Trap-assisted recombination in polymer light-emitting diodes

Kuik, Martijn

Trap-assisted recombination in polymer light-emitting diodes.

Martijn Kuik

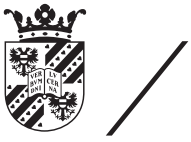

university of groningen

Trap-assisted recombination in polymer light-emitting diodes
Martijn Kuik
PhD thesis
University of Groningen, The Netherlands

Zernike Institute PhD thesis series 2012-2016
ISSN: 1570-1530
ISBN: 978-90-367-5628-0 (Printed version)
978-90-367-5629-7 (Electronic version)

The work described in this thesis was performed in the research group Molecular Electronics and Physics of Organic Semiconductors (MEPOS) part of the Zernike Institute for Advanced Materials at the University of Groningen, The Netherlands. The work was part of the open technology program of the Technology Foundation STW.

PUBLISHED BY: Martijn Kuik
COVER DESIGN: Monique Koers (mocards.nl)
PRINTED BY: Ipskamp Drukkers B.V. (proefschriften.net)

university of groningen / faculty of mathematics and natural sciences / zernike institute for advanced materials

RIJKSUNIVERSITEIT GRONINGEN

Trap-assisted recombination in polymer light-emitting diodes

Proefschrift

ter verkrijging van het doctoraat in de
Wiskunde en Natuurwetenschappen
aan de Rijksuniversiteit Groningen
op gezag van de
Rector Magnificus, dr. E. Sterken,
in het openbaar te verdedigen op
vrijdag 29 juni 2012
om 11.00 uur

door

Martijn Kuik
geboren op 1 september 1977
te Amsterdam

Promotor	:	Prof. dr. ir. P. W. M. Blom
Beoordelingscommissie	:	Prof. dr. D. M. De Leeuw Prof. dr. N. C. Greenham Prof. dr. rer. nat. habil. G. Paasch

Contents

1. A little history of organic light emitting diodes **1**
A little bit of history of materials **2**
The origin of conductive behavior **3**
Breakthrough of the field of organic electronics **4**
Model materials **6**

2. The operation of polymer light emitting diodes **10**
The basics **11**
Fundamental physics in a PLED **14**
Hole and electron current in conjugated polymers **18**
Density dependence of the charge carrier mobility **21**
Unification of a Pool-Frenkel-type and density dependence mobility **23**
Trap-limited electron current **26**
Charge recombination in PLEDs **31**
PPVs **32**
Scientific challenges **33**
Scope of this thesis **34**

3. Optical detection of deep electron traps in PPV light-emitting diodes **41**
Introduction **42**
Electron transport in 'Gilch' MDMO-PPV and 'sulfinyl' MDMO-PPV **43**
Photothermal deflection spectroscopy (PDS) **45**
Internal photo-emission spectroscopy (IPE) **46**
Conclusion **47**

4. Determination of the trap-assisted recombination strength in polymer light emitting diodes **50**
Introduction **51**
Recombination mechanisms in an organic solar cell **52**
Recombination mechanisms in a PLED **54**
Influence of the trap-assisted recombination strength in the PLED operation **55**
Conclusion **58**

5. Trap-assisted and Langevin-type recombination identified via luminance ideality factors in organic light-emitting diodes **60**
Introduction into the ideality factor **61**
Luminance ideality factor **63**
Conclusion **67**

6. The origin of trap-assisted recombination in disordered organic semiconductors **69**
Introduction **70**
Temperature dependence of the capture coefficients in trap-assisted recombination **72**
The mobility dependence of trap-assisted recombination in a white-emitting copolymer **75**
Predictive modeling **76**
Conclusion **77**

7. Non-radiative recombination losses in polymer light-emitting diodes **80**
Introduction **81**
Cathode quenching **82**
Bimolecular and non-radiative trap-assisted recombination **83**
Results and discussion **83**
The profile of current efficiency curves **85**
Magnitude of both loss processes **87**
Conclusion **91**

8. The effect of ketone defects on the charge transport and charge recombination in polyfluorenes **94**
Introduction into polyfluorenes **95**
Optical investigation of ketone defects in PFO **97**
Determination of the luminance ideality factors **99**
Hole transport in PFO and PFO-F **101**
Electron transport in PFO and PFO-F **103**
Conclusion **108**

Summary **112**
Samenvatting **115**
List of publications **119**
Acknowledgements **121**

Chapter 1

A little history of organic light emitting diodes

Over the last decades, organic electronics has become a field of material science advancing rapidly into the commercial domain. After Sony presented in 2008 the world's first commercially available 11 inch organic light emitting diode (OLED) television, as of January 2012, LG announced the development of a 55 inch OLED television only 4 mm thick which will be released by september 2012. In 2010 Samsung introduced its smartphone model Galaxy S featuring a 4 inch active matrix OLED display. Its superior display was a main reason that it became the best sold smartphone line in the world, only 2 years later. Also scientifically the field of organic electronics is expanding fast. For its 50^{th} birthday *Appl. Phys. Lett.* published a list of the top 50 most highly sited papers over the past 50 years in this popular scientific journal. Of these 50 papers, 12 are related to organic electronics.

A little bit of history of materials

OLEDs rely on the conductive and light emissive properties of a specific class of organic, i.e. carbon-based, molecules. As early as 1953 the conductive properties of anthracene crystals were investigated by Mette *et al.*[1], inspired by earlier work on organic dyes as Pyranthron and Violanthron.[2], [3] (**Figure 1**). Not much later Akamatu *et al.* reported on the fairly good conductivity of a perylene-bromide complex in 1954 (**Figure 1**).[4]

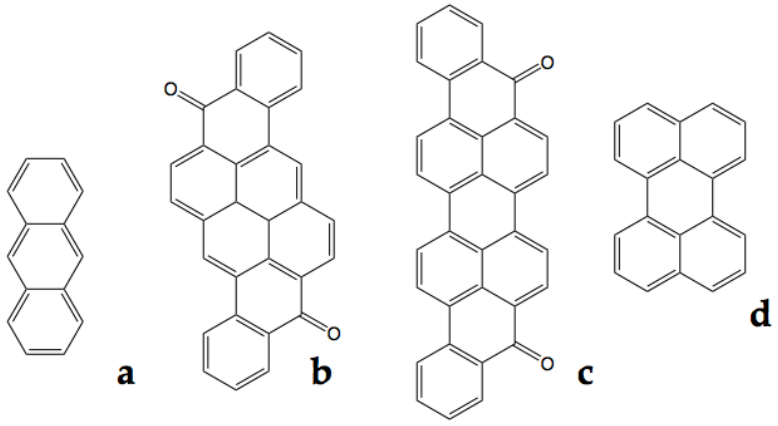

***Figure 1. a**) anthracene, **b**) Pyranthron, **c**) Violanthron and **b**) perylene.*

The first electrically driven light emission, electroluminescence (EL), from organic molecules was reported in the same decade by Bernanose and co-workers when they applied a high alternating current (AC) signal on a thin film of Acridine orange and Quinacrine (**Figure 2**).[5] A little later in the early 1960s Pope *et al.* perhaps laid the foundation for all modern OLEDs by the development the direct current (DC) operating OLED structure incorporating anthracene as light emitting material. [6]

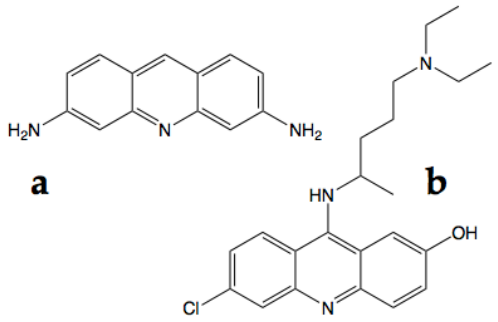

***Figure 2. a**) Acridine orange and **b**) Quinacrine.*

Pyranthron, Violanthron, anthracene and perylene are all of the family of polycyclic aromatic hydrocarbons (PAH) where the latter two are substances commonly found in oil, coal and tar. Acridine orange and quinacrine are of the acridine family and are closely related to anthracene where the difference is that one of the central carbon-hydrogen groups is replaced by a nitrogen atom.

The origin of conductive behavior

The origin of the conduction and light emission in these materials lies in the aromatic structure. An aromatic hydrocarbon implies alternating single and double bonds, i.e. conjugation, between the carbon atoms in a ring. Important to note is that when one carbon atom is replaced by oxygen, sulfur or nitrogen, according to Hückel's rule, the ring shaped molecule still possesses aromatic properties. [7] Actually, the term 'aromatic' was assigned by the fact that most aromatic compounds have a sweet scent.

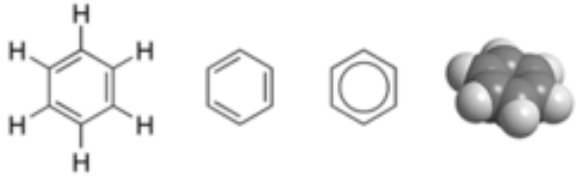

Figure 3. *Various notations for benzene*

Benzene is the simplest of the aromatic hydrocarbons (**Figure 3**). Each carbon in the hexagonal has four electrons to share (**Figure 4**), one for the hydrogen, two for the neighboring carbon bonds and one extra to freely share for a double bond with it's neighboring carbon atoms . In more physical terms, the in-plane C-C and C-H single bonds, σ-bonds, are formed by electrons in so-called sp^2 orbitals where the remaining electron occupies the out-of-plane p_z orbital which due to hybridization with a neighboring p_z orbital forms a π-bond. Since the π-bonds are out of plane with respect to the atoms, these orbitals can interact with each other freely, and become delocalized, hence the schematic representation of a benzene ring (**Figure 4**).

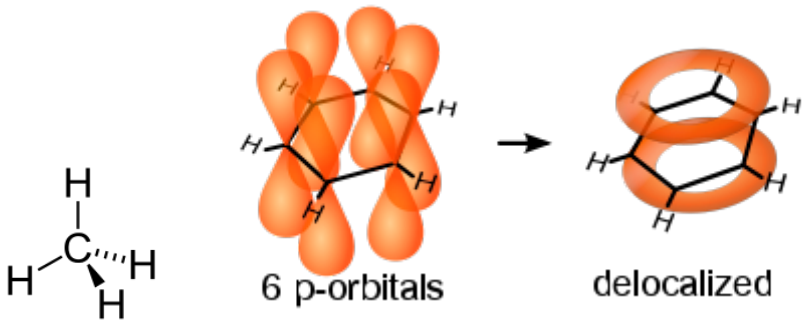

Figure 4. *Schematic structure of methane; a carbon atom comprises four bonding electrons, p orbitals orthogonal to the plane in benzene and delocalized electrons in benzene.*

The out-of-plane π-bond implies that instead of being tied to one carbon atom, each electron is shared by all six carbon atoms in the ring. Thus, there are not enough electrons to form double bonds on all the carbon atoms, but the "extra" electrons strengthen all of the bonds on the ring equally. This is why a benzene ring is smaller and stronger than one would expect from the carbon bonds alone. The delocalization of electrons lies at the origin for the conductive behavior in this class of compounds, since in this system the electrons can 'move freely' between the different atoms in the molecules. The light emission in organic materials is the result of an electron in an energetically higher (sub) orbital, excited either electrically or optically, decaying radiatively via the selection rules for electromagnetic transitions down to a (sub) orbital lower in energy.

Breakthrough of the field of organic electronics

The big breakthrough in the field of organic electronics came when it was shown by Heeger, Shirakawa and MacDiarmid, that the conduction in organic materials is not restricted to aromatic compounds alone. Rewarded in 2000 with the Nobel prize in chemistry, they showed in 1977 that by chemically doping polacetylene (**Figure 5**) with chlorine or bromine, the conductance of the polymer increased dramatically.[8]

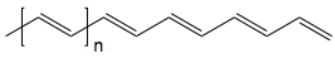

Figure 5. *Schematic structure of polyacetylene, where n indicates the number of repetitions of this structure.*

This work implied that even conjugation in hydrocarbon polymers could lead to conduction when the system is doped. But more importantly, polymers possess much better tunable properties than the organic crystals studied so far. The initial excitement about this new class of materials decreased in the subsequent years because the doped conducting polymers were unfortunately unstable in air, brittle, and still difficult to process. The interest for organic materials in organic electronics picked up actual momentum after the realization of an evaporated double layer OLED by Eastman Kodak developed by Tang and VanSlyke in 1987, exhibiting respectable performance.[9] This diode comprised compounds from a subgroup in organic materials denoted as small molecules. The active layers in this diode consisted of Alq3 stacked on top of an aromatic diamine, TPD (**Figure 6**).

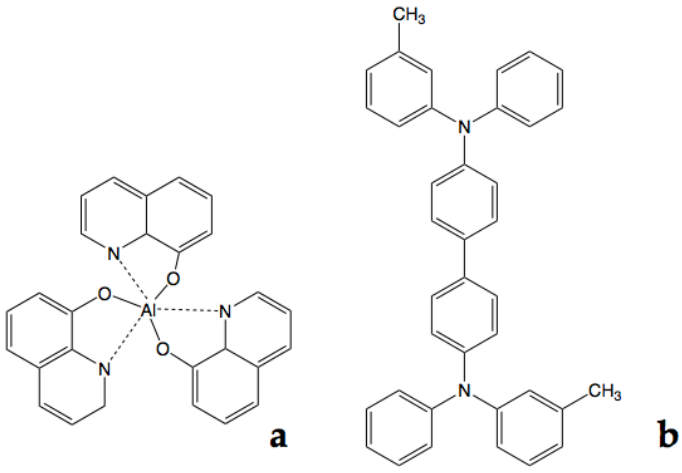

***Figure 6. a**) Alq3 and **b**) TPD*

Interesting results in other disciplines of organic electronics quickly followed hereafter. Subsequently, field-effect transistors made from polythiophene (PT) [10], [11] and from small conjugated oligomers (alpha T6) [12]were reported (**Figure 7**).

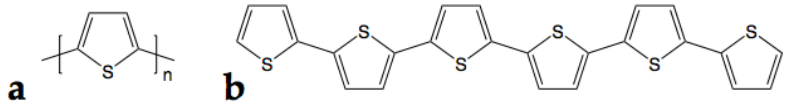

***Figure 7. a**) Polythiophene and **b**) alpha sexithienyl (alpha T6)*

Another major advancement was made by Cambridge University when they reported in 1990 electroluminescence from a conjugated polymer alone. [13] The first polymer light emitting diode (PLED) was born. This diode consisted of a poly(*p*-phenylene vinylene) (PPV) (**Figure 8**) applied via a solution processable precursor route sandwiched between a transparent indium-oxide anode and an aluminum cathode.

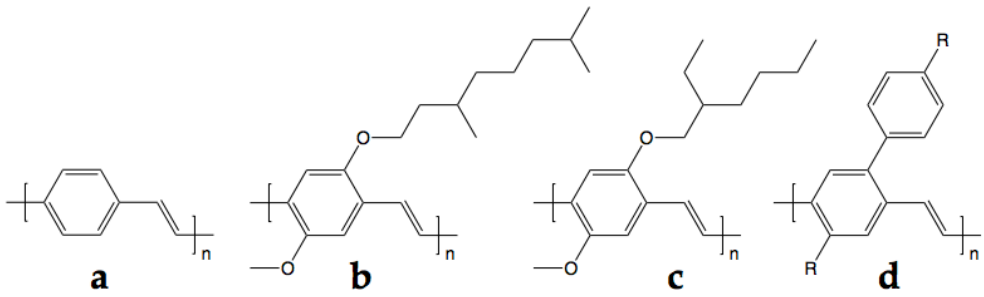

Figure 8. a) *PPV,* ***b)*** *MDMO-PPV,* ***c)*** *MEH-PPV and* ***d)*** *SY-PPV. The R indicates the possibility for additional branches.*

As a result of their fairly undemanding processing conditions PPVs have become a workhorse material for the field of organic electronics for the years that followed. The beneficial property of the tune-ability of polymer molecular structures has led to materials as MEH-PPV and Super Yellow(SY)-PPV, commonly used in PLEDs (**Figure 8**). In fact, due to its relatively high efficiency SY-PPV has served as backlight material in some commercial products early on. By the addition of the branches to the PPV backbone, the requirement for a precursor application route is left redundant since the polymer is now solvable in common organic solvents. Therefore, simple and cheap deposition techniques as spin-coating and rotogravure are common goods these days. Additionally, another PPV, MDMO-PPV, (**Figure 8**) has served as one of the two basic compounds in the first relatively efficient organic solar cell reported in 2001, comprising a conversion efficiency of about 2.5%.[14]

Model materials

At the time of writing this thesis, the polymers designed for usage in organic solar cells and PLEDs often constitute of multiple chemical segments. For example, 'backbone' materials as polythiophene [15], [16], polyphenylene, polyfluorene [17], [18] and polydithiophene [19] are often combined with monomers as triarylamine [20], [21] , benzothiadiazole [22], spirobifluorene [23] and diketopyrrolopyrolle [24] (and many more) (**Figure 9**). Together with

a large variety in side-branches (R), these chemical combinations are chosen in order to fine-tune properties as morphology, charge carrier mobility, solvability, energy levels (i.e. color) and thus overall performance of the electronic devices.

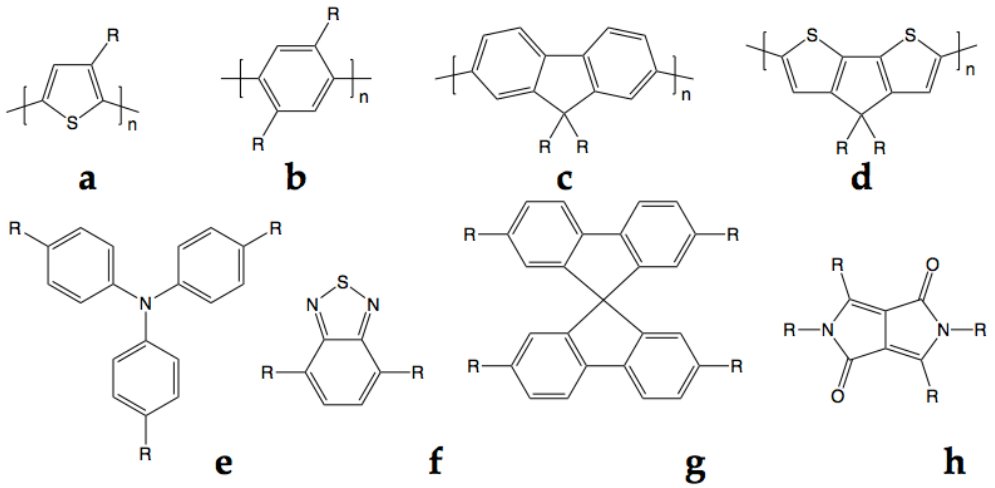

Figure 9. ***a****) polythiophene,* ***b****) polyphenylene,* ***c****) polyfluorene,* ***d****) polydithiophene,* ***e****) triarylamine,* ***f****) benzothiadiazole,* ***g****) spirobifluorene and* ***h****) diketopyrrolopyrolle.*

Where in the time of Bernanose the AC voltages over a thin film device were typically 500-2000V, and where Pope applied a DC voltage of 400V over a 10-20μm thick anthracene crystal, these days for PLEDs with a typical layer thickness of 100nm and the DC operating voltage is around 3 to 4V, depending on the energy levels of the device.

Most of the improvements in the PLEDs of today arise from better synthesis procedures for the polymer compounds leading to a higher purity in the end products, discovery of new chemical 'backbone' and monomer structures, a better choice for organic solvents to favorably influence the morphology and better choices for the anode and cathode materials contacting with the polymer layer. Additionally, since the device structures consist of stacked layers with thicknesses all in the nanometer range, it is now well understood that the preparation and processing of the devices requires special measures and a clean working environment. Dust particles, for example, are typically of micrometer size, which is significantly larger than the total typical diode stack altogether. Hence, most of the PLEDs today are produced in cleanrooms; a laboratory with an exceptionally low level of environmental pollutants.

References

[1] H. Mette and H. Pick, "Elektronenleitfähigkeit von Anthracen-Einkristallen," *Z. Physik*, vol. 134, no. 5, pp. 566–575 (1953).

[2] H. Akamatu and H. Inokuchi, "On the Electrical Conductivity of Violanthrone, Iso-Violanthrone, and Pyranthrone," *J. Chem. Phys.*, vol. 18, no. 6, p. 810 (1950).

[3] S. Mrozowski, "Semiconductivity and Diamagnetism of Polycrystalline Graphite and Condensed Ring Systems," *Phys. Rev.*, vol. 85, no. 4, pp. 609–620 (1952).

[4] H. Akamatu, H. Inokuchi, and Y. Matsunaga, "Electrical Conductivity of the Perylene–Bromine Complex," *Nature*, vol. 173, no. 4395, pp. 168–169 (1954).

[5] A. Bernanose, "Electroluminescence of organic compounds," *British J. of Appl. Phys.* paper 9, p. 54 (1955).

[6] M. Pope, H. P. Kallmann, and P. Magnante, "Electroluminescence in Organic Crystals," *J. Chem. Phys.*, vol. 38, no. 8, p. 2042 (1963).

[7] E. Hückel, "Quantentheoretische Beiträge zum Benzolproblem," *Z. Physik*, vol. 70, no. 3, pp. 204–286 (1931).

[8] H. Shirakawa, E. Louis, A. MacDiarmid,C. Chiang, and A. J. Heeger "Synthesis of electrically conducting organic polymers: halogen derivatives of polyacetylene,(CH) x," *J. Chem. Soc.*, com. 474, pp. 578-580 (1977).

[9] C. W. Tang and S. A. VanSlyke, "Organic electroluminescent diodes," *Appl. Phys. Lett.*, vol. 51, no. 12, p. 913 (1987).

[10] H. Koezuka, A. Tsumura, and T. Ando, "Field-effect transistor with polythiophene thin film," *Synthetic Met.*, vol. 8, pp. 699-704, (1987).

[11] A. Tsumura, H. Koezuka, and T. Ando, "Polythiophene field-effect transistor: Its characteristics and operation mechanism," *Synthetic Met.*, vol. 25, pp. 11-23 (1988).

[12] G. Horowitz, D. Fichou, X. Peng, and Z. Xu, "A field-effect transistor based on conjugated alpha-sexithienyl," *Solid State Comm.*, vol. 72, no. 4, pp. 381-384 (1989).

[13] J. H. Burroughes, D. D. C. Bradley, A. R. Brown, R. N. Marks, K. Mackay, R. H. Friend, P. L. Burns, and A. B. Holmes, "Light-emitting diodes based on conjugated polymers," *Nature*, vol. 347, no. 6293, pp. 539–541 (1990).

[14] S. E. Shaheen, C. J. Brabec, N. S. Sariciftci, F. Padinger, T. Fromherz, and J. C. Hummelen, "2.5% efficient organic plastic solar cells," *Appl. Phys. Lett.*, vol. 78, p. 841 (2001).

[15] H. Sirringhaus, N. Tessler, and R. H. Friend, "Integrated Optoelectronic Devices Based on Conjugated Polymers," *Science*, vol. 280, no. 5370, pp. 1741–1744, (1998).

[16] Z. Bao, A. Dodabalapur, and A. J. Lovinger, "Soluble and processable regioregular poly(3-hexylthiophene) for thin film field-effect transistor applications with high mobility," *Appl. Phys. Lett.*, vol. 69, no. 26, pp. 4108–4110 (1996).

[17] N. S. Cho, D.-H. Hwang, J.-I. Lee, B.-J. Jung, and H.-K. Shim, "Synthesis and Color Tuning of New Fluorene-Based Copolymers," *Macromolecules*, vol. 35, no. 4, pp. 1224–1228, (2002).

[18] Q. Pei and Y. Yang, "Efficient photoluminescence and electroluminescence from a soluble polyfluorene," *J. Am. Chem. Soc.*, vol. 118, no. 31, pp. 7416–7417 (1996).

[19] J. Peet, J. Y. Kim, N. E. Coates, W. L. Ma, D. Moses, A. J. Heeger, and G. C. Bazan, "Efficiency enhancement in low-bandgap polymer solar cells by processing with alkane dithiols," *Nat. Mater.*, vol. 6, no. 7, pp. 497–500 (2007).

[20] G. Casalbore-Miceli, A. Degli Esposti, V. Fattori, G. Marconi, and C. Sabatini, "A correlation between electrochemical properties and geometrical structure of some triarylamines used as hole transporting materials in organic electroluminescent devices," *Phys. Chem. Chem. Phys.*, vol. 6, no. 12, pp. 3092–3096 (2004).

[21] M. A. Parshin, J. Ollevier, M. van der Auweraer, M. M. de Kok, H. T. Nicolai, A. J. Hof, and P. W. M. Blom, "Hole transport in blue and white emitting polymers," *J. Appl. Phys.*, vol. 103, no. 11, pp. 113711 (2008).

[22] Y.-S. Huang, S. Westenhoff, I. Avilov, P. Sreearunothai, J. M. Hodgkiss, C. Deleener, R. H. Friend, and D. Beljonne, "Electronic structures of interfacial states formed at polymeric semiconductor heterojunctions," *Nat. Mater.*, vol. 7, no. 6, pp. 483–489 (2008).

[23] H. T. Nicolai, A. Hof, and J. Oosthoek, and. P. W. M. Blom, "Charge Transport and Recombination in Polyspirobifluorene Blue Light−Emitting Diodes," *Adv. Funct. Mater.*, vol. 21 (8), pp. 1505-1510 (2011)

[24] J. C. Bijleveld, A. P. Zoombelt, S. G. J. Mathijssen, M. M. Wienk, M. Turbiez, D. M. de Leeuw, and R. A. J. Janssen, "Poly(diketopyrrolopyrrole−terthiophene) for Ambipolar Logic and Photovoltaics," *J. Am. Chem. Soc.*, vol. 131, no. 46, pp. 16616–16617 (2009).

Chapter 2

The operation of polymer light emitting diodes

Although OLEDs are already commercially available for quite some years, the physics with regard to their operation is not yet fully understood. The fine-tuning of the properties of OLED devices has been more a trail-and-error approach so far, only partly based on a deep and sound investigation into the mechanisms. Research into the physics of OLEDs is mostly hampered by the ability to synthesize a material with a combination of desired properties. Many materials that would be theoretically interesting to synthesize turn out to also contain properties that do not make them suitable for e.g. fabrication into devices. On the other hand, a lack of detailed understanding of the physics of the materials impedes the design of ideal materials possessing ideal device properties. Hence, the science of organic electronics is not a very straight forward one. In this chapter an overview of the developments concerning to the physics of polymer light emitting diodes (PLEDs) is discussed.

The basics

As specified in the little history section, the operation of a PLED relies on the conductive and emissive properties of the polymer layer. Light emission originates from the fact that in the polymer electrons in a higher energetic state decay radiatively down to a state lower in energy. I order to facilitate this process the contacts to the polymer layer are chosen such that at the cathode the electrons are injected into the polymer layer at a high energy level, whereas the anode is chosen such that the electrons lower in energy can be extracted (i.e. hole injection). This implies that electrons can flow only in one direction since the electrons moving in the reverse direction will experience a large energetic barrier at the cathode, hence a diode (Figure 10).

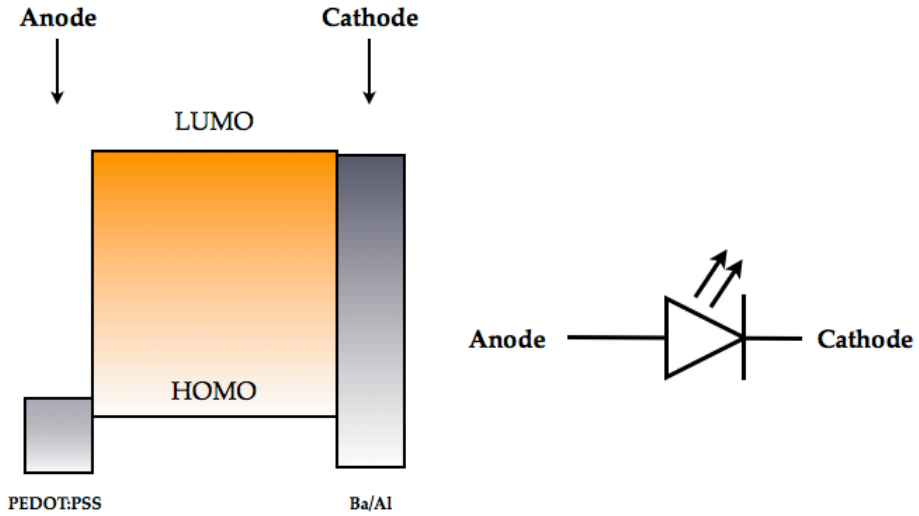

Figure 10. Schematic picture of the energy levels in a PLED and the electric symbol for an LED.

Since the purpose of a PLED is to emit as much light as possible at least one of the contacts to the polymer layer needs to be transparent enough to allow the created light to escape the device structure. Therefore, PLEDs are typically fabricated on top of transparent glass or plastic foil substrates.

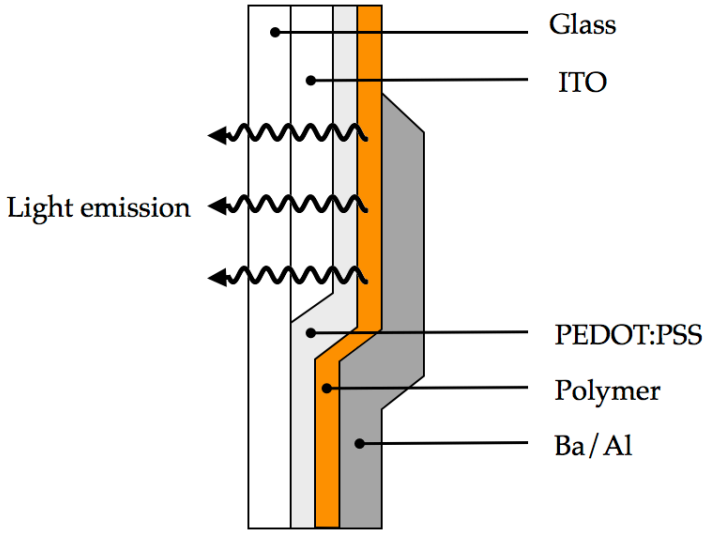

Figure 11. Schematic cross section of a PLED structure.

Clearly, all the following subsequent layers need to be transparent as well, up to the light emitting polymer layer. The first layer on top of a substrate is typically a layer of indium tin oxide (ITO). ITO is one of the most widely used conductive transparent oxides because of the combination of electrical conductivity and optical transparency, as well as the ease with which it can be deposited as a thin film. ITO is applied through evaporation or sputtering onto the substrate forming pre-patterned areas on the substrate that will form the basis of the emitting parts of the PLED structure. Following careful cleaning of the ITO structured substrate, a layer of PEDOT:PSS is applied from a water based solution by means of spin-coating covering the entire substrate, after which the water is driven out by heat. The layer of PEDOT:PSS functions both as a buffer layer in-between the rather rough ITO surface and the light emitting polymer layer, as well as the anode, a hole injecting contact, extracting electrons from low energetic energy levels in the light emitting polymer (hole injection). Then, the light emitting polymer is applied via spin-coating from an organic solvent based solution, again covering the entire substrate. To finish the device Ba and subsequently Al are evaporated through a mask in a vacuum system on top of the light emitting polymer layer, patterned in correspondence with the ITO bottom structure. Instead of Ba also Ca, Cs, CsF, ZnO or Cs_2CO_3 are common cathode materials. These particular materials possess the property of being able to inject electrons in high energy levels of the light emitting polymer, completing the requirements for a diode. The areas where the ITO bottom structure and the Ba / Al top contact overlap will form the emissive part of the PLED (**Figure 11**).

In very general terms, when now a typical bias voltage is applied to the PLED device, electrons will be injected into the polymer from the Ba/Al cathode and holes will enter the polymer from the PEDOT:PSS layer. Somewhere in the polymer layer an electron will feel the Coulombic attraction of a hole and they will form an exciton, a bound state of an electron and hole pair. The electron in the exciton will decay radiatively down in energy, resulting in light emission (**Figure 12**). The color of the light emission is determined by the energy of the exciton, that is reduced with regard to the electrical band gap. The band gap generally refers to the energy difference (in electron volts) between the top of the valence band and the bottom of the conduction band in insulators and semiconductors) with the exciton binding energy. (**Figure 12 and 13**).

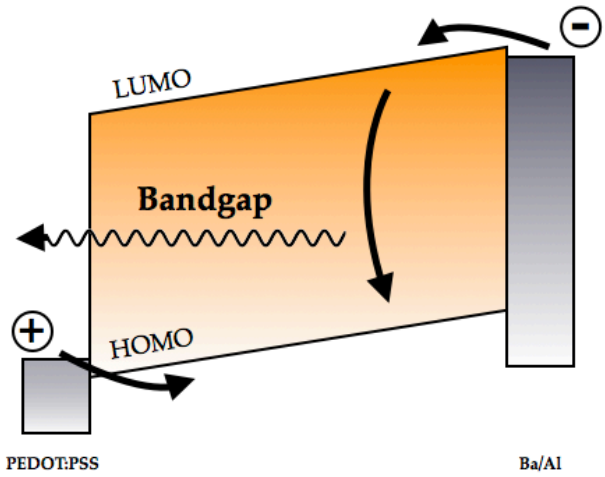

Figure 12. *Schematic representation of the light emission from a PLED at a voltage larger than the band gap of the material.*

As briefly mentioned earlier, the advantage of conjugated polymers over other popular organic materials as for example small molecules is that by modification of their chemical structure they can be made soluble in common organic solvents. As a consequence, polymer-based OLEDs can be processed from solution by cheap and simple processing techniques as spin-coating, inkjet printing or coating techniques as slot-die coating. This feature enables for example a low-cost high-speed production via roll-to-troll fabrication of electronic devices. Therefore the ease of processing of conjugated polymers makes them promising candidates to provide large-area, flexible, light weight lighting systems, integrated circuits and solar cells of the future.

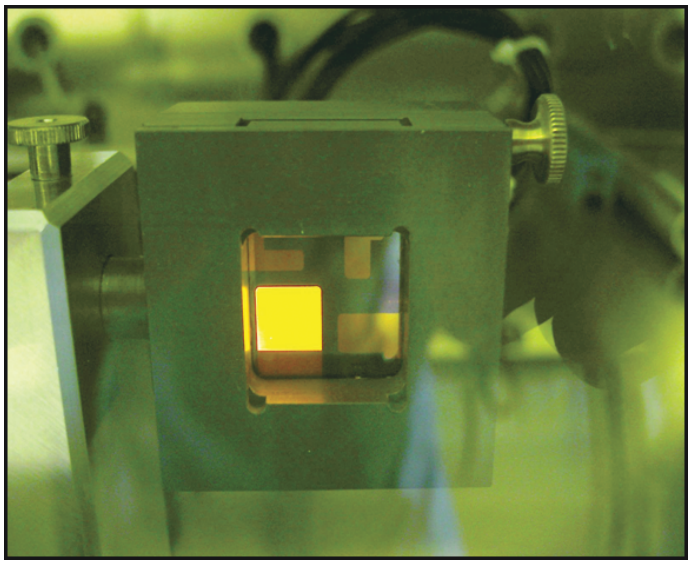

Figure 13. *A picture of a PLED in a measurement setup.*

Fundamental physics in a PLED

Typical molecular weights for conjugated polymers used in PLEDs may vary from about 10000 up to 250000, which results in chain lengths of roughly 10nm to as much as 600nm (depending on the specific structure and synthesis routes). Obviously, the short polymer chains never cover the distance from the anode to the cathode for a typical 100nm layer, even when the chain would be totally straight. However, the very long polymers will never cover this distance, since it is impossible for long polymer chains to exhibit a straight configuration due to phenomena as kinks and twists in the backbone, Van der Waals forces, the size of the side branches or other defects. In fact, longer polymer chains are usually more subjective to these effects and are therefore harder to dissolve, making them difficult to handle during the device fabrication process. Consequently, their use in practical application is limited. The length of the chain, the sandwich device structure and wet deposition techniques as spin-coating or otherwise will in general not lead t chains standing up straight, orthogonal to the surface, thereby forming a single channel of conduction from anode to cathode. Rather, the polymers are randomly distributed similar to spaghetti (without the meatballs) smeared out flat across the surface area. Inevitably, the structural disorder in these organic semiconductors is also reflected in an energetic disorder.

The large disorder comprises a fundamental difference when comparing conjugated polymers to inorganic semiconducting materials with regards to

the charge transport mechanism. The crystalline lattices of inorganic semiconductors are featured by long-range ordered and strongly coupled atoms. The diffraction of quantum mechanical electron waves (orbitals) in these periodic crystals lattices leads to the formation of long-distance well defined delocalized energy bands with a gap in which electrons are forbidden. Additionally, due to the periodicity, the charges can move along these bands with a relatively large average free-path. In contract, conjugated polymers are mostly amorphous or disordered. Although the delocalized electrons can move along the π-orbitals of the polymer backbone, the conjugation length is short and limited by chemical impurities or structural and conformational defects with a scale limit of about 5nm.

The energetic disorder in conjugated polymers is most notably expressed in the definition for the energy bands in these materials. Analogue to the valence and conduction band in *inorganic* semiconductors, the energy bands in *organic* molecules are defined as the highest occupied molecular orbital (HOMO) and the lowest unoccupied molecular orbital (LUMO) respectively (**Figure 10 and 12**). However, in disordered materials these orbitals do not represent a single energy level in particular but are formed by the sum of a bundle of energy levels accompanied by a certain distribution that is related to the amount of disorder.

Due to the short conjugation lengths and the energetic disorder, localized states are formed and the concept of band conduction therefore does not apply in organic semiconductors. Instead, in order to facilitate the conduction process electrons have to be able to jump from one localized state to the other, which evidently depends on the degree of overlap between the orbitals. The carriers may overcome an energy difference between localized states by absorbing or emitting phonons; energies associated with the vibrations of the surrounding matter. This mechanism of phonon-assisted tunneling, or 'hopping', was originally put forward by Mott [1] and Conwell[2] in 1956 in relation to charge transport between impurity states in *inorganic* semiconductors. Miller and Abrahams [3] proposed that the transition rate W_{ij} for hopping from an occupied state i with an energy ε_i to an unoccupied state j with an energy ε_j is described by

$$W_{ij} = \nu_0 e^{(-2\alpha R_{ij})} \begin{cases} e^{\left(-\frac{\varepsilon_j - \varepsilon_i}{k_B T}\right)} & \text{for } \varepsilon_j > \varepsilon_i, \\ 1 & \text{for } \varepsilon_j < \varepsilon_i, \end{cases} \tag{9}$$

where ν_0 is the attempt-to-jump frequency, R_{ij} is the distance between the states i and j, α is the inverse localization length, k_B is the Boltzmann's constant, and

T is the temperature. The wave function (orbital) overlap of states i and j is described by the first exponential term in **Eq (1)**, while the second exponential term accounts for the temperature dependence of the phonon density.

In pioneering work Bässler and coworkers validated in 1993 that when the electron-phonon coupling, i.e. the deformation of the surrounding region by the presence of an electron, is sufficiently weak, the hopping rate in disordered organic systems can be described by the Miller-Abrahams formalism assuming a Gaussian, bell shaped, distribution of site energies (Gaussian disorder model, GDM) with a standard deviation of σ; a parameter for the magnitude of disorder (**Figure 14**).[4] This distribution is in line with the central limit theorem of Lindeberg-Levy in probability theory that states that the sum of a sufficiently large number of independent random variables, each with finite mean and variance, will be approximately a Gaussian function. This work implies that the HOMO and LUMO levels in PLEDs embody a Gaussian shaped density of states (DOS). It should also be noted that it follows from **Eq (1)** that hopping to a lower energy site is more favorable than to a site higher in energy. In the framework of a Gaussian distribution this suggests that the charge carriers do not reside homogeneously distributed throughout the Gaussian DOS, but only the tail states of the distribution are occupied due to a relaxation process of the charge carriers (**Figure 14**).

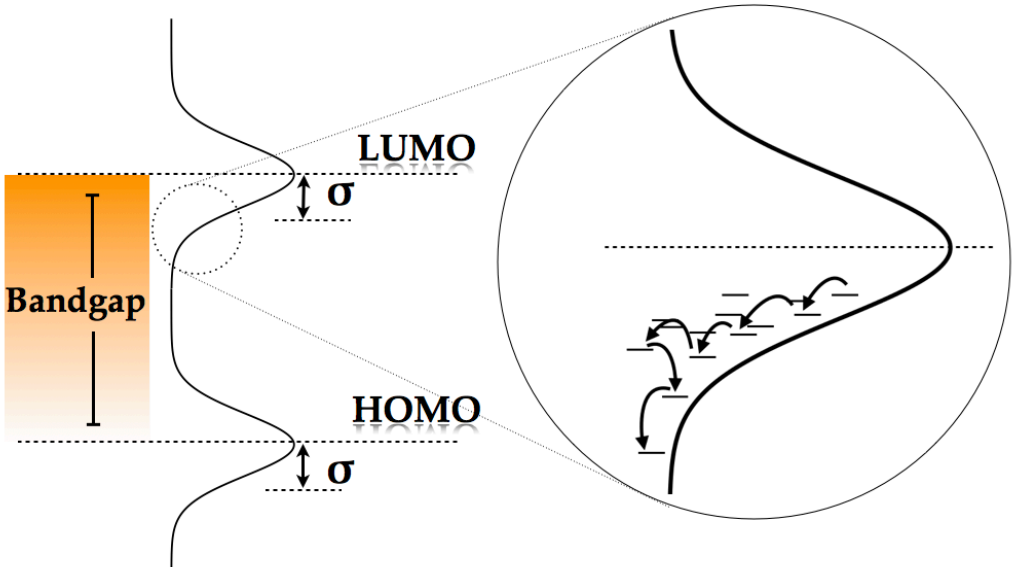

Figure 14. *Schematic representation of the energy levels and the DOS in a PLED as well as the hopping and relaxation process for electrons.*

The drift current relies, per definition, on the presence of an electric field, F (= voltage/thickness), according to

$$J = q\mu pF, \tag{10}$$

where q is the elementary charge, p the density of charge carriers (usually p denotes density of holes and n the density of electrons) and μ the mobility, the speed at which a charge carrier can move through a semiconductor when pulled by an electric field. It was found that for a broad voltage range the mobility in disordered materials could be described using a Poole-Frenkel type electric-field dependence of the form

$$\mu_{PF} = \mu_0 e^{\left(\gamma\sqrt{F}\right)}. \tag{11}$$

In this equation, μ_0 denotes the zero-field mobility and γ is the field activation parameter. For many disordered organic semiconductors the increase of the mobility with increasing voltage has been described using **Eq (3).** In the GDM by Bässler using Monte Carlo simulations (a method of investigation a set of basic equations by repeated random sampling using a computer) leads to a more advanced expression for the charge carrier mobility [4], namely:

$$\mu_{GDM} = \mu_\infty e^{-\left(\frac{2\sigma}{3k_BT}\right)^2} \begin{cases} e^{C\left[\left(\frac{\sigma}{k_BT}\right)^2 - \Sigma^2\right]\sqrt{F}} & \text{for } \Sigma \geq 1.5, \\ e^{C\left[\left(\frac{\sigma}{k_BT}\right)^2 - 2.25\right]\sqrt{F}} & \text{for } \Sigma < 1.5. \end{cases} \tag{12}$$

In this expression μ_∞ is the mobility in the limit $T \rightarrow \infty$, C is a constant that is related to the lattice spacing and Σ describes the positional disorder. Note the similar field dependence as the Poole-Frenkel relation, **Eq(3)**. However, it was found that when applying the standard GDM only the experimental results at high electric fields ($>10^8$ V/m, i.e. >10V across a 100nm thin film) could be satisfactory explained. [5] Gartstein and again Conwell found in 1995 that agreements with experiments could be improved by taking spatial correlations between site energies into account (Correlated disorder model, CDM). [6] In this model the energies are correlated over a greater length then the distances between hopping sites and the mobility takes the form

$$\mu_{CDM} = \mu_\infty e^{-\left(\frac{3\sigma}{5k_BT}\right)^2} e^{0.78\left[\left(\frac{\sigma}{k_BT}\right)^{\frac{3}{2}} - \Gamma\right]\sqrt{\frac{qaF}{\sigma}}}, \tag{13}$$

where a is the intersite spacing, and Γ is the positional disorder of transport sites, Γ=2 for organic materials. This model was successfully used to describe the transport of charges in molecularly doped polymers. Again, in the CDM the field dependence is, albeit controlled by a pre-factor, still very similar to the Poole-Frankel relation (**Eq(3)**). In sum, the major features in the models developed in the mid-90's for transport in organic disorder materials are that the DOS is approximated by a Gaussian function and, additionally, the mobility is depending on temperature as well as on the electric field through a variation on the Pool-Frenkel effect.

Hole and electron current in conjugated polymers

It was mentioned earlier that in order for a PLED to work properly a particular choice is made for the anode and cathode materials. For the anode material the work-function, the minimum energy to remove an electron from the solid, has to align with the HOMO of the polymer and the cathode work-function has to align with that of the LUMO. A poor choice for the energy alignment of the contact materials will introduce injection barriers which will limit the luminous efficacy of a PLED. Materials for the anode are usually 'high' work-function materials as PEDOT-PPS, Au, Pd or MoO_3 and the cathode usually consists of 'low' work-function materials as Ba or others, as mentioned before. However, these injection barriers can also be used beneficially for studying electron and hole transport individually.[7] In a device structures as glass/ITO/PEDOT-PSS/polymer/Au both the PEDOT-PSS and the Au align with the HOMO of a polymer as MEH-PPV. The injection barrier for electrons in this device is so large that they will not enter the polymer layer. Thus the only current that will flow in a device such as this will originate from hole transport, hence a holy-only device (**Figure 15**). Likewise, a typical glass/Al/polymer/Ba/Al device will allow electrons to enter from the Ba/Al contact but the Al bottom contact will block the holes from entering the polymer film, hence an electron-only device (**Figure 15**).

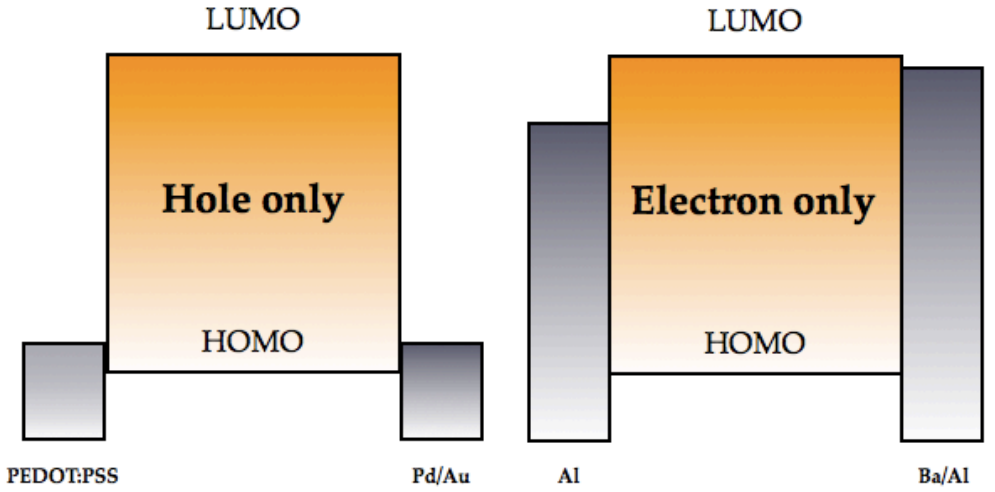

Figure 15 *Schematic picture of the energy levels in a hole only and electron only device.*

A first glance at the MEH-PPV *J-V* characteristics for the comparison of a double carrier (PLED), hole-only and electron-only device in **Figure 16** already clearly reveals one important feature. The transport in a PPV PLED is dominated by hole transport since the hole current is comparable to that of the double carrier device for the same thickness, while the electron current is much lower.

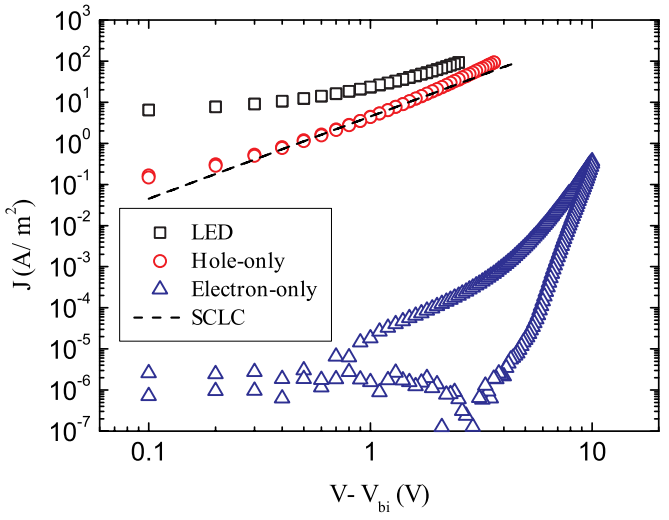

Figure 16 *Current voltage characteristic of a 160nm thick PPV PLED, hole-only and electron-only device. Current voltage characteristics, J-Vs, are commonly presented as*

a current density, current per surface area, to allow comparison with other device configurations.

The organic semiconductors used in PLEDs are not intentionally doped, as a result the intrinsic charge carrier density and the conductivity is very low. When a voltage is applied over these materials charges are injected into the organic semiconductor from the contacts, that are not neutralized by counter charges, as in case of doping. As a result the injected charges are able to form a space charge, a charge distribution over a region of space in the medium. The presence of this space-charge sets an electrostatic limit to the amount of charges that can enter the materials, hence space-charge limited current. Space-charge limited current (SCLC) is generally described at low electric fields by the Mutt-Gurney square law [8] according to,

$$J = \frac{9}{8}\varepsilon_0\varepsilon_r\mu\frac{V^2}{L^3}, \tag{14}$$

where ε_0 is the permittivity of vacuum, ε_r is the relative dielectric constant of the semiconductor materials (typically about 3 for organic materials) and L the device thickness. Clearly observable in **Figure 16**, contrary to the electron current, the hole current in MEH-PPV exhibits clear space charge limited behavior from which a typical hole mobility of 5×10^{-11} m^2/Vs can be determined. At higher biases the current density starts to increase more rapidly with voltage and **Eq (6)** does no longer describe the experimental data. A possible explanation for this current increase could be that the mobility increases with the applied voltage via an earlier discussed Pool-Frenkel like behavior. Applying the SCLC equation to *J-V* characteristics for different temperatures leads to an adjustment to the Pool-Frenkel relation, first suggested by Pai in 1970 on PVK [9],

$$\mu = \mu_0 e^{\left(-\frac{\Delta}{k_B T}\right)} e^{\left(\gamma\sqrt{F}\right)}, \tag{15}$$

where where μ_0 is the zero field mobility and Δ represents the zero-field activation energy. This empirical result seems to contradict the prediction of the temperature dependence in the GDM and CDM models (**Eq (4) and Eq (5)**) since the first term in these mobility expressions predicts a $1/T^2$ dependence. Nonetheless, the empirical result for an Arrhenius type, $1/T$, behavior for the mobility is quite strong since it is measured and confirmed in a rather wide range of organic materials, **Figure 17**.[10]

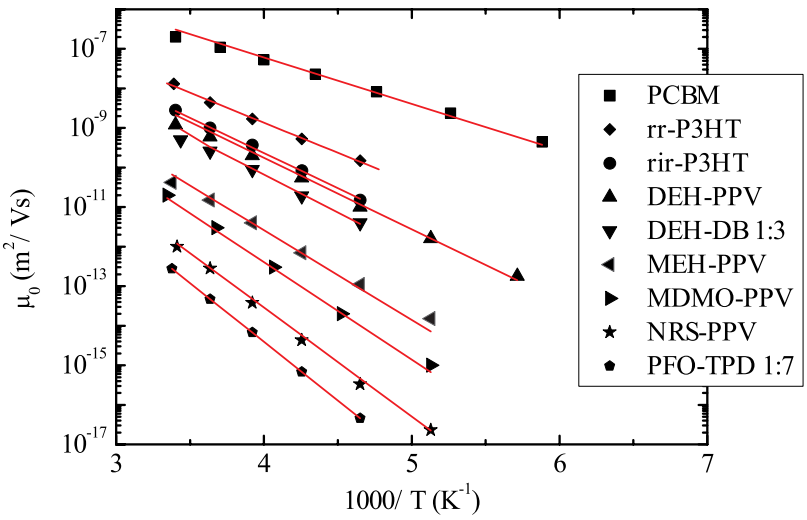

Figure 17 *Arrhenius type behavior of the zero field mobility for a broad range of organic semiconductors. Data taken from Craciun et al.* [10]

Density dependence of the charge carrier mobility

Interestingly, parallel to the development of models describing charge transport in disordered diodes, for another electrical element, the organic field effect transistor (OFET), the mobility was proposed to rely on a phenomena not considered in diodes. A field effect transistor is a three terminal device which relies on the basic principle of a current that flows through a material in-between two contacts, denoted as the source and drain electrode, that can be modulated by applying a voltage to a third contact, the gate electrode. In this configuration the gate electrode is electrically decoupled from the semiconducting material by an insulating layer (**Figure 18**). By applying positive of negative gate voltages, induced charge carriers accumulate or deplete in the semiconductor close to the semiconductor/insulator interface. In this manner the field-effect current can be varied in the source-drain channel.

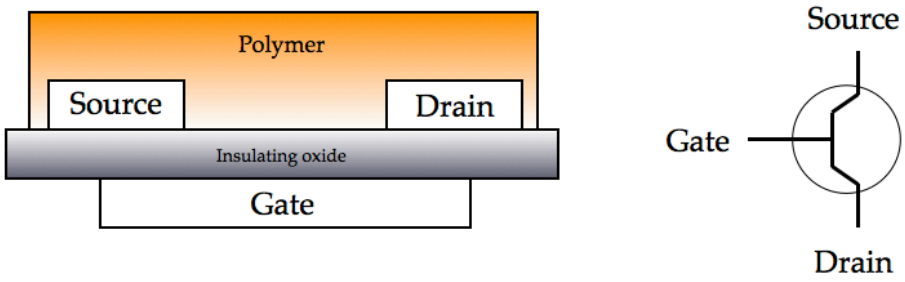

***Figure 18**. Schematic OFET structure and the electric symbol for a FET.*

In contrast to conventional mono-crystalline silicon, the transport properties of disordered organic semiconductors are dominated by hopping to and from localized states according to Miller-Abrahams[3], **Eq (1)**. Based on work by Monroe published in 1985 [11], Vissenberg and Matters proposed in 1998 that when a voltage is applied to the gate of an OFET, the accumulating charge carriers at the interface will fill the lower localized states in the tail of the DOS due to charge relaxation as described in the Miller-Abraham hopping process (**Eq (1)**).[12] Any additional charge in the system will occupy states at relatively higher energy levels, which means that they will need less activation energy to jump to other sites contributing to the total transport process. Consequently, the mobility will be enhanced and is expected to increase with charge carrier density, a dependence not considered in diodes thus far.

The model proposed by Vissenberg and Matters depends on the principle of variable range hopping. This implies that charge carriers may either hop over a small distance with a high activation energy or hop over a long distance comprising a low activation energy, while taking into account the filling of the low energetic localized states. This comprises a fundamental difference with for example the GDM model developed by Bässler, which is a one particle system.[4] The Vissenberg-Matters model predicts that the transport properties are determined by the tail of the Gaussian DOS, which for this case can be approximated by an exponential DOS. Using percolation theory they derived an expression for the mobility in an OFET as,

$$\mu_{FET} = \frac{\sigma_0}{q}\left[\frac{\left(\frac{T_0}{T}\right)^4 \sin\left(\pi\frac{T}{T_0}\right)}{(2\alpha)^3 B_C}\right]^{\frac{T_0}{T}} p^{\frac{T_0}{T}-1}, \tag{16}$$

where σ_0 is a conductivity prefactor, α is again the inverse localization length as an effective overlap parameter of the orbitals as reported earlier in **Eq (1)**, B_c is related to the onset of percolation and has typically a value of 2.8 (in a 3D lattice and assuming uniform spheres for the volume fractions), and T_0 denotes a characteristic parameter describing the width of the density of states. It should be noted that the mobility in this expression results in a 1/T dependence as well.

Unification of a Pool-Frenkel-type and density dependence mobility

Clearly, the average charge carrier density in an organic diode is lower than in the conduction channel of an OFET simply because there is no extra orthogonal field present in a diode configuration to induce and confine additional charge carriers in the organic semiconductor. Carrier densities in typical organic diodes are in the range of about 10^{20} to 10^{21} m^{-3},where the densities in OFET range from 10^{23} up to 10^{25} m^{-3}.

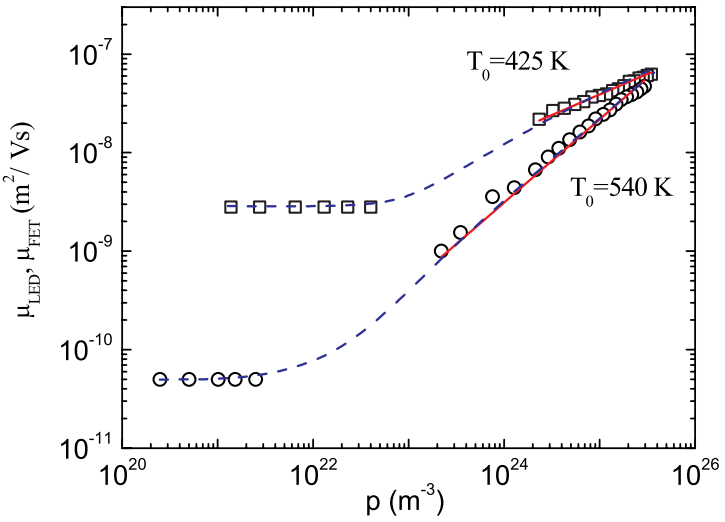

Figure 19 *Mobility as a function of hole density p in a hole only diode and OFET for P3HT and MDMO-PPV.*

In 2003 Tanase *et al.* was the first to show that the mobility at low carrier concentrations as observed in diodes, and at higher carrier concentrations, as observed in OFETs, are part of one continuous function[13], **Figure 19** resulting in an expression for the mobility, at zero electric field, as,

$$\mu = \mu_0 + \frac{\sigma_0}{q}\left[\frac{\left(\frac{T_0}{T}\right)^4 \sin\left(\pi\frac{T}{T_0}\right)}{(2\alpha)^3 B_C}\right]^{\frac{T_0}{T}} p^{\frac{T_0}{T}-1} \quad (17)$$

The charge carrier density, *p*, is in general the result of the sum of background carriers, already present in the organic semiconducting material, and the injected charges from the contacts. At very low voltages the amount of injected charges is lower than the amount of background charges. In that case, the amount of charges is nearly independent on voltage and the current follows a linear relation on voltage, Ohms law. At a sufficient voltage, the amount of injected charges becomes dominant, such that the charge carrier concentration increases linearly with voltage, leading to SCLC. As stated above, an increasing charge carrier density also leads to an increased filling of the tail of the localized states. It was demonstrated by Bässler *et al*. that the maximum occupation of the Gaussian DOS is located at the so called equilibrium energy, given by $-\sigma^2/k_BT$. For low enough carrier densities the Fermi level is below this equilibrium level, meaning that the starting point for hopping transport is independent on the concentration.[14] As a result, for low carrier densities in the mobility is independent on carrier concentration, hence the first term on the right hand side in **Eq (9)**, and the plateau in left of **Figure 19**. For higher carrier densities the Fermi-level exceeds the equilibrium level and the mobility further increases with increasing concentration.[15] Thus increasing or decreasing the mobility according to the power law, (T_0/T)-1, in the second term of **Eq (9)**. It was demonstrated by Tanase *et al.* that this density dependence of the mobility consistently explains the voltage- and thickness dependence of the *J-V* characteristics of MDMO-PPV based hole-only devices at room temperature.[16]

Furthermore, it has been shown in 2008 that the the charge carrier density at zero bias by charge carrier diffusion from the contacts also becomes relevant and *does* influence the mobility for very thin devices.[17] For these very thin devices (< 100nm) the diffusion regions from the anode and cathode overlap, thereby increasing the average carrier density in the layer and thus the mobility. As a consequence, it was demonstrated that a field dependence based on a Pool-Frenkel-type description for the carrier mobility alone in a diode is not sufficient.

As a matter of fact, it can be shown as well as argued that the mobility in most organic diodes at room temperature and low fields is solely dominated by charge carrier density effects and that for lower temperatures the field dependence becomes more important. At room temperature the carriers

occupy higher states in the DOS such that the required energy step for transport is relatively low. For lower temperatures however, the charge carriers are less energetic and reside at much lower energetic states due to relaxation into the deep tail states of the DOS. Consequently, the activated hops between neighboring sites are strongly reduced since escaping these deep states is more difficult, hence suppressing the charge transport. Yet, application of an electric field leads to energetic tilting, reducing the energetic barriers for these charge carriers to hop in the direction of the field, which results in a strong field dependence of the mobility for low temperatures.

Based on this experimental work a parameterization for the temperature, field and density dependence of the charge carrier mobility was introduced by Pasveer *et al.*, using a three dimensional master equation approach.[18] A master equation approach is a computation technique used to describe the time-evolution of a system that can be modeled as being in exactly one of a countable number of states at any given time, where switching between states is treated probabilistically. This work comprises an expansion of the GDM model, designated as the extended Gaussian disorder model (EGDM), and results in the factorized expression for the mobility as,

$$\mu_{EGDM} = \mu_0 \times \mu_F \times \mu_p, \tag{18}$$

where,

$$\begin{aligned} \mu_0 &= \mu_0^* c_1 e^{(-c_2\hat{\sigma})} \\ \mu_F &= e^{0.44\left(\hat{\sigma}^{3/2}-2.2\right)} e^{\sqrt{1+0.8\left(\frac{Fqa}{\sigma}\right)^2}-1} \\ \mu_p &= e^{\frac{1}{2}\left(\hat{\sigma}^2-\hat{\sigma}\right)\left(2pa^3\right)^{\delta}} \end{aligned} \tag{19}$$

,

with,

$$\delta \equiv 2\frac{\ln\left(\hat{\sigma}^2-\hat{\sigma}\right)-\ln(\ln 4)}{\hat{\sigma}^2} \quad \text{and} \quad \mu_0^* \equiv \frac{a^2\nu_0 q}{\sigma}.$$

In these equations $\hat{\sigma} = \sigma/k_BT$, and σ is the width of the density of states and a is the intersite distance according to $a = N_t^{-1/3}$, where N_t is the density of transport sites. For the temperature domain at which in typically transport measurements are performed, **Figure 15**, it has been shown that this model for sufficient filling indeed accounts for a $1/T$ dependence of the mobility. [19], [20]

Trap-limited electron current

The results covered so far only represented the investigation on the hole transport in PPV based polymers. However, as is visible in **Figure 16**, in contrast to the hole transport the electron transport is not characterized by a SCLC behavior, but shows a much steeper voltage dependence. Actually, it turns out that this asymmetric charge transport behavior is prototypical for a vast majority of organic materials. Only recently an increasing amount of compounds are reported of which the carrier mobilities are nearly equal or where the electron transport is dominating the hole transport. [21], [22]

A closer look at **Figure 16** reveals that the current of the electron only device displays some very distinctive features. First, the current is much lower than when compared to the current of the hole only device. Second, the back sweep from high to low bias does not follow the same scan as from going from low to high. And third, for the entire scan the current exhibits a much stronger dependence on the applied electric field. Additionally, but not shown in **Figure 16**, the temperature dependence was found to be reduced and the thickness dependence was found to have increased; when compared to the hole current.

This behavior has been explained by assuming free electron transport in the LUMO [23], [24] accompanied by the presence of electron traps, inside the band gap. The electrons that get stuck on the trap sites reside much longer at that particular site then free electrons would on a free hopping site. As a result, in thermal equilibrium they do not contribute to the charge transport. Hence the electron current is strongly surpressed. Similar to the holes, the total amount of electrons or space-charge, in this case the sum of free and trapped electrons, is dependent on the applied voltage, similar to the workings of a capacitor. The steepness of the *J-V* characteristics is then dependent on the energetic distribution of the traps in the band gap. However, in contract to holes the electron current exhibits hysteresis. This behavior is perhaps best explained using the characteristic electron only feature of an 'envelope' curve depicted in **Figure 20.**

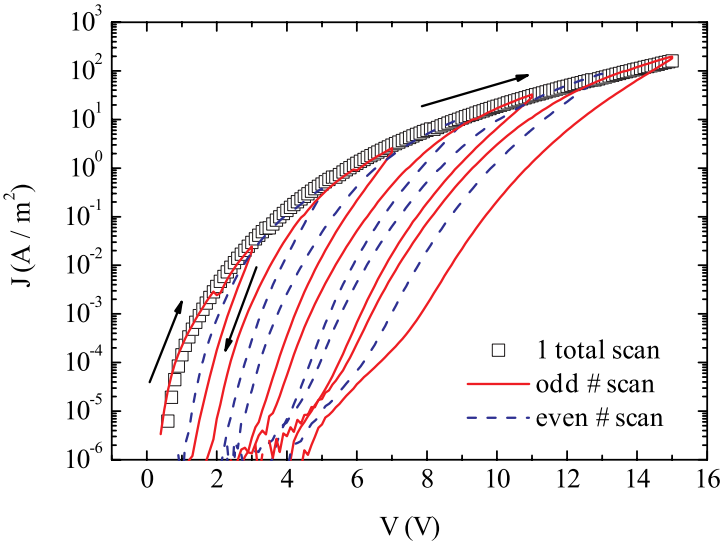

***Figure 20**. The 'envelope' curve of an Al/MEH-PPV/Ba/Al electron only device with a thickness of 150 nm. The lines represent the measurements of consecutive voltage scans where every sweep the maximum voltage is increased with 2 V. The symbols represents the up-scan measurement f another J-V measurement for a fresh device of the same thickness L=150 nm, the 'envelope' curve.*

In **Figure 20** it is shown that the behavior of an electron only *J-V* can be explained by the presence of trap levels inside the band gap. The device starts electrostatically neutral. Once a voltage is applied charges fill up the traps. When a maximum voltages is reached and the down sweep is made, part of the electrons are released and part of the electrons reside longer, i.e. stay trapped, than the time it takes for the scan to release them. At zero voltage, meaning that electrostatically there should be no net charges present, there are still trapped electrons on the film and the device is out of thermal equilibrium. When a subsequent up scan is made the still trapped electrons block the entering of additional electrons at first. When the applied voltage surpasses the maximum voltage of the previous scan the *J-V* scan follows the original 'envelope' curve, filling up additional traps. Hence, once an electron-only device is measured it is brought out of electrostatic equilibrium permanently and can not be scanned again. It should be noted that it has been shown that part of the traps responsible for the hysteresis can be removed by proper purification of the polymer batch.[25]

A quantitative analysis of the electron transport has been lacking for a long time, since it proved to be very difficult to produce reliable electron only

devices or to rule out that the traps are actually a bulk property and not contact effects. It was first proposed by Burrows and Forrest in 1994, through measurements on Alq3, that the electron current could be explained by assuming an exponentially shaped trap level in the presence of the LUMO of the small molecules.[26]

In their work Burrows and Forrest used the Mark and Helfrich formalism to describe the trap limited electron current.[27] Mark and Helfrich deduced this relation in 1962 for the explanation of conductivity measurements on organic single crystals of *p*-therphynel, *p*-quaterphynel and the well-known compound anthracene, of which they showed that contained exponentially distributed hole traps. The Mark and Helfrich equation in the work of Burrows and Forrest is represented by,

$$J = A\mu q^{(1-m)} \left(\frac{m\varepsilon_0\varepsilon_r}{N_{tr}\,(m+1)} \right)^m \left(\frac{2m+1}{m+1} \right)^{m+1} \left(\frac{V^{m+1}}{L^{2m+1}} \right), \tag{20}$$

where A is a prefactor and m is simply a fit parameter amounting to 8±0.5 for Alq3. They estimated, based on their findings, the electron trap concentration, N_{tr}, at about 10^{25} m^{-3}.

The work of Mandoc *et al.* in 2006 conveyed that electron devices of conjugated polymers *can* be reliable fabricated when using the right fabrication procedures and choosing the right materials for the hole blocking bottom contact.[28] Additionally, they showed that the device characteristics can indeed be well explained by assuming this exponential trap distribution using an adjustment of the Mark and Helfrich formalism. This additiona took into acocunt that the transport band is a Gaussianly shaped DOS and the mobility is now governed by a temperature, field and density dependence,

$$J = N_c\mu q \left(\frac{\varepsilon_0\varepsilon_r}{qN_{tr}e^{\frac{(E_{tc}-E_a)}{k_B T_t}}} \right)^r \left(\frac{2r+1}{r+1} \right)^{r+1} \left(\frac{r}{r+1} \right)^r \left(\frac{V^{r+1}}{L^{2r+1}} \right), \tag{21}$$

where N_c is the effective density of states, N_{tr} the total concentration of traps, E_{tc} the trap level relative to E_a, which is a characteristic energy related to the DOS that mimics the role of the conduction band edge, where the DOS is a Gaussian distribution with variance σ and T_t is the trap temperature, which is a characteristic parameter determining the shape of the exponential trap, and $r = T_t/T$, **Figure 21**.[29]

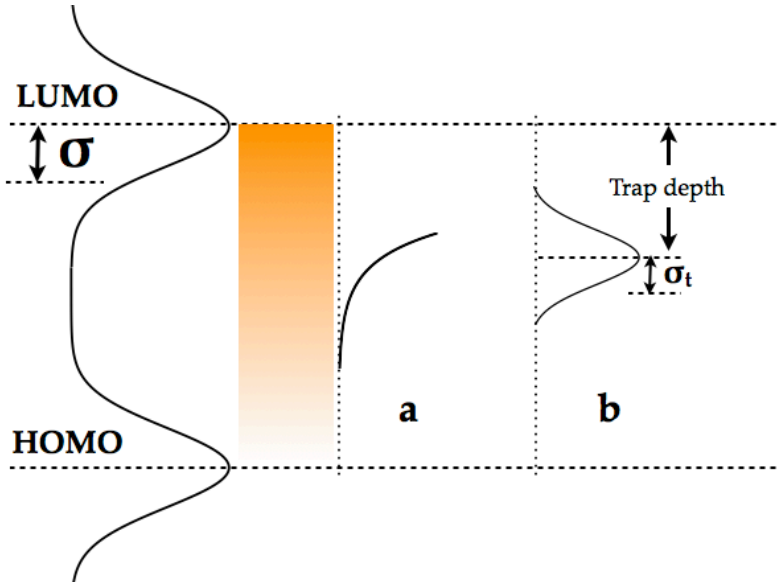

Figure 21 *Schematic representation of* ***a****) an exponential and* ***b****) a Gaussian trap distribution.*

However, a drawback of this model is that the actual trap depth as well as the total amount of traps cannot be determined independently since they are both in the prefactor of **Eq (13)**. Thus in practice the denominator in the first term of **Eq (13)** is taken as an effective trap density incorporating both the number and the depth:

(22) $$N_{tr(eff)} = N_{tr} e^{\frac{(E_{tc}-E_a)}{k_B T_t}}.$$

Typical values for $N_{tr(eff)}$ in PPVs are found in the range of 1×10^{24} m^{-3}.

Recently Nicolai *et al*. introduced a full description of the PPV-based electron current using a Gaussianly shaped trap distribution (**Figure 21**).[30] This work comprises a unification of a description of a shallow and deep Gaussianly shaped trap DOS based on work of Hwang and Kao for the shallow [31] and Nespurek and Smejtek for the deep Gaussianly distributed traps [32] using a recently reported Gauss-Fermi approximation of Paasch and Scheinert.[33] If one assumes the transport DOS to be Gaussianly shaped due to the disorder in the material it follows naturally that a distribution for the traps should also be influenced by this disorder. Therefor a Gaussian trap distribution is much more intuitive than an exponential distribution. Additionally, it was shown that electron only currents in the materials MDMO-PPV, MEH-PPV and NRS-PPV can be equally well described using a Gaussian trap distribution as compared

to an exponential one. And besides that, using a Gaussianly shaped trap distribution has one rather important advantage. It allows a disentanglement of the number of traps and their depth, which was not possible for an exponential trap distribution. MEH-PPV, MDMO-PPV and NRS-PPV are all reported to contain about 3×10^{23} m^{-3} traps at a depth centered at about 0.75 eV below their LUMO (for all these materials the LUMO level is about the same). [30]

The depth of 0.75 eV for the traps in PPVs seems rather deep but recent experiments confirm that the traps limiting the electron transport must be at least deeper than 0.4 eV below the LUMO of a MDMO-PPV. The work of Zhang *et al*. showed that by n-type doping the PPV the electron current with decamethylcobaltocene (DMC), the electron transport can retain its trap free property.[23] Since all the traps are shown to be filled, this must imply that the electrons of the HOMO of the dopant DMC have filed all the traps. Hence, since the HOMO of the dopant DMC is at 3.3 eV, the trap level must lie deeper than 3.3 eV in order to have filled them all. Because the LUMO of MDMO-PPV is located at 2.9 eV the depth of the traps must be deeper than 0.4 eV below the LUMO of the MDMO-PPV, as depicted in **Figure 22**. In this work a rough estimate is made for the number of traps, leading to a number of about 10^{23} m^{-3}.

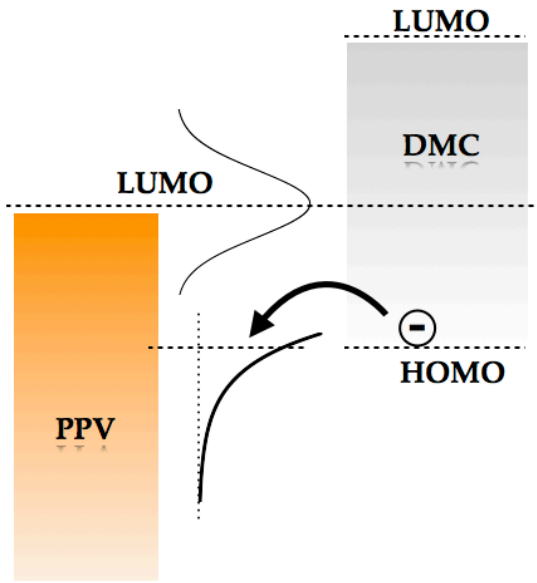

Figure 22 *Schematic picture of the energy levels for the n-type doping of MDMO-PPV with DMC, filling op the electron traps in MDMO-PPV. The trap is depicted as an exponential in favor of the clarity of the picture.*

It has been suggested that the trap limited behavior originates from a change in disorder for the electron transport.[34]. However, it has already been convincingly shown that the traps limiting the electron transport lay energetically well separated from the LUMO for the case of PPVs.[23] At the same time, it is shown that the trap limited behavior can be undone by the addition of electron doping, restoring back to the free hole only current behavior, possessing the same field, density and temperature dependence for the mobility.[23] This implies that the influence of disorder caused by traps in the charge transport, for PPVs at least, is negligible small.

The exact origin of the traps giving rise to the trap-limited electron current in semiconducting polymers is still under debate. Defects such as kinks in the polymer back- bone[35], [36], impurities remaining from the synthesis, or contamination from the environment[37] have been proposed as possible sources. Techniques such as thermally stimulated currents (TSC) and deep level transient spectroscopy (DLTS) have been employed to obtain information on the properties of traps.[38-40] Generally it is suspected that species as water or oxygen are responsible for the trapping behavior although this unfortunately has not been convincingly proven yet.

Charge recombination in PLEDs

Recombination of electrons and holes in PLEDs is a very important process, as it determines the actual efficiency of the device. Bimolecular recombination in organic semiconductors is of the Langevin type; i.e., the rate limiting step is the diffusion of electrons and holes toward each other in their mutual Coulomb field. Such a behavior is characteristic for materials in which the mean free path of the charge carriers is smaller than the critical Coulombic capture distance,

$$r_c = \frac{q^2}{4\pi\varepsilon_0\varepsilon_r k_B T}, \tag{23}$$

at which the Coulomb binding energy between an electron and hole is larger than the thermal energy k_BT. The hopping nature of the charge transport in organic semiconductors is characterized by a typical hopping distance of 1-3 nm. The critical capture distance for an electron and hole recombination, r_c amounts to about 18.5 nm at T = 300 K (ε_r = 3), which is much larger than the typical hopping distance. As a result, the occurrence of Langevin recombination in organic semiconductors was already predicted through

Monte Carlo simulations and later on experimentally verified.[41] This implies for the bimolecular Langevin recombination rate that

$$R_L = B_L np, \tag{24}$$

where the Langevin recombination constant [42] , B_L, is given by

$$B_L = \frac{q}{\varepsilon_0 \varepsilon_r} (\mu_n + \mu_p) . \tag{25}$$

It is important to note that the mobilities in the Langevin expression for B_L, follow the normal temperature, field en density dependence, as derived from the single carrier devices,

$$B_L = \frac{q}{\varepsilon_0 \varepsilon_r} (\mu(T, F, n) + \mu(T, F, p)) . \tag{26}$$

An increase in the mobility will simply also increase the probability that charge carriers find each other in their attractive Coulomb field as expressed in **Eq (18)**.

Even though the presence of Langevin recombination is widely recognized, some studies suggest modifications to the classical Langevin expression, **Eq (17)**[43] due to bipolar mobilities [44] or inclusion of lateral hops.[45] However, all these studies suggest only negligible adjustments.

PPVs

It is clear that historically, most of the scientific experiments, in order to disentangle the physics in PLEDs, have been performed on PPV derivatives, confirming that PPVs have been the work horse compound for the field. But, more importantly, the parameters found and used in the modeling, for PPVs, are now accurately known and undisputed. For example, the zero field mobility of MEH-PPV has been consistently reported by many groups to amount to 5×10^{-11} m^2/Vs for the past 16 years. [46-50] This certainty provides a solid basis for a sound and structural deeper investigation of the physics in PLEDs today using PPVs as prototypical material.

Scientific challenges

From the previous section it may seem that most of the physics in PLEDs is already well established, however this is merely appearance. Some key ingredients for a predictive PLED description are unfortunately still missing. For example, although thus far several unique models exist that attempt to describe the trapping behavior of the electrons in PLED materials [29], [30], [34], [51], the true description of the trap limited electron transport is hampered by the fact that it remains unclear what exactly the origin of this trapping behavior is. There is a strong lack of experiments that validate the amount and depth of electron traps in organic compounds as a whole. In fact, it has even not been satisfyingly proven if the trapping behavior originates from intrinsic properties caused by the synthesis or design of the chemical structures or if the behavior is universal resulting from the presence of extrinsic molecular as water or oxygen, or even a combination of both.

Due to the absence of a thorough understanding of the trapping behavior, the rol of the presence of electron traps on the recombination in PLEDs has never been considered. Very early work did suggest that the presence of trapped charges must have some influence, but this subject has been left unexplored. [52] Although a mechanism as trap-assisted recombination is a well-established process in inorganic (Si) electronics it has never been introduced in the organic device characterization. Moreover, modern day white emitting copolymer light emitting diodes most probably rely on principles as a trap-assisted recombination process due to the various energy levels introduced by the dyes into the polymer backbone. [53], [54] Remarkably, also here a description was never established.

Suppose a mechanism as trap-assisted recombination is present, the question of interest is then, is it an emissive or a non-emissive mechanism? Or can one have both? In inorganic electronics trap-assisted recombination is a non-radiative process. It is therefore not unreasonable to a priori assume that this will also be the case for organic electronics. And if so, this would then reveal a loss mechanism in PLEDs, never accounted for before. Interestingly however, it has also been mentioned previously that white emitting copolymer light emitting diodes most probably rely on a radiative version of trap-assisted recombination. In order to establish some clarity on this subject, research is needed.

Due to the presence of electron traps the electrons injected from the cathode diffuse less far into the polymer layer as compared to the holes. As a result of that, the place where they meet and recombine, the emission zone, is relatively

close to the metallic Ba/Al contact.[55], [56] In general metals have a quenching effect on excitons, which means that energy from the exciton is transferred to the metal non-radiatively. Hence, a loss process. When a clear knowledge of the trapping behavior is lacking also this loss mechanism in PLEDs can unfortunately not be well accounted for. Moreover, without any prior knowledge of the influence on the recombination process by the trapped electrons, it will be difficult to predict the magnitude of both these processes.

Scope of this thesis

Although significant progress has been made in understanding the physics of PLEDs, some key features are still missing. The main theme of this thesis is to investigate the influence of the presence of electron traps on the recombination mechanisms in PLEDs. First, the trapping behavior in PPVs is discussed. In order to gain more understanding of the trapping behavior of trapped electrons in PPVs, and validate a trap depth of 0.75 eV below the LUMO for PPVs, two optical probing techniques are presented in **Chapter 3**. Nicolai *et al*. showed that for the materials MDMO-PPV, MEH-PPV and NRS-PPV the trap depth as well as the trap number are remarkably similar and hinted at a common origin for the trapping behavior for these materials. In **Chapter 3** the trapping behavior of two types of MDMO-PPV is investigated. The two types of MDMO-PPV are basically identical except for the fact that one is synthesized through a dehydrohalogenation route, more famously known as the 'Glich' route, and the other is synthesized via the 'sulfinyl' route, which utilizes an asymmetric chloro-, sulfinyl- substituted monomer. The asymmetry in the 'sulfinyl' monomer leads to a higher regularity in the polymer chain due to less head-to-head or tail-to-tail additions during polymerization. Consequently, 'sulfinyl' MDMO-PPV constitutes fewer defects that may act as trap sites then regular 'Gilch" MDMO-PPV. Modeling of the electron only currents as well as the optical techniques Photothermal deflection spectroscopy (PDS) and photo-emission spectroscopy (IPE) confirm a trap depth of 0.75 eV for both PPV derivatives. Remarkably, electrical and optical measurements reveal no clear distinction between the trapping behavior for both polymers, which reinforces the suspicion of a common extrinsic origin for the trapping behavior.

Studies of recombination mechanisms in OLEDs usually involve using Monte Carlo simulations, no real systematic measurement method has been presented yet. Interestingly, investigating recombination mechanisms in solar cells is a bit more straight forward. In the operation of a solar cell under exposure of light, at the open circuit Voltage (V_{oc}) no current flows from the contacts, hence all excitons created by the incoming light recombine again. As a result, the dependence of the V_{oc} on the light intensity is a sensitive measure for the

recombination processes in a solar cell. In **Chapter 4** this technique is exploited using the established theory for trap free and trap-assisted recombination in organic solar cells by treating a PLED as an organic solar cell, and examining the V_{oc} response to the light intensity. It is found that apart from free carrier recombination, also trap-assisted recombination is observed in PPV PLEDs. The measured strength of this trap-assisted recombination perfectly fills the gap for the 'missing' recombination mechanism in the normal operation of a PLED. Additionally, the inclusion of non-radiative trap-assisted recombination perfectly describes both the *J-V* characteristics as well as the current efficiency. It follows from the calculation of the rates of both individual recombination mechanisms that the trap-assisted recombination is the dominant mechanism at low operating voltages. At low voltages most of the injected electrons immediately occupy a trap state after which they recombine with a free hole. The influence of this behavior on the current in the diffusion regime is discussed in **Chapter 5**. It is shown that ideality factor in the Shockley equation for the diffusion regime is determined by the presence of trap-assisted recombination. Additionally, it is demonstrated that the ideality factor for the photocurrent can be used to determine the origin of recombination for the red and blue peaks in the emission profile of a white organic light emitting polymer (WOLED). In doing so, **Chapter 5** conveys that the trap-assisted recombination process is not restricted to PPVs alone but applies to all materials containing traps. Additionally, it yields that the trap-assisted recombination mechanism is not restricted to a non-radiative characteristic alone. **Chapter 6** investigates the origin of the description of trap-assisted recombination by examining the influence of temperature variation on this process. The strength of the trap-assisted recombination process is thermally activated. In fact, the trap-assisted recombination in disordered organic semiconductors is demonstrated to be governed by the diffusion of the free carrier (hole) towards trapped carrier (electron), similar as to the free carrier, Langevin, recombination, except in this case the electron mobility is zero (trapped). Since it follows from **Chapter 6** that when knowing the carrier mobilities and the amount of traps, the entire recombination process can be predicted, without any additional parameters, the influence of trap-assisted on the current efficiency is reexamined in **Chapter 7**. Thin PLED devices (<100 nm) suffer from severe quenching from the cathode, accompanied by a significant contribution of non radiative trap-assisted recombination. However, thick devices (>100 nm) lose up to 45% of current efficiency by the presence of non-emissive recombination with trapped electrons. **Chapter 8** presents an analysis and comparison of the electron and hole transport and recombination mechanisms of the popular blue emitting compound poly(9,9-dioctylfluorene) (PFO) and PFO contaminated with ketone defects, a common chemical defect for this type of material. For the examination of the recombination processes,

the technique discussed in **Chapter 5** is used. It is demonstrated that ketones in PFO will lead to hole trapping and additional electron trapping on the ketone specie. Moreover, the additional green emission in the emission spectrum of ketone contaminated PFO is shown originate from trap-assisted recombination on the ketone moiety. Hence, **Chapter 8** serves as a practical example of the application of the knowledge and analysis methods resulting from the work presented in this thesis.

References:

[1] N. Mott, "On the transition to metallic conduction in semiconductors," *Canadian J. of Phys.*, vol. 34, no. 12, pp. 1356–1368 (1956).

[2] E. Conwell, "Impurity Band Conduction in Germanium and Silicon," *Phys. Rev.*, vol. 103, no. 1, pp. 51–61, (1956).

[3] A. Miller and E. Abrahams, "Impurity conduction at low concentrations," *Phys. Rev.*, vol. 120, no. 3, pp. 745–755, (1960).

[4] H. Bässler, "Charge transport in disordered organic photoconductors, a Monte Carlo simulation study," *Physica status solidi (b)*, vol. 175, no. 1, pp. 15–56 (1993).

[5] L. Schein, A. Peled, and D. Glatz, "The electric field dependence of the mobility in molecularly doped polymers," *J. Appl. Phys.*, vol. 66, no. 2, pp. 686–692 (1989).

[6] Y. N. Gartstein and E. Conwell, "High-field hopping mobility in molecular systems with spatially correlated energetic disorder," *Chem. Phys. Lett.*, vol. 245, no. 4, pp. 351–358 (1995).

[7] I. D. Parker, "Carrier tunneling and device characteristics in polymer light-emitting diodes," *J. Appl. Phys.*, vol. 75, no. 3, p. 1656 (1994).

[8] N. F. Mott and R. W. Gurney, "Electronic Processes in Ionic crystals," *Oxford University Press (*1948).

[9] D. M. Pai, "Transient Photoconductivity in Poly(N-vinylcarbazole)," *J. Chem. Phys*, vol. 52, no. 5, pp. 2285–2291 (1970).

[10] N. I. Craciun, J. Wildeman, and P. W. M. Blom, "Universal arrhenius temperature activated charge transport in diodes from disordered organic semiconductors," *Phys. Rev. Lett.*, vol. 100, no. 5, p. 056601 (2008).

[11] D. Monroe, "Hopping in Exponential Band Tails," *Phys. Rev. Lett.*, vol. 54, no. 2, pp. 146–149 (1985).

[12] M. C. J. M. Vissenberg and M. Matters, "Theory of the field-effect mobility in amorphous organic transistors," *Phys. Rev. B*, vol. 57, no. 20, pp. 12964–12967 (1998).

[13] C. Tanase, E. W. Meijer, P. W. M. Blom, and D. M. de Leeuw, "Unification of the hole transport in polymeric field-effect transistors and light-emitting diodes," *Phys. Rev. Lett.*, vol. 91, no. 21, p. 216601 (2003).

[14] H. Bässler, "Charge transport in disordered organic photoconductors a Monte Carlo simulation study," *Physica status solidi (b)*, vol. 175, no. 1, pp. 15–56 (1993).

[15] R. Coehoorn, W. F. Pasveer, P. A. Bobbert, and M. Michels, "Charge-carrier concentration dependence of the hopping mobility in organic materials with Gaussian disorder," *Phys. Rev. B*, vol. 72, no. 15, p. 155206 (2005).

[16] C. Tanase, P. W. M. Blom, D. M. de Leeuw, and E. J. Meijer, "Charge carrier density dependence of the hole mobility in poly(p-phenylene vinylene)," *Phys. stat. sol. (a)*, vol. 201, no. 6, pp. 1236–1245 (2004).

[17] N. I. Craciun, J. J. Brondijk, and P. W. M. Blom, "Diffusion-enhanced hole transport in thin polymer light-emitting diodes," *Phys. Rev. B*, vol. 77, no. 3, p. 035206, (2008).

[18] W. F. Pasveer, J. Cottaar, C. Tanase, R. Coehoorn, P. A. Bobbert, P. W. M. Blom, D. M. de Leeuw, and M. A. J. Michels, "Unified description of charge-carrier mobilities in disordered semiconducting polymers," *Phys. Rev. Lett.*, vol. 94, no. 20, p. 206601, (2005).

[19] S. L. M. van Mensfoort, S. I. Vulto, R. A. J. Janssen, and R. Coehoorn, "Hole transport in polyfluorene-based sandwich-type devices: Quantitative analysis of the role of energetic disorder," *Phys. Rev. B*, vol. 78, no. 8, p. 085208 (2008).

[20] I. I. Fishchuk, A. K. Kadashchuk, J. Genoe, M. Ullah, H. Sitter, T. B. Singh, N. S. Sariciftci, and H. Bässler, "Temperature dependence of the charge carrier mobility in disordered organic semiconductors at large carrier concentrations," *Phys. Rev. B*, vol. 81, no. 4, p. 045202 (2010).

[21] Z. Chen, M. J. Lee, R. Shahid Ashraf, Y. Gu, S. Albert-Seifried, M. Meedom Nielsen, B. Schroeder, T. D. Anthopoulos, M. Heeney, I. Mcculloch, and H. Sirringhaus, "High-Performance Ambipolar Diketopyrrolopyrrole-Thieno[3,2-b]thiophene Copolymer Field-Effect Transistors with Balanced Hole and Electron Mobilities," *Adv. Mater.*, vol. 24, no. 5, pp. 647–652 (2011).

[22] H. Yan, Z. Chen, Y. Zheng, C. Newman, J. R. Quinn, F. Dötz, M. Kastler, and A. Facchetti, "A high-mobility electron-transporting polymer for printed transistors," *Nature*, vol. 457, no. 7230, pp. 679–686 (2009).

[23] Y. Zhang, B. de Boer, and P. W. M. Blom, "Trap-free electron transport in poly(p -phenylene vinylene) by deactivation of traps with n -type doping," *Phys. Rev. B*, vol. 81, no. 8, p. 085201 (2010).

[24] L.-L. Chua, J. Zaumseil, J.-F. Chang, E. C. W. Ou, P. K. H. Ho, H. Sirringhaus, and R. H. Friend, "General observation of n-type field-effect behaviour in organic semiconductors," *Nature*, vol. 434, no. 7030, p. 194 (2005).

[25] N. I. Craciun, Y. Zhang, A. Palmaerts, H. T. Nicolai, M. Kuik, R. J. P. Kist, G. A. H. Wetzelaer, J. Wildeman, J. Vandenbergh, L. Lutsen, D. Vanderzande, and P. W. M. Blom, "Hysteresis-free electron currents in poly(p-phenylene vinylene) derivatives," *J. Appl. Phys.*, vol. 107, no. 12 (2010).

[26] P. E. Burrows and S. R. Forrest, "Electroluminescence from trap-limited current transport in vacuum deposited organic light emitting devices," *Appl. Phys. Lett.*, vol. 64, no. 17, p. 2285 (1994).

[27] P. Mark and W. Helfrich, "Space-Charge-Limited Currents in Organic Crystals," *J. Appl. Phys.*, vol. 33, no. 1, p. 205 (1962).

[28] M. M. Mandoc, B. de Boer, and P. W. M. Blom, "Electron-only diodes of poly(dialkoxy-p-phenylene vinylene) using hole-blocking bottom electrodes," *Phys. Rev. B*, vol. 73, no. 15, p. 155205 (2006).

[29] M. M. Mandoc, B. de Boer, G. Paasch, and P. W. M. Blom, "Trap-limited electron transport in disordered semiconducting polymers," *Phys. Rev. B*, vol. 75, no. 19, p. 193202 (2007).

[30] H. T. Nicolai, M. M. Mandoc, and P. W. M. Blom, "Electron traps in semiconducting polymers: Exponential versus Gaussian trap distribution," *Phys. Rev. B*, vol. 83, no. 19 (2011).

[31] K. C. Kao, and W. Hwang, "Studies of the theory of single and double injections in solids with a Gaussian trap distribution," *Solid State Electron.*, vol. 19, pp. 1045–1047 (1976).

[32] S. Nešpůrek and P. Smejtek, "Space-charge limited currents in insulators with the Gaussian distribution of traps," *Czechoslovak J. of Phys.*, vol. 22, no. 2, pp. 160–175 (1972).

[33] G. Paasch and S. Scheinert, "Charge carrier density of organics with Gaussian density of states: Analytical approximation for the Gauss–Fermi integral," *J. Appl. Phys.*, vol. 107, no. 10, p. 104501 (2010).

[34] S. L. M. van Mensfoort, J. Billen, S. I. Vulto, R. Janssen, and R. Coehoorn, "Electron transport in polyfluorene-based sandwich-type devices: Quantitative analysis of the effects of disorder and electron traps," *Phys. Rev. B*, vol. 80, no. 3 (2009).

[35] P. Yang, E. R. Batista, S. Tretiak, A. Saxena, R. L. Martin, and D. L. Smith, "Effect of intramolecular disorder and intermolecular electronic interactions on the electronic structure of poly- p -phenylene vinylene," *Phys. Rev. B*, vol. 76, no. 24 (2007).

[36] W. Graupner, G. Leditzky, G. Leising, and U. Scherf, "Shallow and deep traps in conjugated polymers of high intrachain order," *Phys. Rev. B*, vol. 54, no. 11, pp. 7610–7613 (1996).

[37] M. Meier, S. Karg, K. Zuleeg, W. Brütting, and M. Schwoerer, "Determination of trapping parameters in poly(p-phenylenevinylene)

light-emitting devices using thermally stimulated currents," *J. Appl. Phys.*, vol. 84, no. 1, p. 87 (1998).
[38] J. G. Simmons and G. W. Taylor, "High-Field Isothermal Currents and Thermally Stimulated Currents in Insulators Having Discrete Trapping Levels," *Phys. Rev. B*, vol. 5, no. 4, pp. 1619–1629 (1972).
[39] D. V. Lang, "Deep-level transient spectroscopy: A new method to characterize traps in semiconductors," *J. Appl. Phys.*, vol. 45, no. 7, p. 3023 (1974).
[40] G. Kavaliauskiene, V. Kazukauskas, V. Rinkevicius, J. Storasta, J. V. Vaitkus, R. Bates, V. O'Shea, and K. M. Smith, "Thermally stimulated currents in semi-insulating GaAs Schottky diodes and their simulation," *Appl. Phys. A*, vol. 69, no. 4, pp. 415–420 (1999).
[41] P. W. M. Blom, M. J. M. de Jong, and S. Breedijk, "Temperature dependent electron-hole recombination in polymer light-emitting diodes," *Appl. Phys. Lett.*, vol. 71, no. 7, pp. 930–932 (1997).
[42] P. Langevin, "Recombinaison et Mobilités des Ions dans les Gaz," *Ann. Chim. Phys*, vol. 28, pp. 433–530 (1903).
[43] C. Groves and N. C. Greenham, "Bimolecular recombination in polymer electronic devices," *Phys. Rev. B*, vol. 78, no. 15, p. 155205 (2008).
[44] J. J. M. van der Holst, F. W. A. van Oost, R. Coehoorn, and P. A. Bobbert, "Electron-hole recombination in disordered organic semiconductors: Validity of the Langevin formula," *Phys. Rev. B*, vol. 80, no. 23, p. 235202 (2009).
[45] S. L. M. van Mensfoort, J. Billen, M. Carvelli, S. I. E. Vulto, R. A. J. Janssen, and R. Coehoorn, "Predictive modeling of the current density and radiative recombination in blue polymer-based light-emitting diodes," *J. of Appl. Phys*, vol. 109, no. 064502 (2011).
[46] P. W. M. Blom, M. J. M. de Jong, and J. J. M. Vleggaar, "Electron and hole transport in poly(p-phenylene vinylene) devices," *Appl. Phys. Lett.*, vol. 68, no. 23, pp. 3308–3310 (1996).
[47] R. H. Friend, R. W. Gymer, A. B. Holmes, J. H. Burroughes, R. N. Marks, C. Taliani, D. D. C. Bradley, D. A. Dos Santos, J. L. Bredas, M. Lögdlun, and W. R. Salaneck, "Electroluminescence in conjugated polymers," *Nature*, vol. 397, no. 6715, pp. 121–128 (1999).
[48] I. H. Campbell, D. L. Smith, C. J. Neef, and J. P. Ferraris, "Consistent time-of-flight mobility measurements and polymer light-emitting diode current–voltage characteristics," *Appl. Phys. Lett.*, vol. 74, no. 19, p. 2809 (1999).
[49] C. Tanase, J. Wildeman, and P. W. M. Blom, "Luminescent Poly(p-phenylenevinylene) Hole-Transport Layers with Adjustable Solubility," *Adv. Funct. Mater.*, vol. 15, no. 12, pp. 2011–2015 (2005).

[50] L. Bozano, S. A. Carter, J. C. Scott, G. G. Malliaras, and P. J. Brock, "Temperature- and field-dependent electron and hole mobilities in polymer light-emitting diodes," *Appl. Phys. Lett.*, vol. 74, no. 8, p. 1132, (1999).

[51] J. M. Montero, J. Bisquert, G. Garcia-Belmonte, E. M. Barea, and H. J. Bolink, "Trap-limited mobility in space-charge limited current in organic layers," *Organic Electronics*, vol. 10, no. 2, pp. 305–312 (2009).

[52] P. E. Burrows, Z. Shen, V. Bulovic, D. M. McCarty, S. R. Forrest, J. A. Cronin, and M. E. Thompson, "Relationship between electroluminescence and current transport in organic heterojunction light-emitting devices," *J. Appl. Phys.*, vol. 79, no. 10, pp. 7991–8006 (1996).

[53] Q. J. Sun, B. H. Fan, Z. A. Tan, C. H. Yang, Y. F. Li, and Y. Yang, "White light from polymer light-emitting diodes: Utilization of fluorenone defects and exciplex," *Appl. Phys. Lett.*, vol. 88, no. 16, p. 163510 (2006).

[54] B. Zhang, C. Qin, J. Ding, L. Chen, Z. Xie, Y. Cheng, and L. Wang, "High–Performance All–Polymer White–Light–Emitting Diodes Using Polyfluorene Containing Phosphonate Groups as an Efficient Electron–Injection Layer," *Adv. Funct. Mater.*, vol. 20, no. 17, pp. 2951–2957 (2010).

[55] G. Vaubel, "Reaction of singlet excitons at an anthracene/metal interface: Energy transfer," *Chem Phys Lett*, vol. 10, no. 3, pp. 334–336 (1971).

[56] G. Cnossen, K. E. Drabe, and D. A. Wiersma, "Fluorescence properties of submonolayers of rhodamine 6G in front of a mirror," *J. Chem. Phys*, vol. 98, no. 7, p. 5276 (1993).

Chapter 3

Optical detection of deep electron traps in PPV light-emitting diodes

The trap-limited electron currents in poly(p-phenylene vinylene) (PPV) derivatives can be modeled using a Gaussian trap distribution that is positioned approximately 0.75 eV below the lowest unoccupied molecular orbital (LUMO) of PPV. Photothermal deflection spectroscopy (PDS) measurements and internal photo-emission spectroscopy (IPE) measurements confirm the claim of a Gaussian shaped trap distribution centered at 0.75 eV below the LUMO of PPV. Additionally, two PPV derivatives that differ in the number of conformational defects incorporated during synthesis exhibit identical electron trapping behavior, showing that the traps do not originate from extrinsic impurities of the synthesis or defects in the polymer chains.

This work has been published as: M. Kuik, J. Vandenbergh, L. Goris, E. J. Begemann, L. Lutsen, D. J. M. Vanderzande, J. V. Manca & P. W. M. Blom, *Applied Physics Letter* **99**, 183305 (2011)

Introduction

In order to increase the efficiency of polymer light-emitting diodes (PLEDs), a fundamental understanding of the charge transport is vital. Investigation of the charge transport in PLEDs of PPV derivatives has led to the insight that charge transport is dominated by space-charge-limited hole current, [1] whereas the electron transport is trap limited.[2] [3]As a consequence, the electrons drift less far into the PLED as compared to the holes. A major disadvantage of the presence of electron traps in the carrier transport is that the recombination process as well as the recombination zone is consequently heavily perturbed. Due to the reduced electron transport, a large amount of excitons is formed close to the cathode, resulting in an energy transfer to the metallic cathode followed by non-radiative decay.[4] This effect leads to a loss of light-output efficiency, especially at low voltages. Therefore, knowledge about the presence and position of trap levels in PLED materials is of vital importance for optimizing the luminous efficiency.

Stated an described before in **Chapter 2**, the trap-limited electron current (TLC) in organic semiconductors has been generally described as free electron transport in the LUMO in the presence of an exponential distribution of electron traps inside the band gap.[3] This exponential distribution of traps leads to a strong voltage and layer-thickness dependence of the *J–V* characteristics, as derived by Mark and Helfrich.[5] However, a drawback of this model is that the actual trap depth as well as the total amount of traps cannot be determined independently. Recently, it has been demonstrated by Nicolai *et al.* that the TLC in PPVs can be equally well described when a, more intuitive, Gaussian trap distribution is assumed (**Chapter 2**).[6] In this work, it is suggested that various PPVs share a common trap origin and a trap depth of about 0.7 to 0.8eV below the LUMO is deduced, as schematically depicted in **Figure 1**.

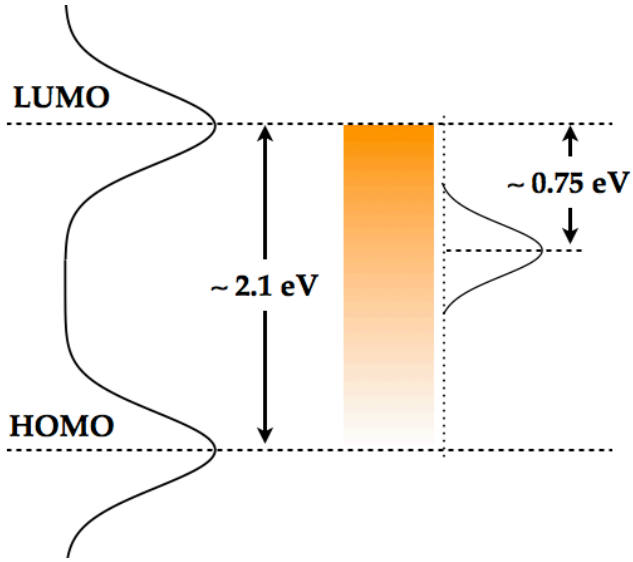

Figure 1. *Schematic representation of the energy levels in MDMO-PPV*

For the validation of this model we investigate the trapping behavior of MDMO-PPV. A common synthetic approach used to obtain MDMO-PPV is a dehydrohalogenation route, also called 'Gilch' route, which uses a dichloro-substituted monomer.[7], [8] An alternative synthesis procedure is the 'sulfinyl' route, which utilizes an asymmetric chloro-, sulfinyl-substituted monomer.[9], [10] The asymmetry in the sulfinyl monomer leads to a higher regularity in the polymer due to less head-to-head or tail-to-tail additions during polymerization. Consequently, 'sulfinyl' MDMO-PPV constitutes fewer defects that may act as trap sites than regular 'Gilch' MDMO-PPV.

Electron transport in 'Gilch' MDMO-PPV and 'sulfinyl' MDMO-PPV

To investigate their electron transport, electron-only devices were fabricated as described in **Chapter 2**; consisting of the structure glass/Al/MDMO-PPV/Ba/Al.[11], [12] These crossbar structured devices were fabricated in a cleanroom environment and kept in nitrogen from the moment the bottom contact of 30nm Al was thermally deposited in vacuum. The polymer layer was consequently spin-coated from toluene after which the structure was topped with a thermally evaporated 5nm Ba and 100nm Al, again in vacuum. The current density measurements were performed in a nitrogen atmosphere as well.

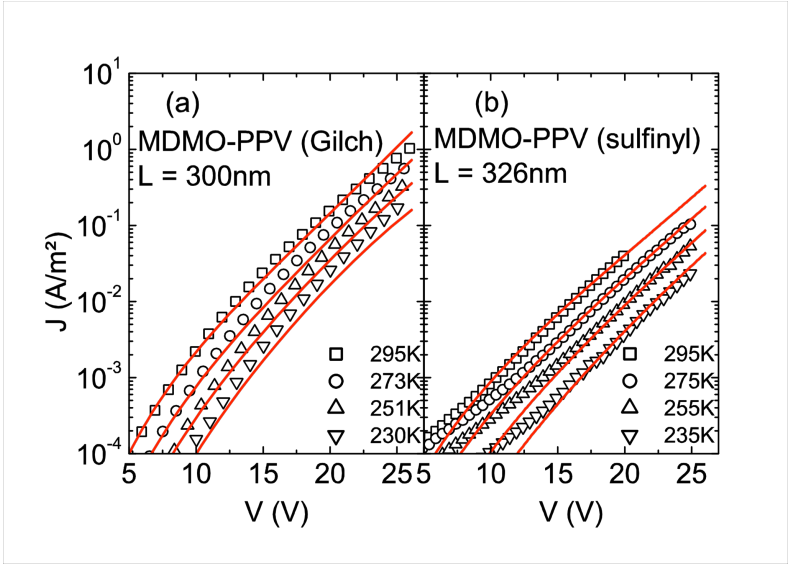

Figure 2. *Experimental (open symbols) and calculated (solid lines) J–V characteristics of a (**a**) 300 nm MDMO-PPV (Gilch) and a (**b**) 326 nm MDMO-PPV (sulfinyl) electron-only device at different temperatures.*

Figure 2(a) depicts the trap-limited electron current at different temperatures for a 300nm 'Gilch' MDMO-PPV layer. Since typically trap-limited transport exhibits hysteresis all the temperature scans have been performed on fresh devices. For the analysis of the trap depth, a benchmarked numerical device model is used [13]that incorporates drift and diffusion of charge carriers, the effect of space charge on the electric field and a density-dependent mobility. [14] The trapping description used in this model is characterized by a Gaussian trap distribution as implemented by Nicolai *et al.* [6]and Paasch *et al.* [15]Identical to an earlier report, the parameters for the Gaussian trap distribution amount to $N_t = 1.3\times10^{23}$ m^{-3}, $\sigma_t = 0.1$ eV and a trap depth of 0.71 eV below the LUMO. For comparison, **Figure 2(b)** illustrates the *J–V* characteristics of a 326nm 'sulfinyl' MDMO-PPV layer. Modeling in this case leads to equal parameters as for the 'Gilch' variant being, $N_t = 1.3\times10^{23}$ m^{-3}, $\sigma_t =$ 0.1 eV, where only the trap level is lowered slightly to 0.74 eV in order to obtain a better fit. The higher regularity in the polymer chain of 'sulfinyl' MDMO-PPV leads to less process-ability of the solution.[9] Therefore the deviation of the fit at lower voltages is caused by parasitical currents in the device and not by the bulk properties of the transport layer. Summarizing, modeling on the electron current demonstrates that the trapping behavior for both materials is exactly the same.

Photothermal deflection spectroscopy (PDS)

Having established again that the trap depth needed to describe the TLC in PPVs is about 0.75 eV below the center of the (LUMO) DOS, we would like to confirm this value via direct measurements. A very sensitive technique for measuring non-radiative decay in thin films is PDS. In this technique the absorption of light of a certain sub-gap wavelength can invoke local non-radiative decay that produces local heating. When the sample is immersed in a liquid characterized by small changes in temperature and large changes in refraction index the probe beam parallel to the surface of the sample (HeNe laser) is able to detect very subtle changes in α(E), the optical absorption coefficient. The samples were prepared by drop casting the MDMO-PPV solution onto Conring 7056 quartz substrates (6×12mm) in nitrogen atmosphere. A detailed description for this method is described elsewhere.[16] All spectra are set on an absolute absorption coefficient scale by measuring separately the transmission/reflection of the PDS-films.

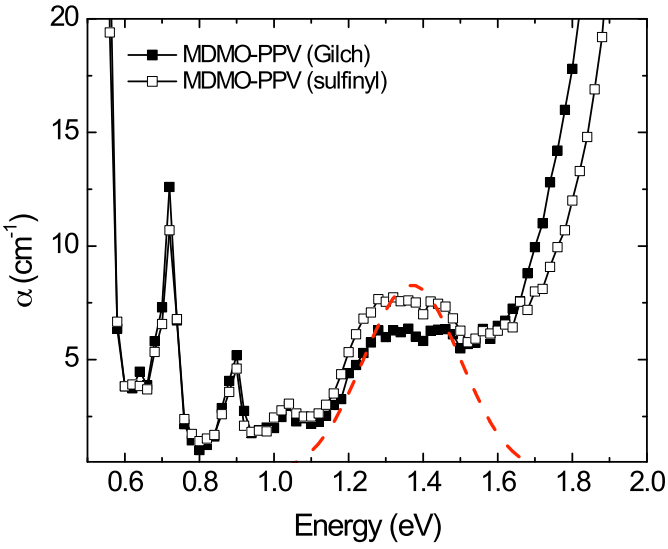

Figure 3. *PDS spectra of 'Gilch' and 'sulfinyl' MDMO-PPV. The dashed curve serves as a guide to the eye for the position of the Gaussian trap distribution at about 0.75 eV below the LUMO for both synthesis routes.*

Figure 3 shows the PDS results for both materials. Below 1.1 eV, multi-phonon absorptions are visible due to vibrational overtones of C-H stretching and bending vibrations.[17], [18] At 1.35 eV, a clear broad peak is discernible after which an incline, due to transitions originating from the tail of the DOS, is observed. It should be noted that optical excitation is a relative measurement, since it also involves the exciton binding energy. An electron is excited from the Highest Occupied Molecular Orbital (HOMO) into a higher energy state. In our measurements, the HOMO-LUMO transition clearly starts to show up for excitation energies that exceed 2 eV. To correct for exciton binding energy effects, the position of the broad peak at 1.35 eV inside the band-gap should be taken relative to the onset of the HOMO-LUMO absorption peak, located at ~2.1 eV (**Figure 1**). As a result, the sub-band-gap absorption at 1.35 eV corresponds with the presence of a Gaussian trap at about 0.75 eV below the LUMO. Also apparent from **Figure 3** is that the position of the trap for both 'Gilch' and 'sulfinyl' MDMO-PPV is at exactly the same energy level, which in turn agrees with the modeling of the *J–V* characteristics. As an alternative to the PDS measurements, another type of optical probe technique is presented.

Internal photo-emission spectroscopy (IPE)

IPE is a common and useful tool to investigate energy level differences, e.g. barrier heights at a metal/semiconductor interface.[19] In general this technique comprises the probing of an induced photocurrent caused by the excitation of charge carriers. Samples were prepared analogue to the fabrication of the electron-only devices, only in this case pre-patterned glass/ ITO substrates were used and the devices were topped with thermally evaporated Ca and Al. **Figure 4** depicts the IPE measurement on the resulting glass/ITO/'Gilch' MDMO-PPV/Ca/Al structure comprising a 700nm polymer layer where the device is irradiated from the ITO side. Since ITO and Ca are known to form ohmic contacts with MDMO-PPV, we can exclude any contribution to the IPE measurements from contact barriers, only transitions inside the band gap of the material will be probed. The samples were irradiated by a Xenon lamp through a series of filters in order to obtain monochromatic light. Since the photocurrent can be very small a lock-in amplifier is used to detect the resulting signal at a chop frequency of 40Hz.

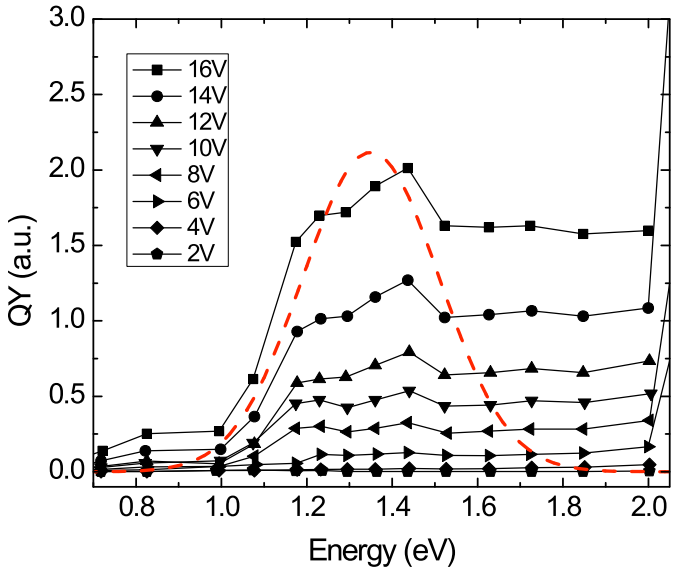

Figure 4. *IPE spectra for a 700 nm 'Gilch' MDMO-PVV device at different driving voltages. The dashed curve serves as a guide to the eye for the position of the Gaussian trap distribution, again at about 0.75 eV below the LUMO.*

A discernible signal onset is centered around 1.35 eV in **Figure 4** This peak is exactly at the same position as the peak in the PDS measurements. In the IPE measurement, this again corresponds to the fact that electrons from the HOMO are excited into an empty trap level that is located about 0.75 eV below the onset of the HOMO-LUMO absorption. In doing so, the electron transport driven by the applied electric field is improved since the fermi level in the device increases due to additional filling up of empty traps. Furthermore, at higher voltages, the chance for electrons to escape from a trap and contribute to a photocurrent increases due to local barrier lowering and tunneling. Above 1.6 eV the signal stays relatively high due to excitation from the HOMO into the tail of the LUMO DOS. To summarize, also this measurement technique demonstrates the position of the onset to agree well with the calculations of a Gaussian trap at about 0.75 eV below the LUMO.

Conclusion

In conclusion, we have verified the presence of deep electron traps in MDMO-PPV by two different types of optical measurements. Both PDS and IPE confirm the trap position of 0.75 eV below the LUMO that was derived from

electrical modeling of the electron transport. Furthermore, we have compared the trap-limited electron current of common 'Gilch' MDMO-PPV to that of 'sulfinyl' MDMO-PPV. Although the 'sulfinyl' variant constitutes a higher regularity in the polymer chain, and therefore possibly less trap sites, no difference in trapping behavior was observed. These results strongly suggest that conformational defects induced in the synthesis are not responsible for the electron trapping in MDMO-PPV and that PPVs share a common physical origin for the trap-limited electron current.

References

[1] P. W. M. Blom, M. J. M. de Jong, and J. J. M. Vleggaar, "Electron and hole transport in poly(p-phenylene vinylene) devices," *Appl. Phys. Lett.*, vol. 68, no. 23, pp. 3308–3310 (1996).

[2] H. Antoniadis, M. A. Abkowitz, and B. R. Hsieh, "Carrier deep-trapping mobility-lifetime products in poly(p-phenylene vinylene)," *Appl. Phys. Lett.*, vol. 65, no. 16, pp. 2030–2032 (1994).

[3] M. M. Mandoc, B. de Boer, G. Paasch, and P. W. M. Blom, "Trap-limited electron transport in disordered semiconducting polymers," *Phys. Rev. B*, vol. 75, no. 19, p. 193202 (2007).

[4] D. E. Markov and P. W. M. Blom, "Migration-assisted energy transfer at conjugated polymer/metal interfaces," *Phys. Rev. B*, vol. 72, no. 16, p. 161401 (2005).

[5] P. Mark and W. Helfrich, "Space-Charge-Limited Currents in Organic Crystals," *J. Appl. Phys.*, vol. 33, no. 1, p. 205 (1962).

[6] H. T. Nicolai, M. M. Mandoc, and P. W. M. Blom, "Electron traps in semiconducting polymers: Exponential versus Gaussian trap distribution," *Phys. Rev. B*, vol. 83, no. 19 (2011).

[7] H. Spreitzer, H. Becker, E. Kluge, W. Kreuder, H. Schenk, R. Demandt, and H. Schoo, "Soluble Phenyl–Substituted PPVs—New Materials for Highly Efficient Polymer LEDs," *Adv. Mater.*, 10, no. 16 (1998).

[8] H. G. Gilch and W. L. Wheelwright, "Polymerization of α-halogenated p-xylenes with base ," *J. Polym. Sci., Part A: Polym. Chem.* (1966).

[9] F. Louwet, D. Vanderzande, J. Gelan, and J. Mullens, "A New Synthetic Route to a Soluble High Molecular Weight Precursor for Poly(p-phenylenevinylene) derivatives," *Macromolecules*, vol. 28, no. 4, pp. 1330–1331 (1995).

[10] T. Munters, T. Martens, L. Goris, V. Vrindts, J. V. Manca, L. Lutsen, W. de Ceuninck, D. Vanderzande, L. de Schepper, J. Gelan, N. S. Sariciftci, and C. J. Brabec, "A comparison between state-of-the-art 'gilch' and 'sulphinyl' synthesised MDMO-PPV/PCBM bulk hetero-junction solar cells," *Thin Solid Films*, vol. 403, pp. 247–251 (2002).

[11] M. M. Mandoc, B. de Boer, and P. W. M. Blom, "Electron-only diodes of poly(dialkoxy-p-phenylene vinylene) using hole-blocking bottom electrodes," *Phys. Rev. B*, vol. 73, no. 15, p. 155205 (2006).
[12] R. Steyrleuthner, S. Bange, and D. Neher, "Reliable electron-only devices and electron transport in n-type polymers," *J. Appl. Phys.*, vol. 105, no. 6, p. 064509 (2009).
[13] L. J. A. Koster, E. C. P. Smits, V. D. Mihailetchi, and P. W. M. Blom, "Device model for the operation of polymer/fullerene bulk heterojunction solar cells," *Phys. Rev. B*, vol. 72, no. 8, p. 085205 (2005).
[14] C. Tanase, P. W. M. Blom, D. M. de Leeuw, and E. J. Meijer, "Charge carrier density dependence of the hole mobility in poly(p-phenylene vinylene)," *Phys. stat. sol. (a)*, vol. 201, no. 6, pp. 1236–1245 (2004).
[15] G. Paasch and S. Scheinert, "Charge carrier density of organics with Gaussian density of states: Analytical approximation for the Gauss–Fermi integral," *J. Appl. Phys.*, vol. 107, no. 10, p. 104501 (2010).
[16] L. Goris, K. Haenen, M. Nesládek, P. Wagner, D. Vanderzande, L. Schepper, J. D'haen, L. Lutsen, and J. V. Manca, "Absorption phenomena in organic thin films for solar cell applications investigated by photothermal deflection spectroscopy," *J Mater Sci*, vol. 40, no. 6, pp. 1413–1418 (2005).
[17] T. Fujii and L. Pan, "Subgap Absorption Spectra in Polysilane Films.," *Jpn. J. Appl. Phys.* (2000).
[18] C. H. Seager, M. Sinclair, D. McBranch, A. J. Heeger, and G. L. Baker, "Photothermal deflection spectroscopy of conjugated polymers," *Synthetic Met*, no. 49-50, pp. 91-97 (1992).
[19] R. H. Fowler, "The Analysis of Photoelectric Sensitivity Curves for Clean Metals at Various Temperatures," *Phys Rev*, vol. 38, no. 1, pp. 45–56 (1931).

Chapter 4

Determination of the trap-assisted recombination strength in polymer light emitting diodes

The recombination processes in PPV based PLEDs are investigated. Photogenerated current measurements on PLED device structures reveal that next to the known Langevin recombination also trap-assisted recombination is an important recombination channel in PLEDs. The dependence of the open-circuit voltage on light intensity enables us to determine the strength of this process. Numerical modeling of the current-voltage characteristics incorporating both Langevin and trap-assisted recombination yields a correct and consistent description of the PLED, without the traditional correction of the Langevin pre-factor. At low bias voltage the trap-assisted recombination rate is found to be dominant over the free carrier recombination rate.

This work has been published as: M. Kuik, H. T. Nicolai, M. Lenes, G. A. H. Wetzelaer, M. Lu & P. W. M. Blom, *Applied Physics Letter* **98**, 093301 (2011)

Introduction

It is widely accepted that the recombination mechanism in PLEDs is bimolecular of the Langevin type, i.e. free electrons recombining with free holes. [1-3] To what extent the trapped electrons also contribute to the recombination in a PLED is an open question (**Figure 1**). Earlier research has already given some indications that this contribution might be considerable.[4], [5] Modeling done on PPV-based PLEDs has shown that using only Langevin recombination is not entirely sufficient to correctly describe the current-voltage behavior of such a PLED. In order to fit the *J–V* curves the strength of the Langevin recombination needs to be enhanced typically by a factor of 3 or 4. [4], [5] This suggests that only taking into account Langevin recombination of free charge carriers is not sufficient and that trap-assisted recombination might play a significant role.

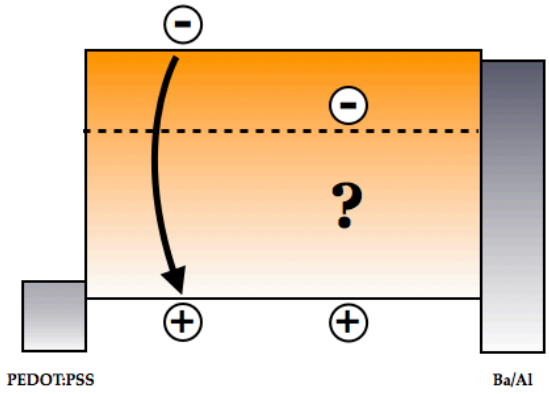

Figure 1. *Schematic representation of the free carrier Langevin-type recombination and the open questions of the presence of trapped electrons.*

An additional recombination channel will increase the recombination strength which will lead to lower device currents. This dependence seems somewhat counter intuitive but can be understood in the following way. When recombination would be absent in the device, the electrons would cross all the way over to the anode and the holes would cross all the way to the cathode. For every injected electron the device will allow an injected hole on the other side, similar to the workings of a capacitor. This process will lead to large currents since in this process, a lot of charge carriers are allowed in the material. However, the recombination process in a PLED is efficient. Virtually none of the electrons reach the anode and none of the holes reach the cathode. Hence, the presence of the recombination process will allow less charges in the

device, thus lowering the device current. Therefore, an increase in the recombination strength will lower the device current.

Recombination mechanisms in an organic solar cell

A similar observation was made in organic solar cells in which trap-limited electron transport is present. At the open circuit voltage (V_{OC}) there is no current extraction and virtually all photogenerated excitons recombine (**Figure 2**). As a result the dependence of the V_{OC} on the light intensity is a sensitive measure for the recombination mechanisms in solar cells.[6-9]

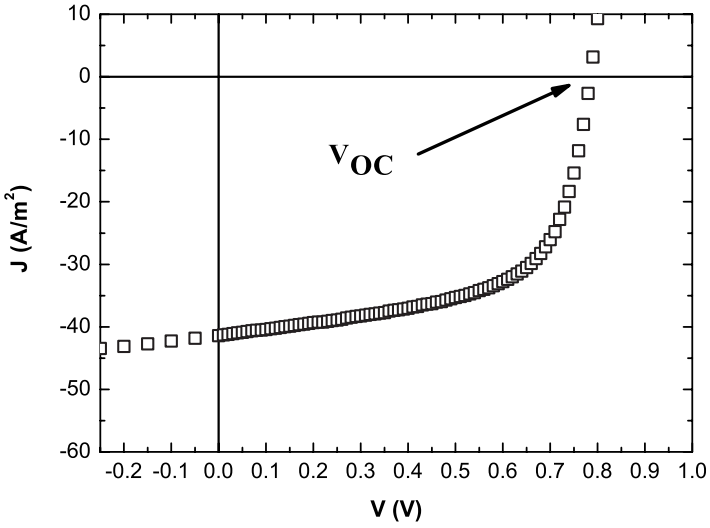

Figure 2. *The current voltage characteristics of a prototypical MDMO-PPV:PCBM solar cell under illumination of standard 1000 W/m² and AM1.5.*

The response of the V_{OC} on the light intensity in trap-free solar cells is given by[10]

$$V_{OC} = \frac{E_{gap}}{q} - \frac{kT}{q} ln\left(\frac{(1-P)\,BN_{cv}^2}{PG}\right) \tag{27}$$

where P is the dissociation probability of bound electron-hole pairs, E_{gap} is the effective energy gap, N_{cv} is the effective density of states B is the recombination strength and G is the generation rate of electron-hole pairs. The generation rate

G is proportional to the light intensity in this equation, directly connecting the V_{OC} to the light intensity. Furthermore, for the bimolecular recombination strength the traditional Langevin relation **Eq. (18)** is used.[11] **Eq. (19)** predicts that the slope of V_{OC} versus the logarithm of the light intensity is equal to the thermal voltage *kT/q*. It has been demonstrated that this relation holds for solar cells in which both the electron- and hole transport are trap-free, which is the case in most polymer:fullerene bulk heterojunction solar cells. [10] However, if one of the carriers exhibits trap-limited transport, the slope exceeds *kT/q*. This increase of the dependence of V_{OC} on light intensity can be explained by considering trap-assisted recombination. [6-9]

The description for the trap-assisted recombination strength is given by the Shockley-Read-Hall (SRH) equation [12], [13]

$$B_{SRH} = \frac{C_n C_p N_t}{[C_n (n + n_1) + C_p (p + p_1)]} \tag{28}$$

where C_n and C_p are the capture coefficients for electrons and holes, respectively, N_t is the density of electron traps, *n* and *p* are the electron density in the conduction band and the hole density in the valence band, respectively, and their product under equilibrium conditions,

$$p_1 n_1 = N_{cv} e^{\frac{-E_{gap}}{k_B}} = n_i^2 \tag{29}$$

where n_i is the intrinsic carrier concentration in the sample. In the solar cell model the strength of the SRH recombination is added to the Langevin recombination strength resulting in the continuity equations

$$\frac{1}{q}\frac{\partial}{\partial x} J_n = -\frac{1}{q}\frac{\partial}{\partial x} J_p = B\left(np - n_i^2\right) = \left(B_L + B_{SRH}\right)\left(np - n_i^2\right) = R \tag{30}$$

,where J_n is the electron current, J_p the hole current and *R* denotes the total recombination rate.

Addition of SRH recombination into the solar cell model then explains the experimentally observed increase of the V_{OC} dependence on light intensity, as shown by Mandoc *et al*. [6], [7] The fact that the increase in the V_{OC} dependency on the light intensity indeed originates from traps was further confirmed by deliberately adding traps to the trap free MDMO:PPV-PCBM

system. [6] In this study we investigate the photovoltaic response of standard PEDOT:PSS/(pristine)PPV/Ba/Al PLED structures and specifically examine the dependence of the V_{OC} on the light intensity. It should be noted that all the PPV derivatives used here exhibit a strongly trap-limited electron transport, hence a deviation of kT/q is expected.[14]

Recombination mechanisms in a PLED

A first glance at the light intensity dependence of the V_{OC} for some well-known PPV derivatives (**Figure 3**) reveals that for all these materials the slope is considerably higher than kT/q, thus indicating the presence of trap-assisted recombination. For the polymer SY-PPV, NRS-PPV and MEH-PPV the slopes are 2.1, 1.7 and 1.7 times the thermal voltage, respectively.

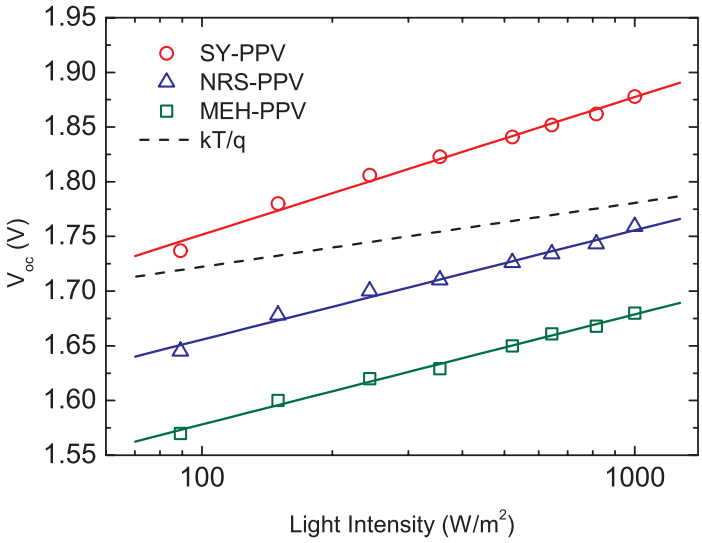

Figure 3. *Light intensity dependence of the V_{OC} at room temperature for SY-PPV (120nm), NRS-PPV (98nm) and MEH-PPV (138nm). The kT/q slope is added as a reference.*

Having established that the trap-assisted mechanism is present in these PPVs it is of importance to know how relevant this mechanism is. Since MEH-PPV is the most thoroughly benchmarked [15] and electrically parameterized[14] polymer of this set, this material will be used for further investigation. A numerical device model [16], in which drift and diffusion of charge carriers, the effect of space-charge on the electric field, density dependent mobility [17], Langevin type recombination [11], exponential trap distribution for the electrons [14] and a field and temperature dependent generation rates of free

charge carriers [16] is included, is used to obtain the segmented line in **Figure 4**.

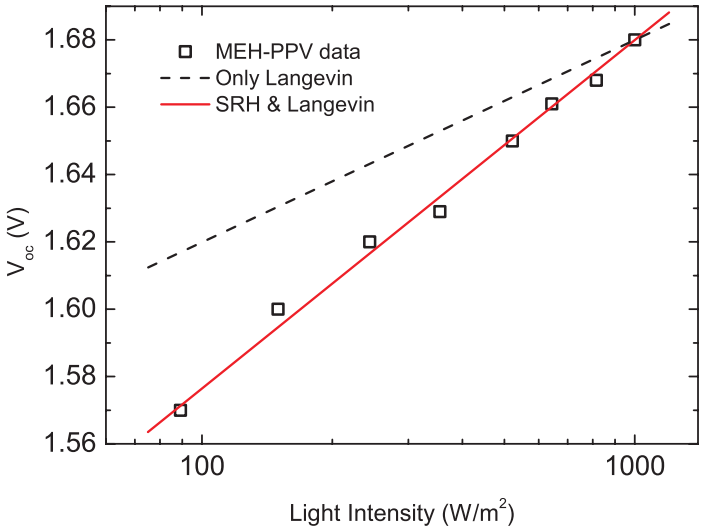

***Figure 4**. Light intensity dependence of the V_{OC} for MEH-PPV. The experimental data (symbols) is fitted (solid line) using an SRH recombination mechanism in addition to the conventional Langevin recombination (dashed line), which has a slope of kT/q.*

One can clearly observe that the strength of the free carrier recombination alone, yielding a *kT/q* slope, is not enough to explain the data correctly. We introduce also for the PLED case the SRH mechanism of recombination with trapped electrons according to **Eq. (20)** and **Eq. (22)**. Using 9.0×10^{-19} m^3/s for the electron and hole capture coefficients, the light intensity dependence for the V_{OC} for the MEH-PPV device is perfectly described. This value for the capture coefficient is nearly equal to the value of 1.4×10^{-18} m^3/s for the case of the polymer:polymer bulk heterojunction solar cell in which also trap-limited electron transport in the acceptor PPV polymer is the limiting factor for the performance of this type of solar cell.[7]

Influence of the trap-assisted recombination strength in the PLED operation

Having determined the strength of the trap-assisted recombination through the V_{OC} light intensity measurement, it is of interest to find out whether the addition and the strength of this mechanism proves to be significant for the operation of a PLED. As observed in previous studies and again apparent in

Figure 5, for PPV PLEDs Langevin recombination alone is not sufficient to describe the *J-V* characteristics.

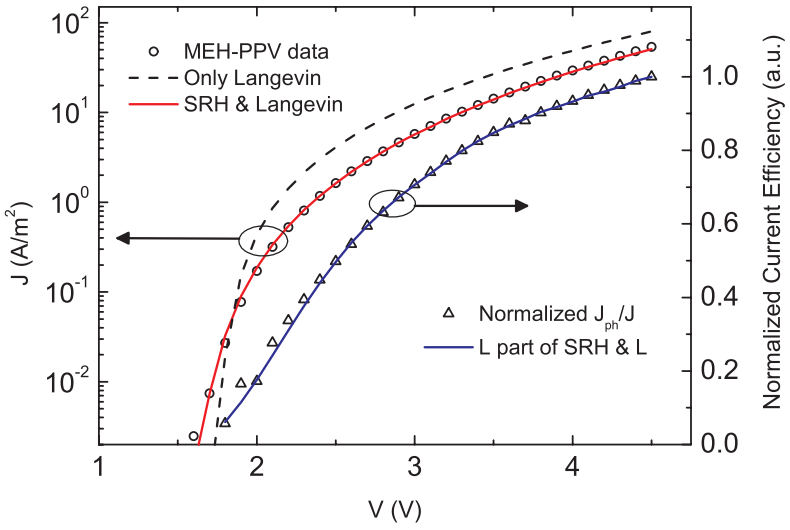

Figure 5. *J-V characteristics of a 165 nm MEH-PPV PLED and the corresponding fit at 295 K. The dashed line represents the simulation of the current when only Langevin recombination is taken into account. The normalized CE data and fit are plotted to the right axis.*

In order to fit the *J-V* characteristics it was needed to increase the Langevin recombination strength by typically a factor 3-4, as mentioned earlier. However, our results, as shown in **Figure 5**, demonstrate that the simulation that does include the trap-assisted recombination, using C_n=C_p=9.0×10^{-19} m^3/s as obtained from the V_{OC} measurements, excellently describes the experimental data, without any correction on the Langevin recombination strength. Moreover, the normalized current efficiency (CE; light output/current) plotted in the same figure on a sensitive double linear scale, taking into account a quenching distance of 8.5 nm from the cathode, is also well described. For the calculation of the CE only free carrier (Langevin) recombination is considered emissive, the trap-assisted recombination is assumed to be non-radiative (**Figure 6**). The electron traps in MEH-PPV are known to be around 0.75 eV in the bandgap (**Chapter 3**), so that radiative recombination of holes with trapped electrons would lead to emission in the near-infrared, which is not observed. [18]

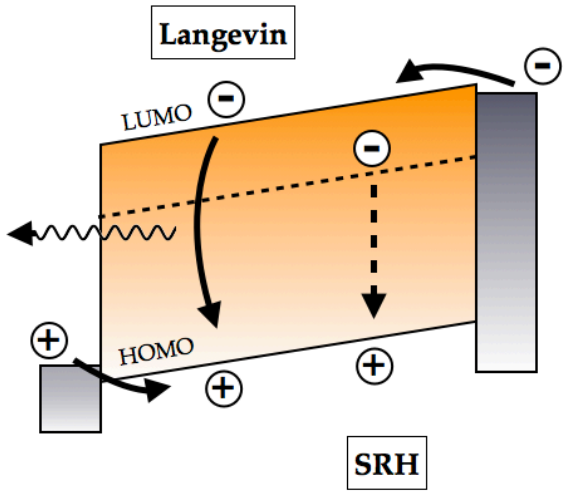

Figure 6 *Schematic depiction of the recombination processes in an MEH-PPV PLED. Only Langevin is considered emissive.*

Taking into account singlet emission and 20% out coupling efficiency [19] the external quantum efficiency (EQE) from the simulation amounts to 1%, which is in good agreement with earlier reports. [4], [20]

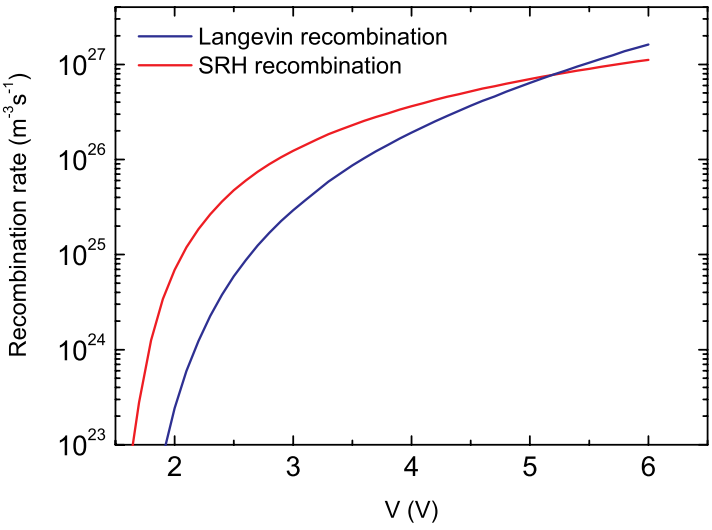

Figure 7. *The recombination rate for the two competing recombination processes. The inset depicts a schematic representation of these processes. Only Langevin is assumed to be radiative.*

The SRH and Langevin recombination rates following from the calculations are depicted in **Figure 7**. The calculations show that the trap-assisted recombination rate is dominant over the free carrier type at low voltage, however being surpassed by Langevin recombination at higher electric fields. The different bias dependence originates from the fact that Langevin recombination rate is quadratic in carrier density [$\sim np$], whereas trap-assisted recombination rate exhibits a linear scaling [$\sim n(p)$]. This implies that at low voltages the majority of the recombination that is taking place is recombination of free holes with electrons that occupy a trap site.

Conclusion

In conclusion, through photovoltaic measurements on PPV diodes we have established the presence and the strength of trap-assisted recombination as a complement to the bimolecular Langevin recombination. Including trap-assisted recombination in the PLED device model leads to a consistent *J-V* and efficiency description. The omission of this process rationalizes the previously observed overestimation of the Langevin pre-factor. The trap-assisted recombination is a dominant loss mechanism in the PLED at low bias voltage, whereas radiative bimolecular recombination takes over at higher electric fields.

References

[1] U. Albrecht and H. Bässler, "Langevin-Type Charge Carrier Recombination in a Disordered Hopping System," *Physica status solidi (b)*, vol. 191, no. 2, pp. 455–459 (1995).

[2] J. C. Scott, P. Brock, J. Salem, S. Ramos, G. Malliaras, S. A. Carter, and L. Bozano, "Charge transport processes in organic light-emitting devices," *Synthetic Met*, vol. 111, pp. 289–293 (2000).

[3] J. Staudigel, M. Stossel, F. Steuber, and J. Simmerer, "A quantitative numerical model of multilayer vapor-deposited organic light emitting diodes," *J. Appl. Phys.*, vol. 86, no. 7, pp. 3895–3910 (1999).

[4] P. W. M. Blom, M. J. M. de Jong, and C. Liedenbaum, "Device physics of polymer light-emitting diodes," *Polym Advan Technol*, vol. 9, no. 7, pp. 390–401 (1998).

[5] P. W. M. Blom, M. J. M. deJong, and S. Breedijk, "Temperature dependent electron-hole recombination in polymer light-emitting diodes," *Appl. Phys. Lett.*, vol. 71, no. 7, pp. 930–932 (1997).

[6] M. M. Mandoc, F. B. Kooistra, J. C. Hummelen, B. de Boer, and P. W. M. Blom, "Effect of traps on the performance of bulk heterojunction organic solar cells," *Appl. Phys. Lett.*, vol. 91, no. 26, p. 263505 (2007).

[7] M. M. Mandoc, W. Veurman, L. J. A. Koster, B. de Boer, and P. W. M. Blom, "Origin of the reduced fill factor and photocurrent in MDMO-PPV : PCNEPV all-polymer solar cells," *Adv. Funct. Mater.*, vol. 17, no. 13, pp. 2167–2173 (2007).

[8] N. C. Giebink, G. P. Wiederrecht, M. R. Wasielewski, and S. R. Forrest, "Ideal diode equation for organic heterojunctions. I. Derivation and application," *Phys. Rev. B*, vol. 82, no. 15, p. 155305 (2010).

[9] D. Cheyns, J. Poortmans, P. Heremans, C. Deibel, S. Verlaak, B. P. Rand, and J. Genoe, "Analytical model for the open-circuit voltage and its associated resistance in organic planar heterojunction solar cells," *Phys. Rev. B*, vol. 77, no. 16 (2008).

[10] L. J. A. Koster, V. D. Mihailetchi, R. Ramaker, and P. W. M. Blom, "Light intensity dependence of open-circuit voltage of polymer : fullerene solar cells," *Appl. Phys. Lett.*, vol. 86, no. 12, p. 123509 (2005).

[11] P. Langevin, "Recombinaison et Mobilités des Ions dans les Gaz," *Ann. Chim. Phys*, vol. 28, pp. 433–530 (1903).

[12] W. Shockley and W. T. Read jr., "Statistics of the recombinations of holes and electrons," *Phys Rev*, vol. 87, no. 5, pp. 835–842, (1952).

[13] R. N. Hall, "Electron-hole recombination in Germanium," *Phys Rev*, vol. 87, no. 2, pp. 387–387 (1952).

[14] M. M. Mandoc, B. de Boer, G. Paasch, and P. W. M. Blom, "Trap-limited electron transport in disordered semiconducting polymers," *Phys. Rev. B*, vol. 75, no. 19, p. 193202 (2007).

[15] D. Braun and A. J. Heeger, "Visible light emission from semiconducting polymer diodes," *Appl. Phys. Lett.*, vol. 58, no. 18, p. 1982 (1991).

[16] L. J. A. Koster, E. C. P. Smits, V. D. Mihailetchi, and P. W. M. Blom, "Device model for the operation of polymer/fullerene bulk heterojunction solar cells," *Phys. Rev. B*, vol. 72, no. 8, p. 085205 (2005).

[17] C. Tanase, P. W. M. Blom, D. M. de Leeuw, and E. J. Meijer, "Charge carrier density dependence of the hole mobility in poly(p-phenylene vinylene)," *Phys. stat. sol. (a)*, vol. 201, no. 6, pp. 1236–1245 (2004).

[18] H. T. Nicolai, M. M. Mandoc, and P. W. M. Blom, "Electron traps in semiconducting polymers: Exponential versus Gaussian trap distribution," *Phys. Rev. B*, vol. 83, no. 19 (2011).

[19] N. C. Greenham, R. H. Friend, and D. D. C. Bradley, "Angular Dependence of the Emission from a Conjugated Polymer Light−Emitting Diode: Implications for efficiency calculations," *Adv. Mater.*, vol. 6, no. 6, pp. 491–494 (1994).

[20] P. W. M. Blom, H. Martens, H. Schoo, M. C. J. M. Vissenberg, and J. Huiberts, "Performance of a polymer light-emitting diode with enhanced charge carrier mobility," *Synthetic Met*, vol. 122, no. 1, pp. 95–98, Jan. 2001.

Chapter 5

Trap-assisted and Langevin-type recombination identified via luminance ideality factors in organic light-emitting diodes

Here we show that the ideality factor of the current of organic light-emitting diodes (OLEDs) in the diffusion-dominated regime has a temperature independent value of 2, which reveals that non-radiative trap-assisted recombination dominates the current. In contrast, the ideality factor of the light output approaches unity, demonstrating that luminance is governed by recombination of the bimolecular Langevin type. This apparent contradiction can be resolved by measuring the current and luminance ideality factor for a white-emitting polymer, where both free and trapped charge carriers recombine radiatively. With increasing bias voltage, Langevin recombination becomes dominant over trap-assisted recombination due to its stronger dependence on carrier density, leading to an enhancement in OLED efficiency.

This work is part of the publication: G. A. H. Wetzelaer, M. Kuik, H. T. Nicolai & P. W. M. Blom, *Physical Review B* **83**, 165204 (2011)

Introduction into the ideality factor

The simplest form of an OLED comprises a thin layer of organic semiconductor sandwiched between two metallic electrodes, which form an Ohmic hole and electron contact, respectively. Due to the difference in work function of the electrodes, a built-in voltage (V_{bi}) across the OLED exists.

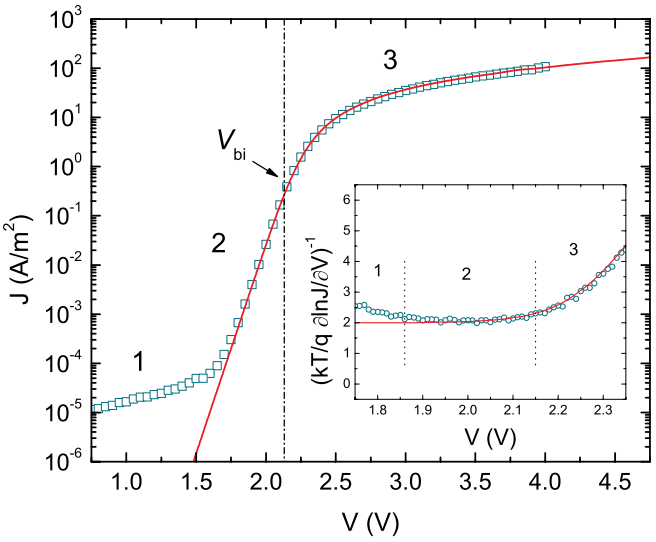

Figure 1 *Experimental J-V characteristics (symbols) of a 43 nm SY OLED and the corresponding calculations (solid line) from a drift-diffusion model, using* $C_n = C_p = 2\times10^{-18}$ *m³/s. The inset shows the differential plot of the data and simulation according to* ***Eq. (2).*** *The leakage (1), diffusion (2), and drift (3) regimes are indicated.*

The *J-V* characteristics of an OLED (**Figure 1**) therefore show three discernible regimes: At low voltages, the current is dominated by parasitical currents between the electrodes, referred to as leakage current, which depends linearly on voltage. The second regime, with V lower than V_{bi}, is diffusion dominated and shows an exponential dependence on voltage according to the Shockley diode equation, given by[1]

$$J = J_0 \left[e^{\left(\frac{qV}{\eta kT}\right)} - 1 \right], \tag{31}$$

where J_0 denotes the saturation current density and η the ideality factor. Hence, the ideality factor is a measure of the slope of the *J-V* characteristics on a

semilogarithmic plot. In the absence of recombination, the ideal diode equation should apply, where η equals unity. At the built-in voltage, a transition from the exponential regime to the drift-dominated, space-charge- limited regime occurs [2], which is characterized by a quadratic dependence of the current on the voltage in the case of trap-free transport, according to the Mott-Gurney square law (**Eq. 6**) [3].

As first described by Sah et al., the ideality factor of a classical *p-n* junction is affected by trap-assisted recombination in the space-charge region.[4] Here, electrons immobilized in trapping sites recombine with free holes as described by the Shockley-Read-Hall (SRH) formalism as described in **Chapter 4**.[5], [6] When SRH recombination is the dominant loss mechanism (as is shown in **Chapter 4**), the ideality factor is expected to be exactly 2.[4] As a result, the ideality factor can be used as a fingerprint for trap-assisted recombination.

In the present study, the OLEDs were prepared on top of a glass substrate, patterned with a transparent indium-tin oxide electrode. For organic semiconductors, a variety of conjugated polymers have been used. A voltage sweep of a typical OLED is depicted in **Figure 1**, where the PPV derivative SY-PPV was used as emitter. As the present study focuses on the ideality factor, the slope of the diffusion regime below V_{bi} is of predominant interest. Conventionally, the ideality factor is determined by fitting the experimental data with **Eq. (23)**. However, in order to prevent erroneous fitting, we determine the ideality factor by numerical differentiation according to

$$\eta = \left(\frac{kT}{q} \frac{\partial ln J}{\partial V} \right)^{-1} . \tag{32}$$

By plotting this quantity against voltage, as shown in the inset of **Figure 1**, the three regimes in the *J-V* characteristics can be distinguished again, where the ideality factor is obtained from the plateau value. The plateau value can be regarded as the steepest exponential incline of the *J-V* characteristics. For a correct determination of the ideality factor, it is of paramount importance that the exponential part is clearly discernible, requiring low leakage currents and high current densities in the space-charge limit. The latter can be achieved for materials with a high charge carrier mobility or by decreasing the layer thickness. As can be seen from **Figure 1**, an ideality factor of 2 was determined for the SY-PPV device, in exact correspondence to the value that is predicted from the Sah-Noyce-Shockley theory in the case of trap-assisted recombination. [4] In addition, both the drift and diffusion regimes can be accurately described by using a numerical drift-diffusion model (**Figure 1**) that, along with

Langevin recombination, includes an additional SRH recombination mechanism, as described in **Chapter 4**.

Luminance ideality factor

As stated above, an ideality factor of 2 in the current of an OLED can be explained by the fact that the dominant recombination mechanism is trap assisted. However, previous studies concluded that charge recombination in organic semiconductors is a bimolecular process of the Langevin type, controlled by the diffusion of oppositely charged free carriers toward each other in their mutual Coulomb field. This apparent discrepancy can be resolved by also studying the ideality factor of the luminance (L) vs voltage (V) characteristics, analogous to the case for the current density. An important requirement for reliable extraction of such a luminance ideality factor is a sufficient luminous efficiency, as the length of the exponential regime is limited by the sensitivity of the photodiode used to record light output. In order to experimentally verify this hypothesis, we studied the L-V characteristics of a diode in which emissive recombination from trapped charge carriers is present, as is the case in host-guest systems, frequently applied in highly efficient OLEDs. An ideal compound for this test is a state-of-the-art white-emitting polymer (Merck) [7], where green- and red- emitting chromophores are incorporated in the blue-emitting backbone. In this polymer the highest occupied molecular orbital (HOMO) levels of the chromophores align with the HOMO of the blue host, whereas the lowest unoccupied molecular orbital (LUMO) levels of the chromophores are substantially below the LUMO of the blue host due to the smaller band gap (**Figure 2**). [8] The chromophores are therefore expected to trap electrons.

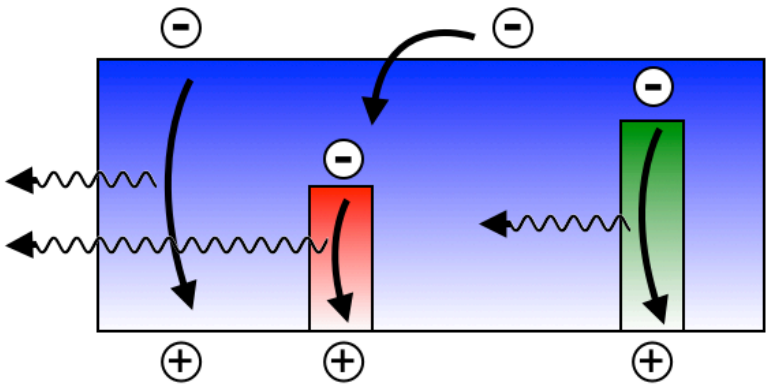

Figure 2. *Schematic representation of the energy levels of the white-emitting copolymer where the HOMO levels of the red and green chromophores align with the HOMO of*

the blue host and the schematic description of the recombination process on the blue backbone (Langevin-type) and on the red chromophore (trap-assisted).

Hence, the blue part of the emission spectrum is assumed to arise from Langevin recombination, whereas the red emission can be ascribed to recombination of holes with electrons that are trapped on the chromophore (**Figure 2**). By measuring the L-V characteristics through selective optical filters, the different recombination mechanisms may be disentangled. Therefore, a blue dichroic filter (serving as a bandpass filter) and a 550 nm longpass filter were used, splitting the electro- luminescence (EL) spectrum into a blue and a red component. As can be observed from **Figure 3(a)**, the ideality factor for the current density again amounts to 2, consistent with materials that lack chromophores.

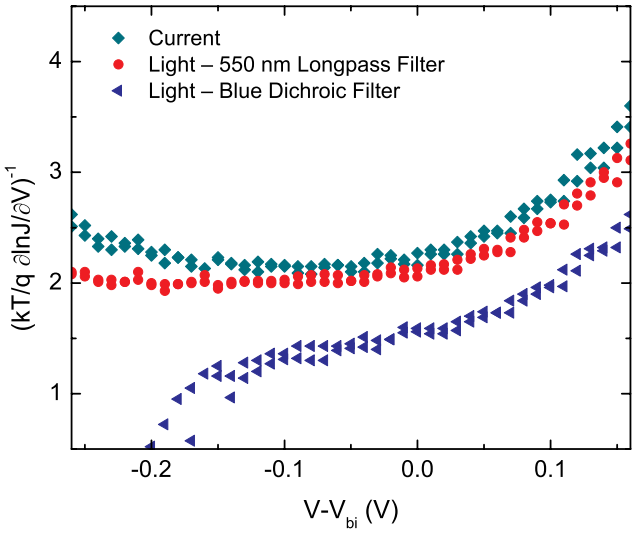

Figure 3. *(**a**) the η-V,*

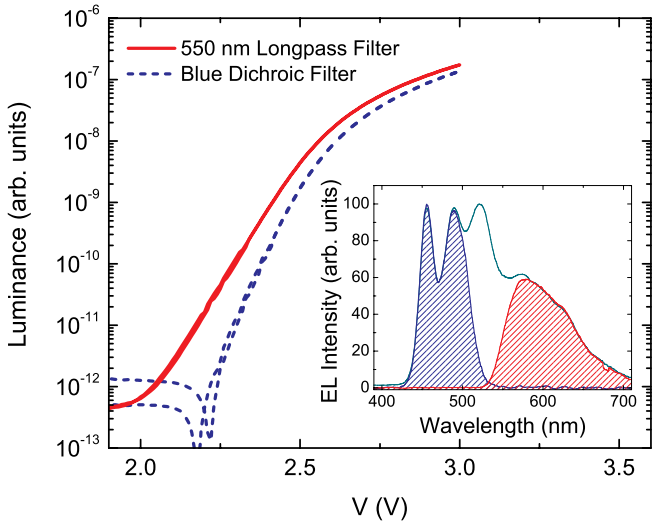

And ***Figure 3.*** *(**b**) the characteristics of a 30 nm white OLED using selective optical filters, indicating the difference in ideality factor for the red and blue light components.The inset shows the corresponding EL spectrum, where the filled areas represent the spectra of the filtered light.*

Remarkably, **Figure 3(b)** shows a clear difference in the slope of the L-V characteristics when either the red or the blue part of the spectrum is measured. The ideality factor for the red light also amounts to 2, confirming that it originates from SRH recombination of an electron that is trapped on the chromophore with a free hole. For the blue emission, a substantially lower ideality factor approaching unity, was observed, in line with the bimolecular Langevin recombination. The unfiltered L-V characteristics are governed by the trap-assisted recombination from the red chromophores, since this mechanism prevails in the low-voltage regime. The observation of a luminance ideality factor shifting to 2 when emissive traps are introduced strongly substantiates that the ideality factor of 2 in OLEDs originates from trap-assisted recombination.

It is evident that the efficiency of a conventional OLED is directly related to the competition between trap-assisted recombination and the radiative bimolecular recombination process. The voltage dependence of this competition can be visualized in the (normalized) EL spectrum of the white OLED (**Figure 4**).

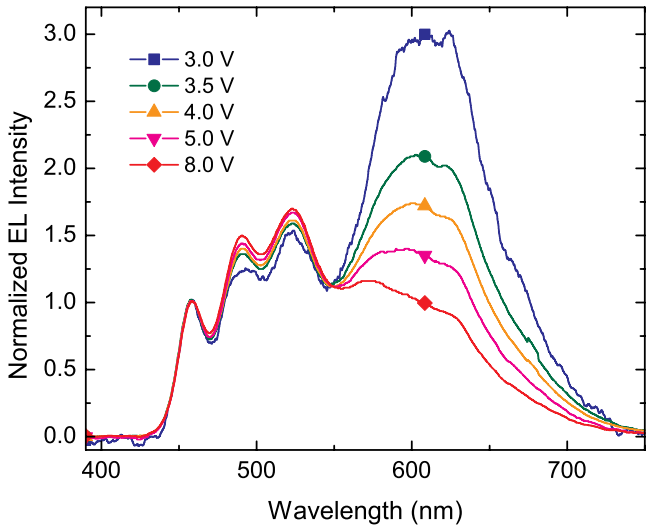

Figure 4 *Voltage dependent EL spectrum of an 80 nm white OLED, normalized at the first blue peak. The red component of the spectrum decreases relative to the blue peak with increasing bias, due to a difference in carrier density dependence of the competing recombination mechanisms.*

We observe that the blue Langevin recombination exhibits a stronger dependence on voltage than the red SRH process, as shown by the relative decrease of red emission compared to the blue peak with increasing voltage. The stronger voltage dependence of the bimolecular Langevin recombination arises from the fact that it is quadratically dependent on the carrier density, whereas SRH recombination only exhibits a linear dependence, as described in **Chapter 4**. The number of trapping sites (red chromophores) is fixed, leading to a strong increase in the free carrier recombination when the traps are filled upon application of a higher voltage. As a result, the blue emission will strongly increase with voltage, whereas the recombination from the trapping sites is limited by the number of traps. This leads to a relative decrease in the intensity of the red feature in the spectrum.

The quantitatively estimation of the relevance of non-radiative trap-assisted recombination has already been performed in **Chapter 4**. Looking again at **Figure 7** in this chapter it becomes apparent that the difference in the slope of the exponential part of the recombination rates is immediately visible, yielding ideality factors of 2 and 1 for SRH and Langevin recombination, respectively, as expected. At low bias voltage, SRH recombination clearly dominates, explaining the observation of a simple ideality factor of 2 for the device

current. As voltage increases, the Langevin recombination gradually approaches the SRH characteristics and becomes dominant above a certain voltage. This competition therefore leads to an intrinsic voltage dependence of the OLED efficiency. In general, the relevance of SRH recombination in OLEDs will depend on the amount of traps, the trap depth, as well as the SRH capture coefficients as will be discussed in the following chapters.

Conclusion

In conclusion, we have confirmed that at low bias the dominant recombination mechanism in OLEDs is trap assisted. A temperature-independent ideality factor of 2 in the current was determined, which evidences the presence of SRH recombination from trapping sites. Furthermore, an ideality factor approaching unity was determined for the luminance, showing that the emissive recombination is determined by a bimolecular Langevin process, and that recombination from trapping sites is non-radiative. This was further confirmed by selective filtering of the blue and red parts of the EL spectrum of a white OLED, where red chromophores incorporated in the blue backbone function as emissive traps, allowing disentanglement of both competing recombination mechanisms by measurement of the luminance ideality factor. At low voltages trap assisted recombination is dominant while when increasing bias Langevin recombination becomes more dominant, which is also reflected in the voltage-dependent emission spectrum of a white OLED.

This study shows that the ideality factor can be regarded as an effective and simple tool for studying the recombination mechanisms in OLEDs for both single-color and white-emitting devices. Accurate determination and understanding of the recombination processes is essential for identification of non-radiative loss mechanisms, thereby providing insights on improving the efficiency of OLEDs.

References

[1] W. Shockley, "The theory of p-n junctions in semiconductors and p-n junction transistors," *Bell Syst. Tech. J*, vol. 28, no. 3, pp. 435–489 (1949).

[2] P. W. M. Blom, M. J. M. deJong, and J. J. M. Vleggaar, "Electron and hole transport in poly(p-phenylene vinylene) devices," *Appl. Phys. Lett.*, vol. 68, no. 23, pp. 3308–3310 (1996).

[3] N. F. Mott and R. W. Gurney, "Electronic Processes in Ionic crystals" Oxford University Press (1948).

[4] C. Sah, R. N. Noyce, and W. Shockley, "Carrier generation and recombination in p-n junctions and p-n junction characteristics," *P Ire*, vol. 45, no. 9, pp. 1228–1243 (1957).
[5] W. Shockley and W. T. Read jr., "Statistics of the recombinations of holes and electrons," *Phys Rev*, vol. 87, no. 5, pp. 835–842 (1952).
[6] R. N. Hall, "Electron-hole recombination in Germanium," *Phys Rev*, vol. 87, no. 2, pp. 387–387 (1952).
[7] M. M.de Kok, W. Sarfert, and R. Paetzold, "Tuning the colour of white polymer light emitting diodes," *Thin Solid Films*, vol. 518, no. 18, pp. 5265–5271 (2010).
[8] M. A. Parshin, J. Ollevier, M. van der Auweraer, M. M. de Kok, H. T. Nicolai, A. J. Hof, and P. W. M. Blom, "Hole transport in blue and white emitting polymers," *J. Appl. Phys.*, vol. 103, no. 11, pp. 113711 (2008).

Chapter 6

The origin of trap-assisted recombination in disordered organic semiconductors

The origin of trap-assisted recombination of electrons and holes in organic semiconductors is investigated. The extracted capture coefficients of the trap-assisted recombination process are shown to be thermally activated with an identical activation energy as measured for the hole mobility μp. We demonstrate that the rate limiting step for this mechanism is the diffusion of free holes towards trapped electrons in their mutual coulomb field, with the capture coefficient given by $(q/\varepsilon)\mu_p$. As a result, both the bimolecular and trap-assisted recombination processes in organic semiconductors are governed by the charge carrier mobilities.

This work has been published as: M. Kuik, L. J. A. Koster, G. A. H. Wetzelaer, & P. W. M. Blom, *Physical Review Letter* **107**, 256805 (2011)

Introduction

As a recapitulation of the introduction in **Chapter 2**, bimolecular recombination (**Figure 1(a)**) in organic semiconductors is of the Langevin type, i.e. the rate limiting step is the diffusion of electrons and holes toward each other in their mutual coulomb field.[1] Such a behavior is characteristic for materials in which the mean free path of the charge carriers is smaller than a critical distance r_c at which the coulomb binding energy between an electron and hole equals k_BT. The charge transport in organic semiconductors is of a hopping nature, with a typical hopping distance of 1-3 nm, whereas r_c amounts to 18.5 nm at T=300 K. Therefore, the manifestation of Langevin recombination in organic semiconductors is expected [2] and experimentally verified.[3] This implies for the bimolecular recombination rate that [1],

$$R_L = B_L\left(np - n_i^2\right) = \frac{q}{\varepsilon_0\varepsilon_r}\left(\mu_n + \mu_p\right)\left(np - n_i^2\right) \tag{33}$$

Even though the presence of Langevin recombination is widely recognized, some studies suggest modifications to the Langevin expression [4] due to bipolar mobilies [5] or inclusion of lateral hops.[6]

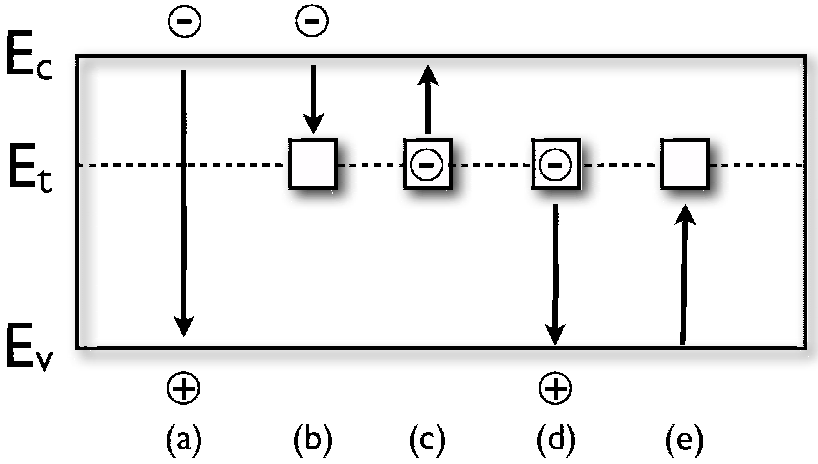

Figure 1. *Schematic representation of bimolecular recombination and the 4 processes involved in recombination by trapping: (**a**) bimolecular, Langevin recombination, (**b**) electron capture, (**c**) electron emission, (**d**) hole capture and (**e**) hole emission.*

Another important recombination process that dominates the recombination in indirect semiconductors as silicon and germanium is trap-assisted recombination.[7,8] This is a two-step process where a trap state, originating from imperfections or impurities in the crystal structure, creating energy levels inside the forbidden energy band gap, captures a charge carrier that subsequently recombines with a mobile carrier of the opposite sign because of their Coulombic interaction. Due to conservation of momentum this process cannot occur without the release of a phonon slowing the recombination process down. Therefore, in most cases the trap sites act as recombination centers for non-radiative recombination. Trap-assisted recombination was first described by Shockley, Read and Hall (SRH) in 1952.[7,8] The four basic steps involved in the recombination by trapping are depicted in **Figure 1** for recombination centers that are neutral when empty, and negatively charged when filled with a trapped electron. First (**Figure 1 (b)**) an electron is captured by a neutral center with a rate governed by a capture coefficient C_n. This trapped electron can subsequently be excited back to the conduction band (**Figure 1(c)**) or is being captured by a hole (**Figure 1(d)**) governed by a capture coefficient C_p. Another option is that an electron is captured from the valence band by a neutral center (**Figure 1(e)**), which is a generation process. In their work, SRH calculated the total trap-assisted recombination rate by assuming thermal equilibrium between the four processes, which requires the rate of capture and the rate of emission to be equal. As a result, the well-known SRH recombination rate is

$$R_{SRH} = B_{SRH}\left(np - n_i^2\right) = \frac{C_n C_p N_{tr}\left(np - n_i^2\right)}{\left[C_n\left(n + n_1\right) + C_p\left(p + p_1\right)\right]} \tag{34}$$

where C_n denotes the probability per unit time that an electron in the conduction band will be captured for the case that the trap is empty and able to capture an electron. Correspondingly, C_p indicates the probability per unit time that a hole will be captured when a trap is filled with an electron and able to capture the hole.

As stated before, in many organic semiconductors the electron currents are strongly trap-limited. For PPV derivatives the trap-limited currents are well described using a model in which the electrons traps, with a typical density of about 2×10^{23} m^{-3}, are Gaussianly distributed in energy, with the center of their distribution located 0.7-0.8 eV below the LUMO (**Chapter 3**).[9] In organic solar cells with trap-limited electron currents, it was demonstrated that the SRH recombination mechanism is responsible for an increased response of the V_{OC} on the incident light intensity.[10] At V_{OC} there is no current extraction and all

generated charge carriers recombine. As a consequence, the V_{OC} behavior is strongly dependent on the presence of specific recombination mechanisms. From the measured response, a capture coefficient of 1.4×10^{-18} m^3/s at room temperature could be deduced. In **Chapter 5**, it was observed that the ideality factor of their current-voltage characteristic is exactly equal to 2, which is a fingerprint of SRH recombination, as derived by Sah *et al.* [11]By measuring V_{OC} as a function of light intensity of PLEDs made from various PPV derivatives in **Chapter 4**, a SRH capture coefficient of 9×10^{-19} m^3/s was derived, in close agreement with the value reported earlier for solar cells.

Temperature dependence of the capture coefficients in trap-assisted recombination

Up to this point, in literature, analysis of trap-assisted recombination has only been performed at room temperature.[10], [12-15] The temperature dependence of the SRH recombination will provide information about the physical origin of this process in organic semiconductors. **Figure 2** depicts the temperature dependence of the V_{OC} - light intensity measurements for a polymer LED consisting of the sandwich structure ITO/PEDOT:PSS/MEH-PPV/Ba(5 nm)/Al(100 nm).

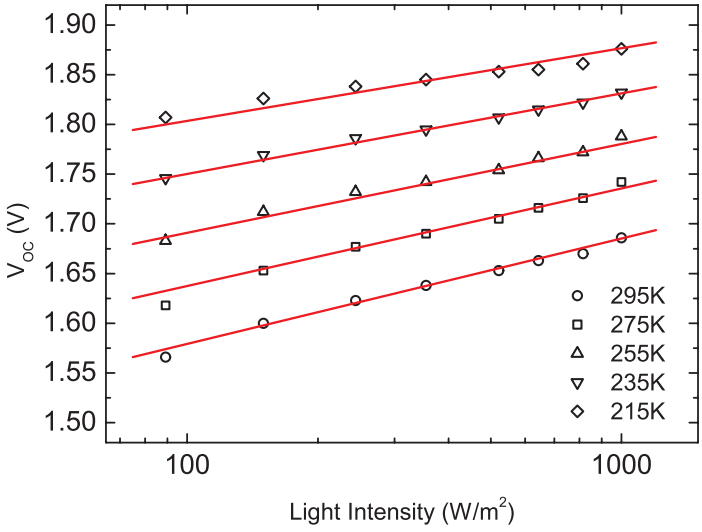

Figure 2. *Measured (symbols) and calculated (solid lines) V_{OC} as a function of the incident light intensity for an MEH-PPV PLED (138nm) at various temperatures.*

The slope is observed to lower slightly from 1.8kT/q at 295K to 1.7kT/q at 215K. To analyze the data, we use a numerical device model [16] in which drift and diffusion of charge carriers, the effect of space-charge on the electric field, density- and field dependent mobility [17], a distribution of traps for the electrons [9], and a field and temperature dependent generation rate of free charge carriers is included. For MEH-PPV, the field-, density- and temperature-dependent mobilities of electron and holes, as well as the trapping behavior of electrons all have been determined independently in previous studies using single carrier devices.[9] As a result, the only unknown parameter to describe the measured light dependence of the V_{OC} is the SRH capture coefficient. The calculated dependence of V_{OC} on light intensity is shown in **Figure 2** by the solid lines.

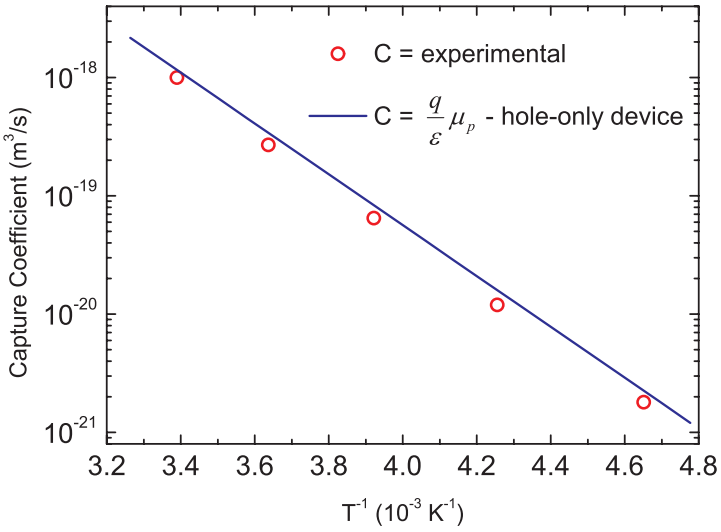

Figure 3. *Arrhenius behavior of the capture coefficient obtained from the V_{OC} - light intensity fit for the 138nm MEH-PPV device (red symbols). Also illustrated are the calculated capture coefficients using* ***Eq. (29)*** *with the effective hole mobility of a 140nm hole-only device (blue line).*

Subsequently, the capture coefficients acquired are depicted in an Arrhenius plot in **Figure 3**. The SRH capture coefficient decreases with decreasing temperature, and is thermally activated with an activation energy of 0.42 eV. Remarkably, the temperature activation of the capture coefficient is exactly equal to the activation energy of the hole mobility as deduced from space-charge-limited currents in MEH-PPV based hole-only devices, structured as ITO/PEDOT:PSS/MEH-PPV/Au(100 nm). This indicates that the SRH capture coefficient is related to the hole mobility.

In order to rationalize this result, we consider two limiting cases for SRH recombination: In the first case $C_p << C_n$, meaning that the time for a hole to capture a trapped electron is significantly larger than the time for an electron to be captured by an empty trap. In LEDs typically $np >> n_1p_1 = n_i^2$ and $n \approx p$, so that the SRH recombination rate reduces to

$$R_{SRH} = C_p N_{tr} p \tag{35}$$

The second case to consider is the opposite of the first, $C_p >> C_n$. For that case, the SRH equation reduces to

$$R_{SRH} = C_n N_{tr} n \tag{36}$$

Both these equations resemble the equation for bimolecular Langevin recombination $R_L=B_Lnp$ ($np >> n_1p_1 = n_i^2$), with B_L replaced by C_n or C_p. In the first case, $C_p<<C_n$, the rate limiting step is the capture of a trapped electron by a free hole, which involves the process of two opposing charges being attracted to each other in their mutual coulomb field, **Figure 1(d)** and **Figure 1(e)**. This process is similar to bimolecular Langevin recombination, with the only difference that the trapped electron cannot move, meaning that $\mu_n=0$. In that case, the SRH recombination coefficient C_p for hole capture by a trapped electron would be

$$C_p = \frac{q}{\varepsilon_0 \varepsilon_r} \mu_p \tag{37}$$

In **Figure 3** the calculated capture coefficient C_p is plotted as a solid line, using the experimentally determined hole mobilities of MEH-PPV. As can be observed in **Figure 3**, the value of the experimental capture coefficients determined from the intensity dependence of the V_{OC} is in very good agreement with the predicted value from **Eq. (29)**. This confirms that the SRH recombination in organic semiconductors is determined by diffusion of the free carrier towards the trapped carrier, similar to Langevin recombination where both free carriers diffuse towards each other.

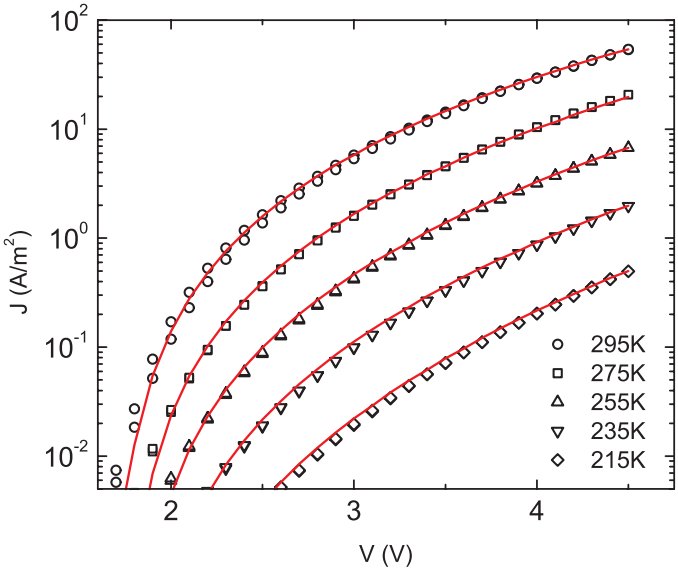

Figure 4. *The J-V characteristics (symbols) of a 165 nm MEH-PPV PLED and the corresponding fits (solid lines) using for the capture coefficient* $(q/\varepsilon)\mu_p$.

Figure 4 comprises excellent fits for the temperature dependence of the *J-V* characteristics of a 165 nm MEH-PPV PLED using **Eq (29)** for the capture coefficients of the trap-assisted recombination process. The fits yield a correct description for the charge transport in the PLED for the whole temperature range.

The mobility dependence of trap-assisted recombination in a white-emitting copolymer

In most organic semiconductors, trap-assisted recombination is of non-radiative nature which denotes SRH recombination as a loss mechanism in LEDs (**Chapter 4**). However, for a white-emitting copolymer, where green- and red- emitting chromophores are incorporated in the blue-emitting polyfluorene backbone, we have demonstrated in **Chapter 5** that the blue part of the emission spectrum arises from Langevin recombination, whereas the red emission originates from SRH recombination of holes with electrons that are trapped on the red chromophore.[18], [19] As a result, both Langevin and SRH can be simultaneously studied by measuring the light output-voltage (*L-V*) characteristics through selective optical filters, as described in **Chapter 5**.

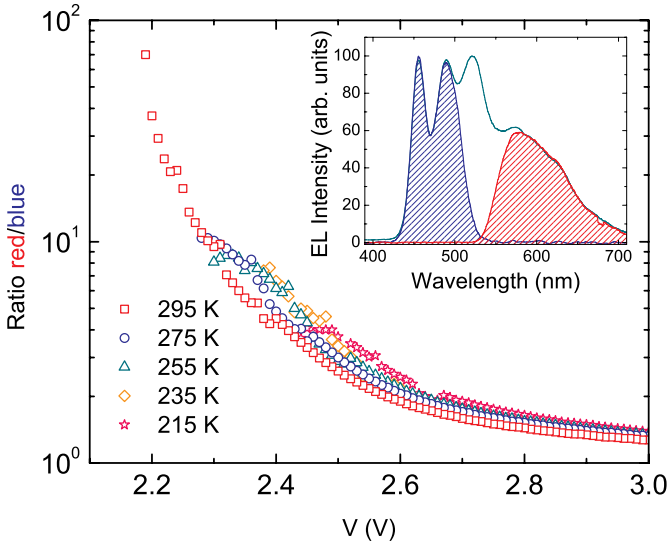

Figure 5. *Ratio of the red (550 nm longpass filter) and the blue light (blue dichroic filter) of a white light-emitting copolymer as a function of voltage for various temperatures.*

Figure 5 depicts the ratio of the red (SRH) and blue (Langevin) emission as a function of voltage for various temperatures. Since Langevin is quadratic in carrier density, whereas SRH is linear, this ratio drops for increasing voltage. More importantly, the ratio is temperature independent: Since the blue-emission rate arises from Langevin recombination, the blue light curve follows the temperature dependence of the highest (hole) mobility in the Langevin expression [**Eq. (25)**]. The trap-assisted red emission on the other hand scales with the capture coefficient C_p [**Eq. (27)**]. The temperature independence of their ratio unambiguously demonstrates that the SRH capture coefficient of the red emission is also dominated by the hole mobility, possessing the same temperature-, field- and density dependence.

Predictive modeling

Understanding of trap-assisted recombination paves the way for a fully predictive description of current transport and recombination of organic LEDs. From single-carrier devices, the electron- and hole mobilities $\mu_n(n,E,T)$ and $\mu_p(p,E,T)$ can be derived, including their dependence on density, electric field and temperature. Furthermore, from electron-only diodes, the number of electron traps N_{tr} can be derived. In a recent study, we demonstrated that at room temperature the inclusion of the measured SRH coefficient in an OLED

device model gives a consistent description of the bipolar PLED characteristics without the need for adjusting the Langevin expression. Moreover, now knowing the origin of SRH in organic semiconductors the modeling of bipolar organic LEDs does not require any additional parameter. The SRH capture coefficient is given by $C_p = (q/\varepsilon)\mu_p$, so that SRH recombination rate can be simply approximated by

$$R_{SRH} = \frac{q}{\varepsilon_0 \varepsilon_r} \mu_p(T, F, p) N_{tr} p \quad , \tag{38}$$

while Langevin recombination rate is given by

$$R_L = \frac{q}{\varepsilon_0 \varepsilon_r} \left[\mu_n(T, F, n) + \mu_p(T, F, p) \right] np \quad . \tag{39}$$

Together with an earlier reported universal Arrhenius relation of the mobility, the result described in this work enables full predictive modeling of organic LEDs.[20] Furthermore, SRH-based loss processes in organic solar cells can from now on be quantitatively predicted.

Conclusion

In conclusion, we have investigated the mechanism of recombination via trapping, as an addition to bimolecular recombination. The temperature behavior of trap-assisted recombination revealed that the capture coefficient is thermally activated, equal to the activation of the experimental hole mobility. We have demonstrated that the trap-assisted recombination in disordered organic semiconductors is governed by the diffusion of the free carrier (hole) towards the trapped carrier (electron), similar as the Langevin recombination for free carriers where both carriers are mobile. As a result, with the charge carrier mobilities and amount of trapping centers known, the complete recombination process in disordered organic semiconductors can be predicted.

References

[1] P. Langevin, "Recombinaison et Mobilités des Ions dans les Gaz," *Ann. Chim. Phys*, vol. 28, pp. 433–530, 1903.

[2] U. Albrecht and H. Bässler, "Langevin-Type Charge Carrier Recombination in a Disordered Hopping System," *Physica status solidi (b)*, vol. 191, no. 2, pp. 455–459 (1995).

[3] P. W. M. Blom, M. J. M. de Jong, and S. Breedijk, "Temperature dependent electron-hole recombination in polymer light-emitting diodes," *Appl. Phys. Lett.*, vol. 71, no. 7, pp. 930–932 (1997).

[4] C. Groves and N. C. Greenham, "Bimolecular recombination in polymer electronic devices," *Phys. Rev. B*, vol. 78, no. 15, p. 155205 (2008).

[5] J. J. M. van der Holst, F. W. A. van Oost, R. Coehoorn, and P. A. Bobbert, "Electron-hole recombination in disordered organic semiconductors: Validity of the Langevin formula," *Phys. Rev. B*, vol. 80, no. 23, p. 235202 (2009).

[6] S. L. M. van Mensfoort , J. Billen, and M. Carvelli, "Predictive modeling of the current density and radiative recombination in blue polymer-based light-emitting diodes," *J. of Appl. Phys.*, no. 109, pp. 064502 (2011).

[7] W. Shockley and W. T. Read jr., "Statistics of the recombinations of holes and electrons," *Phys Rev*, vol. 87, no. 5, pp. 835–842 (1952).

[8] R. N. Hall, "Electron-hole recombination in Germanium," *Phys Rev*, vol. 87, no. 2, pp. 387–387 (1952).

[9] H. T. Nicolai, M. M. Mandoc, and P. W. M. Blom, "Electron traps in semiconducting polymers: Exponential versus Gaussian trap distribution," *Phys. Rev. B*, vol. 83, no. 19 (2011).

[10] M. M. Mandoc, W. Veurman, L. J. A. Koster, B. de Boer, and P. W. M. Blom, "Origin of the reduced fill factor and photocurrent in MDMO-PPV : PCNEPV all-polymer solar cells," *Adv. Funct. Mater.*, vol. 17, no. 13, pp. 2167–2173 (2007).

[11] C. Sah, R. N. Noyce, and W. Shockley, "Carrier generation and recombination in p-n junctions and p-n junction characteristics," *P Ire*, vol. 45, no. 9, pp. 1228–1243 (1957).

[12] R. A. Street and M. Schoendorf, "Interface state recombination in organic solar cells," *Phys. Rev. B*, vol. 81, no. 20, p. 205307 (2010).

[13] T. Kirchartz, B. E. Pieters, J. Kirkpatrick, U. Rau, and J. Nelson, "Recombination via tail states in polythiophene: fullerene solar cells," *Phys. Rev. B*, vol. 83, no. 115209 (2011).

[14] L. Tzabari and N. Tessler, "Shockley–Read–Hall recombination in P3HT: PCBM solar cells as observed under ultralow light intensities," *J. Appl. Phys.*, vol. 109, no. 064501 (2011).

[15] S. R. Cowan, W. L. Leong, N. Banerji, G. Dennler, and A. J. Heeger, "Identifying a Threshold Impurity Level for Organic Solar Cells: Enhanced First-Order Recombination Via Well- Defined PC84BM Traps in Organic Bulk Heterojunction Solar Cells," *Adv. Func. Mater.*, vol. 16, no. 16, pp. 3083-3092 (2011)

[16] L. J. A. Koster, E. C. P. Smits, V. D. Mihailetchi, and P. W. M. Blom, "Device model for the operation of polymer/fullerene bulk heterojunction solar cells," *Phys. Rev. B*, vol. 72, no. 8, p. 085205 (2005).

[17] W. F. Pasveer, J. Cottaar, C. Tanase, R. Coehoorn, P. A. Bobbert, P. W. M. Blom, D. M. de Leeuw, and M. Michels, "Unified description of charge-carrier mobilities in disordered semiconducting polymers," *Phys. Rev. Lett.*, vol. 94, no. 20, p. 206601 (2005).

[18] M. M. de Kok, W. Sarfert, and R. Paetzold, "Tuning the colour of white polymer light emitting diodes," *Thin Solid Films*, vol. 518, no. 18, pp. 5265–5271 (2010).

[19] M. A. Parshin, J. Ollevier, M. van der Auweraer, M. M. de Kok, H. T. Nicolai, A. J. Hof, and P. W. M. Blom, "Hole transport in blue and white emitting polymers," *J. Appl. Phys.*, vol. 103, no. 11, pp. 113711 (2008).

[20] N. I. Craciun, J. Wildeman, and P. W. M. Blom, "Universal arrhenius temperature activated charge transport in diodes from disordered organic semiconductors," *Phys. Rev. Lett.*, vol. 100, no. 5, p. 056601 (2008).

Chapter 7

Non-radiative recombination losses in polymer light-emitting diodes

In this chapter we use the predictive nature of the previous chapter and present a quantitative analysis of the loss of electroluminescence in LEDs based on MEH-PPV due to the combination of non-radiative trap-assisted recombination and exciton quenching at the metallic cathode. It is demonstrated that for an MEH-PPV LED the biggest efficiency loss, up to 45%, arises from extrinsic non-radiative recombination via electron traps. The loss caused by exciton quenching at the cathode proves only to be significant for devices thinner than 100 nm. Removal of electron traps by purification is expected to enhance the efficiency of polymer LEDs by more than a factor of two.

This work has been published by: M. Kuik, L. J. A. Koster, A. G. Dijkstra, G. A. H. Wetzelaer, & P. W. M. Blom, *Organic Electronics*, **13**, 969-974 (2012)

Introduction

As stated before, investigation of the charge transport in PLEDs of the model compound PPV, and its derivatives, has led to the knowledge that the charge transport in the polymer is intrinsically dominated by holes.[1] The reduced electron transport is attributed to the presence of electrons traps,[2], [3] causing the electrons to drift less far into the PLED as compared to the holes. A major disadvantage of this unbalanced charge transport is that the recombination zone culminates close to the metallic cathode. The excitons formed relatively close to the cathode may transfer their energy to the metallic contact and decay non-radiatively [4], [5], leading to a loss in luminous efficacy (**Figure 1(a)**). Together with the fraction of the singlet exciton formation, photoluminescence efficiency and optical out-coupling efficiency, exciton quenching at the cathode is regarded as one of the prime limitations to the PLED performance. The second key ingredient in the PLED operation, emissive charge recombination, is generally considered to be described as the Coulombic attraction between two free charge carriers of the opposite sign as depicted in **Figure 1(b)**. However, the previous chapters have demonstrated that the trapped, immobile electrons in PPVs also actively participate in the recombination process through trap-assisted recombination with free holes. But, the recombination is in this case shown to be non-radiative, which designates the presence of electron traps in the active layer as the origin of an additional loss mechanism (**Figure 1(c)**). In this chapter, non-radiative trap-assisted recombination and exciton quenching at the cathode are quantitatively addressed. Through modeling of MEH-PPV PLED devices, we shed light on the influence- and magnitude of both these loss processes on the device performance.

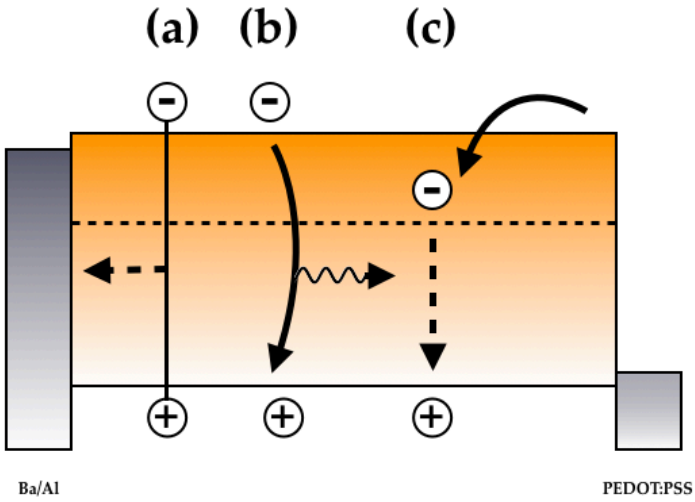

Figure 1. *Schematic illustration of* ***a****) The quenching of the exciton by the metallic cathode,* ***b****) bimolecular, Langevin-type, recombination, and* ***c****) trap-assisted, SRH, recombination*

Cathode quenching

Quenching at the metallic cathode is a balance of two processes. First, the energy from the excited polymer is transferred to the metal non-radiatively via long-range dipole-dipole interaction, as depicted in **Figure 1(a)**. The occurrence of non-radiative energy transfer to the metal will lead to a gradient in the exciton population close the metallic film. As a result, excitons will diffuse towards the interface, which increases the overall exciton quenching process even more. In order to quantify the exciton quenching mechanism a one-dimensional continuity equation is used for the exciton density distribution *E(x,t)*[6], [7]

$$\frac{\partial E(x,t)}{\partial t} = D\frac{\partial^2 E(x,t)}{\partial x^2} - \frac{E(x,t)}{\tau_\infty}\left(1+\frac{x_0^3}{x^3}\right) + R_L \quad (40)$$

The first term on the right-hand side represents the one-dimensional exciton diffusion. The second term accounts for the exciton decay in the polymer (exciton lifetime, τ_∞), further enhanced by non-radiative exciton energy transfer to the metal, described by the inverse cubic distance dependence.[6], [8] The last term describes the exciton generation process which is the generation of excitons governed by the emissive Langevin recombination rate.

At both polymer film interfaces the boundary conditions $E(x=0,\ x=L)=0$ is applied, representing negligible surface quenching on both boundaries. For MEH-PPV, the diffusion coefficient, D, and exciton decay time, τ_∞, have been measured in earlier work to be 1.1e-7 m^2/s and 455 ps which leaves the characteristic range of the energy transfer, x_0, the characteristic distance from the cathode at which most of the excitons formed at a distance larger than this range will decay radiatively and excitons formed closer then this range will transfer their energy to the metal, as a fit parameter for a steady-state exciton density profile.[9]

Bimolecular and non-radiative trap-assisted recombination

The workings of the bimolecular, Langevin-type, recombination has been described extensively throughout this thesis so far. The rate of the emissive bimolecular recombination, R_L, is given by **Eq. (25)**. Equally, the presence of the mechanism of non-radiative trap-assisted recombination in PLEDs has been convincingly validated and demonstrated in the previous chapters. The rate of the trap-assisted recombination is given by **Eq. (26)** except that from now on we use the mobility dependent capture coefficient as described in **Chapter 6**. As a result, when taking $C_n=C_p$ [10-13] the addition of trap-assisted recombination conveniently does not introduce new parameters into the model enabling predictive modeling.

Results and discussion

Throughout this work the analysis of both loss mechanism is performed using again the numerical model [14] in which drift and diffusion of charge carriers, the effect of space-charge on the electric field, density dependent mobility [15], Gaussian trap distribution for the electrons [16], quenching at the cathode [17], [18], free carrier and trap-assisted recombination is included. We have investigated MEH-PPV PLEDs with an active layer thickness of 75 and 165 nm, using PEDOT:PSS and Ba/Al as the anode and cathode respectively. The temperature, field and density dependent hole mobility for both thicknesses was deduced by means of hole-only devices, resulting in the a hole mobility of 5×10^{-11} m^2/Vs for MEH-PPV at zero field and room temperature. For the full characterization of the field and density dependence of the mobility, the description and parameters derived by Tanase *et al.* were used.[15] The electron transport is taken as limited by the presence of electron traps, with for the free electrons $\mu_n=\mu_p$, as was shown in both field-effect transistors[19] and diodes where the effect of traps was eliminated by *n*-type doping.[20] These electron traps are described as a Gaussian-shaped distribution of trap states centered at

0.75 eV below the LUMO with a width σt of 0.10 eV and the number of traps equal to N_{tr}=1.1×10^{23} m^{-3}, as discussed in **Chapter 3**.[16] **Figure 2** depicts the experimental *J-V* data and the according perfect fits at 295K.

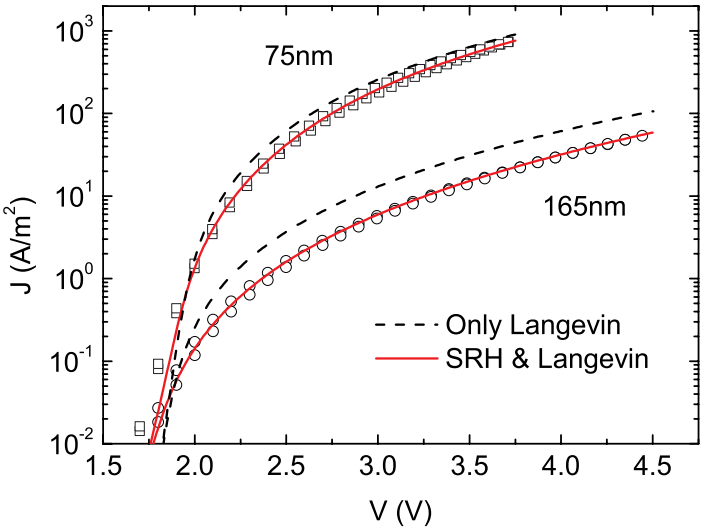

Figure 2. *Current-voltage characteristics of a 75 nm and 165 nm MEH-PPV PLED and the corresponding fits. The dashed lines represent the simulations of the current when only Langevin recombination is taken into account and the contribution of SRH recombination is neglected.*

In order to confirm that the calculations for the *J-V* fits are accurate, the current efficiency (CE; light output/current) is plotted on a sensitive linear scale in **Figure 3** for both thicknesses. In the CE calculations both free carrier and trap-assisted recombination are incorporated, though only free-carrier recombination is taken emissive and sensitive to quenching from the metallic cathode. Good CE fits are obtained for both thicknesses on a sensitive linear scale using a typical energy transfer range of 4 nm. Even on a sensitive linear scale the model evidently explains the voltage dependence of the efficiency of both the thick and thin device well

.

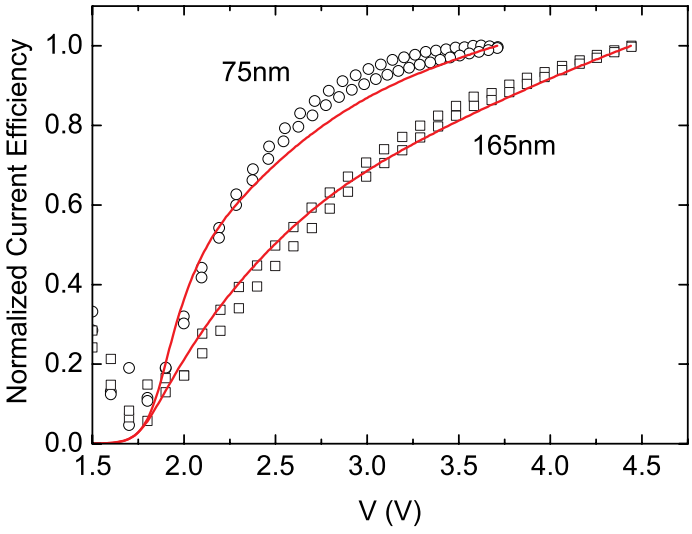

Figure 3. *Normalized current efficiency data and the corresponding fits for a 75 nm and 165 nm PLED. Only Langevin recombination is considered to be emissive.*

The profile of current efficiency curves

Generally in a PLED, electrons flow in at the cathode and holes flow in from the anode. The number of electrons eventually flowing out at the anode and holes at the cathode define the portion of surface recombination at the contacts. In the model, we take the recombination at the surface of the contacts such that it allows for the hole current at the cathode Jp(0)≠0, and on the other side Jn≠(L)0. Nevertheless, it follows from the calculations that even at the maximum applied voltage across the 75nm device, Jp(0) represents only 1.7% of the total current at the cathode and Jn(L) is negligible at the anode. Therefore, to a good approximation, electrons do not flow out at the anode, nor do holes flow out at the cathode. Thus recombination is efficient and governs the device current according to,

$$J = J_n(L) - J_n(0) = q \int R(x)dx \tag{41}$$

,which leads to *J=qRL*, where *R* is the average recombination rate. The conversion efficiency, CE, is defined as the ratio emitted photons per injected electrons. When assuming that Langevin recombination is the only radiative process, the CE is thus represented by

(42)
$$\eta = \frac{\int R_L dx}{J/q} = \frac{\int R_L dx}{\int R_L + R_{SRH} dx}$$

for the case that the current is governed by both the Langevin and SRH recombination rates. It can be understood from **Eq. (34)** that the measured CE depicted in **Figure 3** can therefore be regarded as a fingerprint for non-radiative SRH recombination. If no traps were present in the polymer layer, SRH recombination would be absent; the CE would be independent of voltage, which is clearly not observed. It should be noted that the influence of exciton quenching at the cathode is not taken into account here yet. The effect of this loss mechanism diminishes for thicker layers, thus without SRH recombination the shape of the CE for thicker devices cannot be described. Interestingly, as a result of the trap-limited electron current, increasing the voltage does not simply shift the recombination zone towards the middle of the device layer which would eliminate the influence of quenching. Although the zone does move to the middle of the layer on average, as can been observed in **Figure 4**, The recombination zone also broadens considerably. Revealing that cathode quenching will never entirely disappear, not even at high electric fields, as can be observed in **Figure 5**. [21]

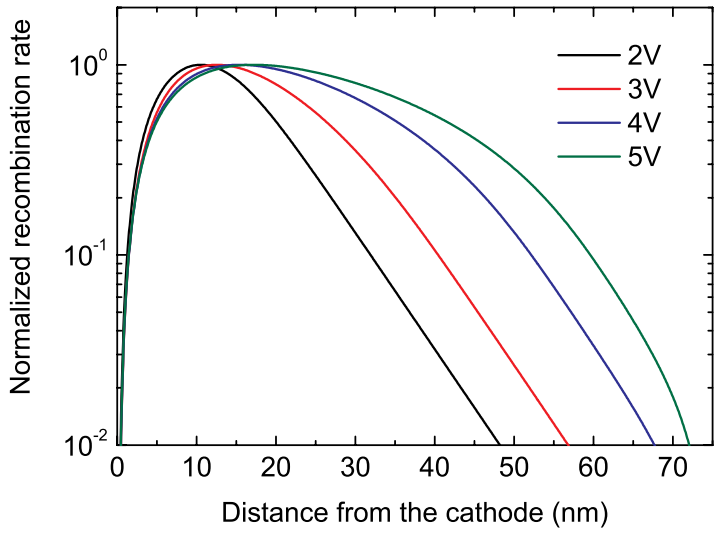

Figure 4. *Calculated and normalized profile of the recombination zone of the 75nm device at various voltages, taking into account emissive Langevin recombination and exciton diffusion.*

Magnitude of both loss processes

An important question is how both individual loss mechanisms compare in magnitude. **Figure 5** represents the calculations of the relative contributions of the loss mechanisms to the CE for the operation of a 75nm device.

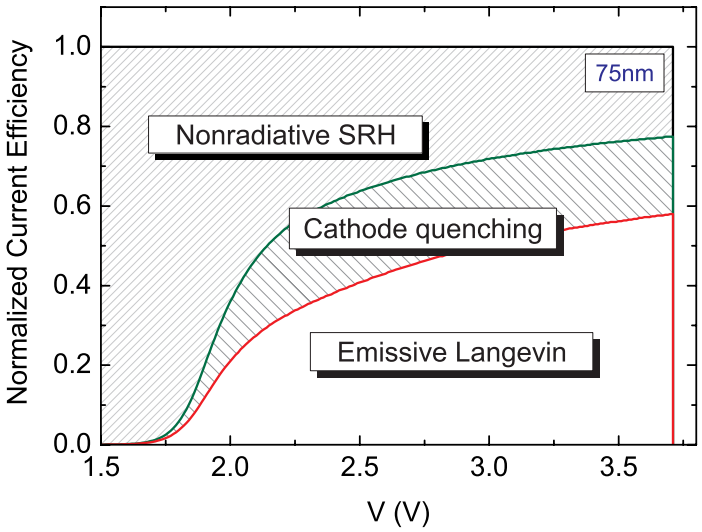

Figure 5. *Calculated contributions of the two loss processes in a 75 nm MEH-PPV PLED. At low voltages nonradiative trap-assisted recombination is the main loss mechanism while at high voltages cathode quenching and nonradiative trap-assisted recombination (SRH) nearly match in contribution to the efficiency loss.*

Despite the small difference in the *J-V* data and the fit comprising only Langevin recombination (dashed line) in **Figure 2**, it is evident from **Figure 5** that in the operation of the device at low voltages the loss process is almost entirely dominated by trap-assisted recombination. For higher voltages both loss processes are of equal magnitude and are each responsible for an efficiency loss of about 20% with regard to the total recombination. Furthermore, with increasing voltage the emissive Langevin recombination becomes more and more important. As the traps are intrinsically present, their number, N_{tr}, is fixed. Therefore, with increased filling of the traps at higher voltages the probability for free carrier recombination increases and becomes dominant when all the traps are filled. In thin PLEDs this process is amplified by the contribution of charge carriers that diffuse from the contacts into the active layer, thereby also enhancing the mobility and partially filling the traps.[22] Consequently, trap-assisted recombination will be less visible in the *J-V*

characteristics of a thin PLED. This phenomenon is perhaps best illustrated in **Figure 5** showing the individual recombination rates for both the 75nm and 165nm device.

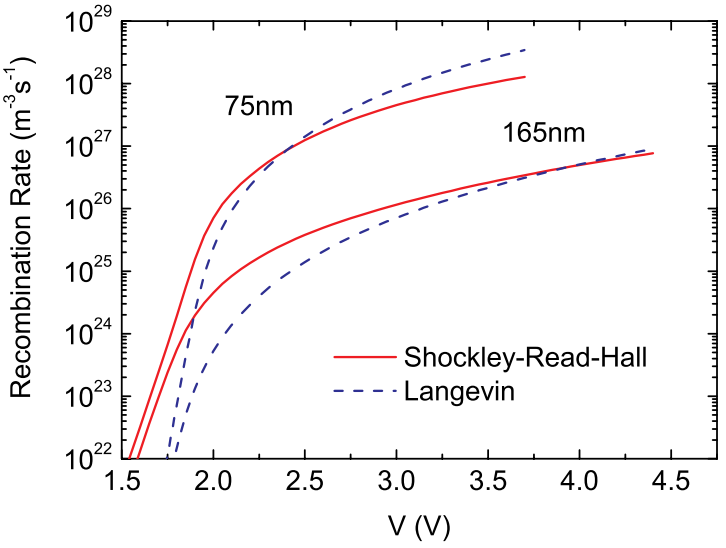

Figure 6. *Calculated individual recombination rates for the 75 nm and 165 nm device. The Langevin recombination for the 75 nm device dominates the total rate earlier then for the 165 nm device due the different dependencies on charge densities of the Langevin and SRH recombination rates, quadratic and linear respectively.*

The point at which the Langevin rate crosses the SRH rate arises at lower voltages for the thin device as compared to the thick PLED. Hence, the current of the 75nm device is largely governed by the Langevin recombination rate, validating the rather small deviation between the fit and the dashed line in **Figure 2**. It should be noted that this behavior can also be observed in systems where both Langevin and SRH recombination are emissive. Also again clearly discernible in **Figure 6** is the difference of the slopes in the diffusion regime, the ideality factor for SRH converges to 2 whereas the Langevin dominated regime converges to 1 as discussed in **Chapter 5**. The little difference between the data and the fit comprising only Langevin recombination in **Figure 2** (dashed line) can thus not been used as a motivation for neglecting trap-assisted recombination. As demonstrated in **Figure 5** trap-assisted recombination is significantly present at all voltages and cannot be disregarded.

In contrast, devices with a thicker active layer are less affected by effects as charge diffusion from the contacts which would expose the true impact of the presence of electron traps even more. **Figure 7** depicts the active layer thickness dependence of both loss mechanisms calculated at a current density of 100 A / m^2.

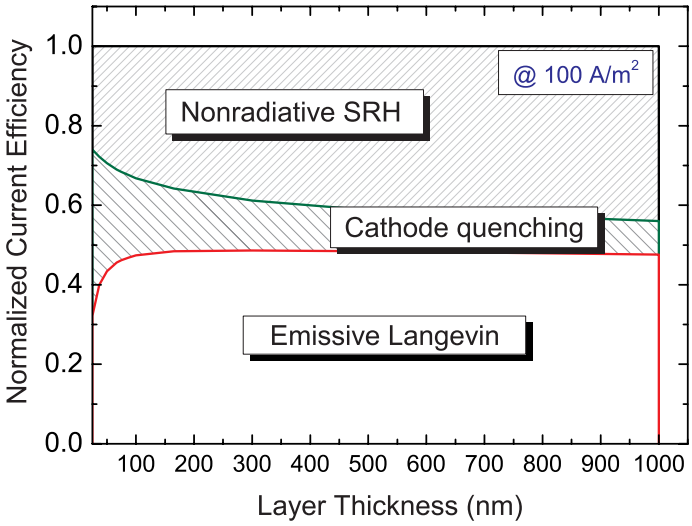

Figure 7. *Thickness dependence of the two loss processes in an MEH-PPV PLED; exciton quenching at the metallic cathode and nonradiative trap-assisted recombination (SRH) calculated at 100 A/m^2*

Clearly, the contribution of the cathode quenching reduces drastically for thicker devices, starting at about 40% for a 25nm device to less than 10% for a 1μm device. Since the electron traps are inherently present in the active layer the non-radiative trap-assisted recombination kicks off at a significant 25% for a 25nm device increasing to a staggering 45% for a 1μm device. This result also shows that quenching at the cathode cannot account for the shape of the CE curves for thicker devices since its influence reduces substantially with increasing thickness. Moreover, nor quenching, nor contact effects can explain the trend of a steep curved CE for the 75nm device and flattening of the CE for the 165nm device in **Figure 3**. It is evident that trap-assisted recombination is the only candidate to which this behavior can be ascribed. Non-radiative trap-assisted recombination dominates the recombination processes at low electric fields, increasing the layer thickness will thus increase the voltage domain at which this recombination process is dominant, thereby flattening the CE curve for thicker devices.

The presence of (filled) electron traps in the MEH-PPV layer is thus detrimental for the device performance in two ways: due to the reduced electron transport the recombination zone is mainly located close to the cathode leading to enhanced quenching of excitons, and furthermore the traps act as non-radiative recombination sites in the active layer. Therefore, the compelling question becomes what the PLED efficiency would be if the amount of electron traps could be reduced. Here we can take advantage of having a complete descriptive device model from which this effect can now be simply predicted. **Figure 8** conveys the influence on the CE by the variation of the number of traps, N_{tr}, taking into account 25% singlet emission and 20% out-coupling efficiency.[23]

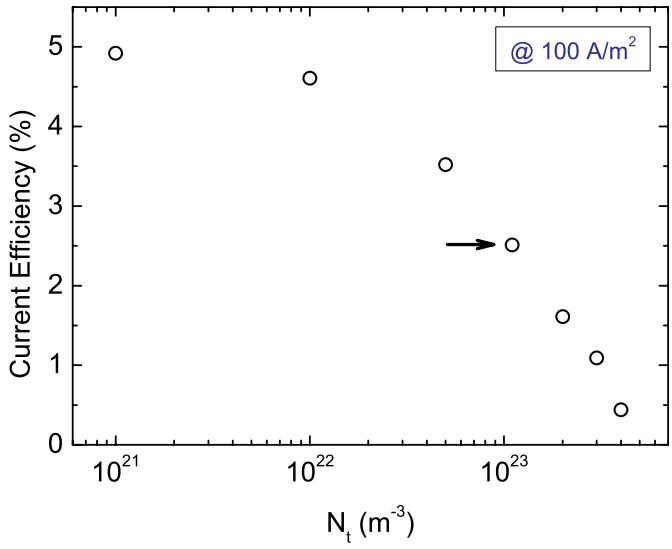

Figure 8. *The current efficiency dependence on the number of electron traps per volume for the 165 nm device. The arrow indicates the number of traps for MEH-PPV as deduced by Nicolai et al. [19], and used in the modeling for the PLEDs.*

Remarkably, it follows that for a reduction of a typical trap number of 1.1×10^{23} m^{-3} for MEH-PPV by one order of magnitude already results in nearly a doubling of the CE. It should be noted that reducing the amount of traps in order to improve the device performance is not an unrealistic endeavor. Craciun *et al.* recently reported that through proper purification of a batch of MEH-PPV hysteresis free electron currents could be obtained.[24] This result implies that whatever electron trapping species is causing the hysteresis as much as 1×10^{22} m-3 of it can be removed by means of proper purification,

which will ultimately lead to an improved device performance. This finding combined with the work presented in this chapter emphasizes the importance of purification of the polymers used for lighting applications even more. Earlier work has already hinted towards an efficiency improvement via proper purification.[25] Equally, Campell *et al.* reported in 2001 that by reducing the large imbalance between both charge carriers in poly(9,9-dioctylfluorene) (PFO) the quantum efficiency was improved.[26]

Conclusion

In conclusion, we have quantitatively addressed the influence of electron traps on the magnitude of non-radiative trap-assisted recombination and exciton quenching from the metallic cathode in PLEDs using the predictive nature of the previous chapter. The results reveal that thin devices (< 100 nm) suffer from severe cathode quenching, accompanied by a significant contribution of non-radiative trap-assisted recombination that increases fast with layer thickness. For devices thicker than 100nm non-radiative trap-assisted recombination is shown to dominate the current efficiency loss by up to 45%. Evidently, future work should focus on the identification and removing of electron traps. This will not only eliminate the non-radiative trap-assisted recombination but in addition, the recombination zone will shift to the center of the device lowering the contribution of cathode quenching, leading to an efficiency improvement of more than a factor of two.

References

[1] P. W. M. Blom, M. J. M. deJong, and J. J. M. Vleggaar, "Electron and hole transport in poly(p-phenylene vinylene) devices," *Appl. Phys. Lett.*, vol. 68, no. 23, pp. 3308–3310 (1996).

[2] M. M. Mandoc, B. de Boer, G. Paasch, and P. W. M. Blom, "Trap-limited electron transport in disordered semiconducting polymers," *Phys. Rev. B*, vol. 75, no. 19, p. 193202 (2007).

[3] H. Antoniadis, M. A. Abkowitz, and B. R. Hsieh, "Carrier deep-trapping mobility-lifetime products in poly(p-phenylene vinylene)," *Appl. Phys. Lett.*, vol. 65, no. 16, pp. 2030–2032 (1994).

[4] G. Vaubel, "Reaction of singlet excitons at an anthracene/metal interface: Energy transfer," *Chem Phys Lett*, vol. 10, no. 3, pp. 334–336 (1971).

[5] G. Cnossen, K. E. Drabe, and D. A. Wiersma, "Fluorescence properties of submonolayers of rhodamine 6G in front of a mirror," *J. Chem. Phys*, vol. 98, no. 7, p. 5276 (1993).

[6] A. L. Burin and M. A. Ratner, "Exciton Migration and Cathode Quenching in Organic Light Emitting Diodes †," *J. Phys. Chem. A*, vol. 104, no. 20, pp. 4704–4710 (2000).
[7] D. E. Markov, J. Hummelen, P. W. M. Blom, and A. Sieval, "Dynamics of exciton diffusion in poly(p-phenylene vinylene)/fullerene heterostructures," *Phys. Rev. B*, vol. 72, no. 4, p. 045216 (2005).
[8] R. R. Chance, A. Prock, and R. Silbey, "Comments on the classical theory of energy transfer," *J. Chem. Phys*, vol. 62, no. 6, p. 2245 (2008).
[9] D. E. Markov, C. Tanase, P. W. M. Blom, and J. Wildeman, "Simultaneous enhancement of charge transport and exciton diffusion in poly(p-phenylene vinylene) derivatives," *Phys. Rev. B*, vol. 72, no. 4, p. 045217, (2005).
[10] M. M. Mandoc, F. B. Kooistra, J. C. Hummelen, B. de Boer, and P. W. M. Blom, "Effect of traps on the performance of bulk heterojunction organic solar cells," *Appl. Phys. Lett.*, vol. 91, no. 26, p. 263505 (2007).
[11] M. M. Mandoc, W. Veurman, L. J. A. Koster, B. de Boer, and P. W. M. Blom, "Origin of the reduced fill factor and photocurrent in MDMO-PPV : PCNEPV all-polymer solar cells," *Adv. Funct. Mater.*, vol. 17, no. 13, pp. 2167–2173 (2007).
[12] G. A. H. Wetzelaer, M. Kuik, H. T. Nicolai, and P. W. M. Blom, "Trap-assisted and Langevin-type recombination in organic light-emitting diodes," *Phys. Rev. B*, vol. 83, no. 165204 (2011).
[13] L. Tzabari and N. Tessler, "Shockley–Read–Hall recombination in P3HT:PCBM solar cells as observed under ultralow light intensities," *J. Appl. Phys.*, vol. 109, no. 6, p. 064501 (2011).
[14] L. J. A. Koster, E. C. P. Smits, V. D. Mihailetchi, and P. W. M. Blom, "Device model for the operation of polymer/fullerene bulk heterojunction solar cells," *Phys. Rev. B*, vol. 72, no. 8, p. 085205 (2005).
[15] C. Tanase, P. W. M. Blom, D. M. de Leeuw, and E. J. Meijer, "Charge carrier density dependence of the hole mobility in poly(p-phenylene vinylene)," *Phys. stat. sol. (a)*, vol. 201, no. 6, pp. 1236–1245 (2004).
[16] H. T. Nicolai, M. M. Mandoc, and P. W. M. Blom, "Electron traps in semiconducting polymers: Exponential versus Gaussian trap distribution," *Phys. Rev. B*, vol. 83, no. 19 (2011).
[17] D. E. Markov and P. W. M. Blom, "Exciton quenching in poly(phenylene vinylene) polymer light-emitting diodes," *Appl. Phys. Lett.*, vol. 87, no. 23, p. 233511 (2005).
[18] D. E. Markov and P. W. M. Blom, "Migration-assisted energy transfer at conjugated polymer/metal interfaces," *Phys. Rev. B*, vol. 72, no. 16, p. 161401 (2005).
[19] L.-L. Chua, J. Zaumseil, J.-F. Chang, E. C. W. Ou, P. K. H. Ho, H. Sirringhaus, and R. H. Friend, "General observation of n-type field-effect

behaviour in organic semiconductors," *Nature*, vol. 434, no. 7030, p. 194 (2005).
[20] Y. Zhang, B. de Boer, and P. W. M. Blom, "Trap-free electron transport in poly(p -phenylene vinylene) by deactivation of traps with n -type doping," *Phys. Rev. B*, vol. 81, no. 8, p. 085201 (2010).
[21] R. Coehoorn and S. L. M. van Mensfoort, "Effects of disorder on the current density and recombination profile in organic light-emitting diodes," *Phys. Rev. B*, vol. 80, no. 8, p. 085302 (2009).
[22] N. I. Craciun, J. J. Brondijk, and P. W. M. Blom, "Diffusion-enhanced hole transport in thin polymer light-emitting diodes," *Phys. Rev. B*, vol. 77, no. 3, p. 035206 (2008).
[23] N. C. Greenham, R. H. Friend, and D. D. C. Bradley, "Angular Dependence of the Emission from a Conjugated Polymer Light−Emitting Diode: Implications for efficiency calculations," *Adv. Mater.*, vol. 6, no. 6, pp. 491–494 (1994)
[24] N. I. Craciun, Y. Zhang, A. Palmaerts, H. T. Nicolai, M. Kuik, R. J. P. Kist, G. A. H. Wetzelaer, J. Wildeman, J. Vandenbergh, L. Lutsen, D. Vanderzande, and P. W. M. Blom, "Hysteresis-free electron currents in poly(p-phenylene vinylene) derivatives," *J. Appl. Phys.*, vol. 107, no. 12 (2010).
[25] A. Menon, H. Dong, Z. I. Niazimbetova, L. J. Rothberg, and M. E. Galvin, "Polydispersity effects on conjugated polymer light-emitting diodes," *Chem Mater*, vol. 14, no. 9, pp. 3668–3675 (2002).
[26] A. J. Campbell, D. D. C. Bradley, T. Virgili, D. G. Lidzey, and H. Antoniadis, "Improving efficiency by balancing carrier transport in poly (9, 9-dioctylfluorene) light-emitting diodes using tetraphenylporphyrin as a hole-trapping, emissive dopant," *Appl. Phys. Lett.*, vol. 79, p. 3872 (2001).

Chapter 8

The effect of ketone defects on the charge transport and charge recombination in polyfluorenes

In the previous chapters we have discussed the effect of trapping on the charge transport and charge recombination in general. In this chapter we apply this new insight for the investigation into the popular material poly(9,9-dioctylfluorene) (PFO) and its oxidized counterpart. Here, the effect of on-chain ketone defects on the charge transport of PFO is investigated. Using MoO3 as ohmic hole contact, the hole transport in a pristine PFO diode is observed to be limited by space-charge, whereas fluorenone contaminated PFO (PFO-F) is shown to be trap limited by the occurrence of an exponential trap distribution with a trap depth of 0.18 eV. The electron transport in PFO is also observed to be trap limited, but in order to describe the electron transport of PFO-F an additional trap level with a depth of 0.46 eV has to be introduced. The obtained energy levels of the fluorenone trapping sites are in close agreement with cyclic voltammetry (CV) measurements reported in literature. As a result, the fluorenone defects are shown to simultaneously act as hole- and electron trap. Moreover, through luminance ideality factor measurements, the green emission associated with these defects is observed to originate from trap-assisted recombination.

This work has been published as: M. Kuik, G. A. H. Wetzelaer, J. G. Laddé, H. T. Nicolai, J. Wildeman, J Sweelssen & P. W. M. Blom, *Adv. Funct. Mater.* **2011**, 21, 4502-4509

Introduction into polyfluorenes

Polyfluorenes (PFs) form an interesting and widely studied class of conjugated polymers for application in polymer light-emitting diodes (PLEDs). The main reason for the interest in these materials is their efficient, deep blue emission making them suitable candidates for full color polymer light emitting displays. In addition, polyfluorenes serve as a backbone host material in many white light-emitting copolymers, making them a common material in polymer lighting applications. However, blue-emitting polyfluorenes are known to suffer from rapid degradation under ambient atmospheres, resulting in the appearance of a broad, featureless green emission band located around 530 nm. [1-4] In fact, early studies reported solely on the green emission of polyfluorenes unaware of this rapid degradation. The origin of this lower energy emission has been a matter of controversy. In initial experiments, reordering of the polymer chains and subsequent aggregation, as well as excimer formation, was assigned as the source of the green emission.[5], [6] Conversely, films of polyfluorenes showed spectral stability upon annealing in N_2 [7]and vacuum[8], [9], rendering the interpretation of aggregate formation questionable and ruling out the effect of excimer formation. Instead, the additional green emission was associated with on-chain defects incorporated during the synthesis.[10] Their oxidation leads to the presence of ketone defects, yielding so-called fluorenone moieties being incorporated in the polymer backbone (**Figure 1b**). Currently, it is widely agreed that ketone defects are definitely responsible for the green emission. However, the precise relaxation processes after excitation of these sites are still subject of discussion. Despite the abundance of publications using optical and chemical methods to identify the on-chain defects, their implications on the electronic transport properties of polyfluorenes have never been studied. A polyfluorene model compound is the dialkyl substituted fluorene-based homopolymer poly(9,9-dioctylfluorene) (PFO) (**Figure 1a**). PFO is highly soluble in common organic solvents and has been vastly studied for its attractive properties.[11], [12]

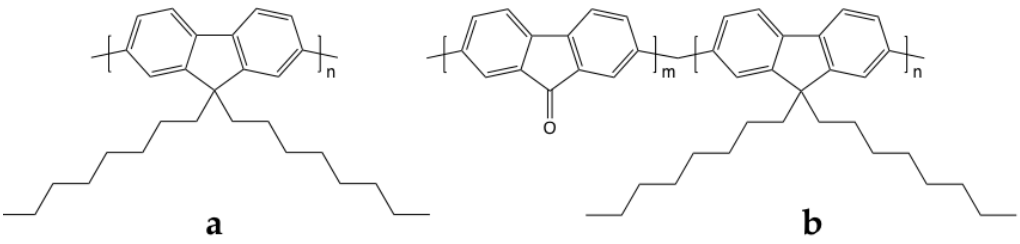

Figure 1. a) *poly(9,9-dioctylfluorene) (PFO) and* ***b)*** *Oxidized PFO contaminated with ketone defects (m), ketone defects in polyfluorenes are called fluorenones.*

Being a deep blue emitting polymer, PFO has a band gap of 3.2 eV, which, however, complicates simultaneous efficient injection of both electrons and holes. While ohmic injection of electrons into the LUMO (~2.6 eV below vacuum)[13] of PFO can be achieved with a Ba/Al cathode, hole injection from standard anodes like PEDOT:PSS is strongly hindered by a large injection barrier. This injection barrier stems from the difference between the HOMO of PFO (~5.8 eV)[11] and the PEDOT:PSS work function of approximately 5.1 eV. [14] The absence of an ohmic hole contact has been impeding the investigation of the hole transport in PFO by means of hole-only diodes. Recently, Nicolai *et al.*[15] have shown that by the incorporation of a molybdenumtrioxide (MoO_3) hole injection layer (HIL) between the polymer and the top electrode ohmic charge injection into the HOMO of PFO can be achieved. Hence, a space-charge limited-current (SCLC) could be observed, from which the hole mobility was determined. As a result, all the important prerequisites are currently present to investigate the effect of the ketone defects on the charge transport. The HOMO and LUMO of fluorenone have been measured to be 5.67 eV and 3.14 eV respectively, as determined by cyclic voltammetry (CV). [16] Considering that both levels are situated within the PFO band gap, the presence of fluorenone species in the polymer backbone should lead to trapping behavior in the electron as well as the hole transport.[17]

Here, we compare the charge transport of deep blue emitting pristine PFO with PFO containing fluorenone elements (PFO-F) in the polymer chain. As a first step optical measurements are conducted to investigate the presence or absence of fluorenone defects. Subsequently, hole transport measurements are conducted using MoO_3 as an ohmic hole contact. Analysis of the current–voltage behavior can provide useful information on the presence of hole traps, which will limit the hole transport of the defect-containing PFO-F when comparing it with pristine PFO. As for the electron transport, which is hindered by a trap distribution as found in a large variety of organic semiconductors, the charge trapping behavior of regular PFO is investigated first. The well-established procedure for studying electron transport in conjugated polymers by means of electron-only diodes is used. In fact, current *J–V* characteristics of the electron transport of standard PFO have not been shown before. Similar to the hole transport measurements, the electron transport of PFO will then be compared with the electron transport of the fluorenone-containing PFO-F, which is expected to contain additional trapping sites. By fitting the *J–V* characteristics of the hole- and electron-only devices using a drift–diffusion model, the amount of traps as well as the energy levels of the trapping sites can be calculated and will be compared to the energy levels predicted from cyclic voltammetry measurements. An important note to realize is that electron- and hole trapping is caused by the same species, which

requires that the number of electron and hole traps is exactly the same. We demonstrate that the fluorenone defects give rise to trapping effects in both the electron and hole current. The trap-depths obtained from numerical modeling of the *J–V* characteristics are in close agreement with the reported energy levels of the fluorenone defects.

Optical investigation of ketone defects in PFO

As stated previously, extensive research has been conducted on ketone defects in PFO, which has focused mainly on the chemical origin of the defects and their optical properties. Therefore, the effect of the presence of these species on the optical properties of PFO is well known, which is advantageous for their identification and provides the opportunity to compare the obtained results with previous research. First, glass/ITO/PEDOT:PSS/polymer/Ba/Al PLEDs were prepared with deep blue emitting PFO and with a PFO that is contaminated with ketone defects.

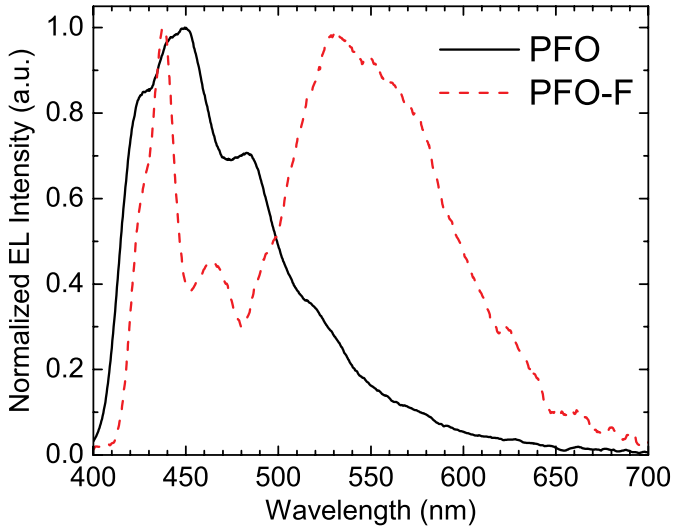

Figure 2. *Electroluminescence spectra of PFO (solid line) and PFO-F (dashed line).*

In **Figure 2** the measured electroluminescence (EL) spectra of regular PFO and PFO-F are shown, normalized to the highest peak. The additional green emission is clearly visible in the PFO-F spectrum. When comparing these results to previous work [7], [8], [16], where fluorenone moieties were deliberately introduced, it convincingly appears that the additional green peak originates from ketone defects. In accordance with these studies, the green emission band is broad and featureless, having its maximum at approximately

530 nm. In order to confirm that this green peak originates from trapping sites, as would be expected from the fluorenone energy levels, a voltage sweep has been performed for the EL spectrum of PFO-F.

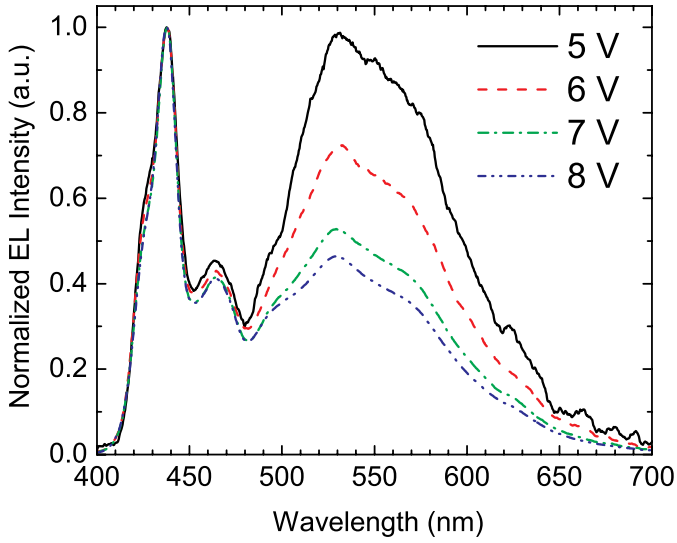

Figure 3. *Electroluminescence spectra of PFO-F at different driving voltages*

Figure 3 shows the EL spectrum at different voltages normalized to the highest blue peak. The green band lowers in intensity relative to the blue peak for higher voltages, analogous to the red and blue peak in the white emitting PLED respectively, as reported in **Chapter 5** . This can be explained by the fact that the blue light originates from bimolecular recombination of free electrons and holes, whereas the green light is generated by charges that are trapped at the fluorenone moieties and subsequently recombine. The number of trapping sites is fixed, leading to a strong increase in the free carrier recombination when the traps are filled upon application of a higher voltage. As a result, the blue emission will strongly increase with voltage, whereas the recombination from the trapping sites is limited by the number of traps. This leads to a relative decrease in the intensity of the green features in the spectrum. In EL measurements, recombination from trapping sites is highly favorable due to their energetic positions. In photoluminescence (PL) measurements however, excitations takes place locally, with the neutral excitons not driven by an electric field, but only diffusing within the exciton diffusion length (~5nm).[18] Consequently, the excitons are less likely to encounter traps prior to recombination as compared to EL measurements. This will strongly reduce the intensity of the green peak in PL measurements. In order to estimate the

amount of ketone defects, photoluminescence measurements have been performed on both PFO and PFO-F.

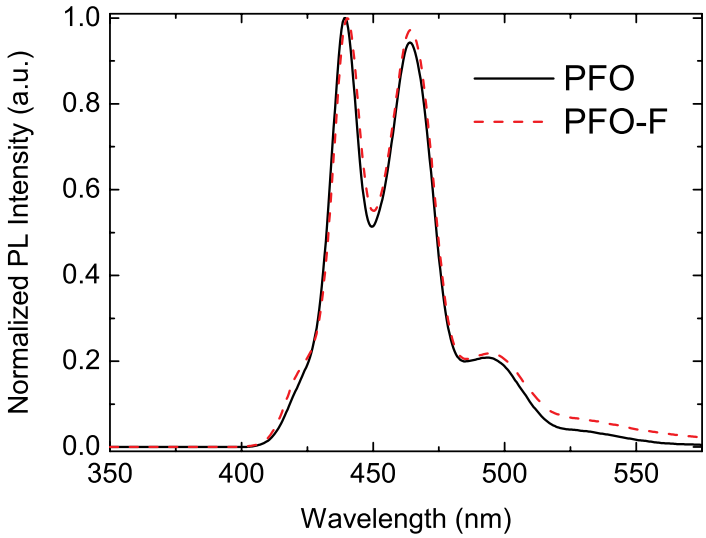

Figure 4. *Photoluminescence spectra of PFO (solid line) and PFO-F (dashed line) thin films.*

As can be seen from **Figure 4**, the difference between the pristine PFO and the fluorenone contaminated PFO-F is negligible in the PL spectra. For comparison, Gong *et al*. reported [16] on the change in PL and absorption spectra by deliberately adding a newly synthesized poly(9,9-dioctylfluorene-co-fluorenone) copolymer, containing 1% fluorenone, to pristine PFO solution. In that report, it was shown that the addition of 0.6 wt. % of the PFO copolymer already results in a small but noticeable change in the PL spectra, indicating that in the PFO-F used in our study the amount of the fluorenone species is even lower. Sims *et al*. have shown a similar decrease in PL intensity of the green band by decreasing the amount of fluorenone molecules blended with the pristine polymer.[6]

Determination of the luminance ideality factors

As stated earlier, the lowering of the green peak relative to the blue peak as a function of voltage (**Figure 3**) suggests the presence of a trap-assisted recombination mechanism at the fluorenone moiety. The difference in bias dependence of trap-assisted and free-carrier recombination has been explained in previous chapters, where the trap-assisted recombination was described by the Shockley-Read-Hall (SRH) formalism.[19], [20] In particular in **Chapter 5**, it

was shown that for the luminance in PLEDs at lower driving voltages the device characteristics are dominated by SRH recombination whereas at higher voltages, the free carrier, Langevin type, recombination takes over, analogous to what is observed in **Figure 3**. Direct evidence for the presence SRH recombination can be obtained by measuring the luminance ideality factor of a PLED. As first described by Sah *et al*. [21] and discussed in **Chapter 5**, the ideality factor is affected by the presence of SRH recombination. When the dominant recombination mechanism is trap assisted, the ideality factor is expected to be exactly equal to 2. As a consequence, the luminance ideality factors, can reveal which recombination mechanism is governing the light emission. Radiative recombination from trapping sites will lead to an ideality factor of 2, while light emission originating from free carrier recombination will lead to an ideality factor closer to 1. **Figure 5** depicts the luminance ideality factors for a 60 nm PFO and 63 nm PFO-F device. As evidenced by the ideality factor of 2, the light output of the PFO-F device is dominated by SRH recombination from the fluorenone moiety.

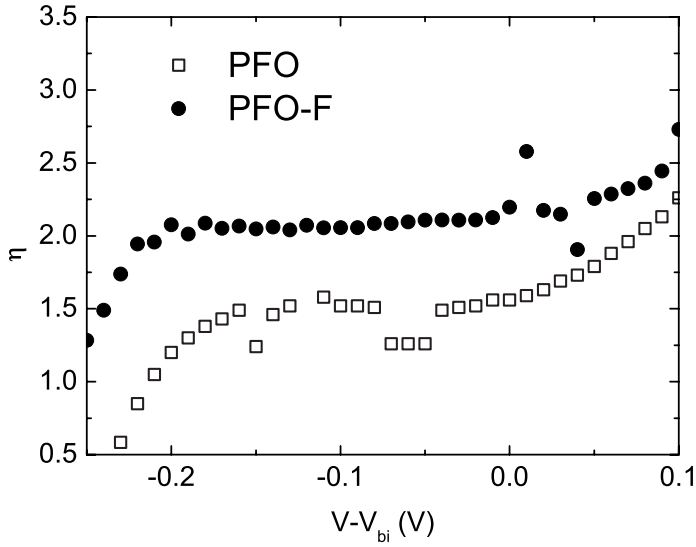

Figure 5. *η–V characteristics extracted from the light output of PFO (open symbols) and PFO-F (closed symbols). The dominance of trap-assisted SRH recombination in PFO-F leads to an ideality factor of 2. Free-carrier recombination in PFO leads to a significantly lower ideality factor.*

In contrast, the PFO device exhibits a substantially lower ideality factor, indicating that free carrier recombination of the bimolecular Langevin-type is dominant. As a consequence, this experiment serves as an additional proof for

the green emission peak to originate from a trap-assisted recombination mechanism on the fluorenone moiety.

Hole transport in PFO and PFO-F

The optical measurements unambiguously point to the presence of a relatively low amount of ketone defects exhibiting a broad green emission band in the EL, originating from trap-assisted recombination. In order to study the effect of these ketone defects on the charge transport, single-carrier diodes were prepared. First, the hole transport was examined; Devices comprising a glass/ITO/PEDOT:PSS/polymer/MoO3/Al structure were fabricated, using the same fabrication method as reported by Nicolai *et al.*[15] **Figure 6** depicts the *J–V* characteristics for PFO and PFO-F for different device thicknesses.

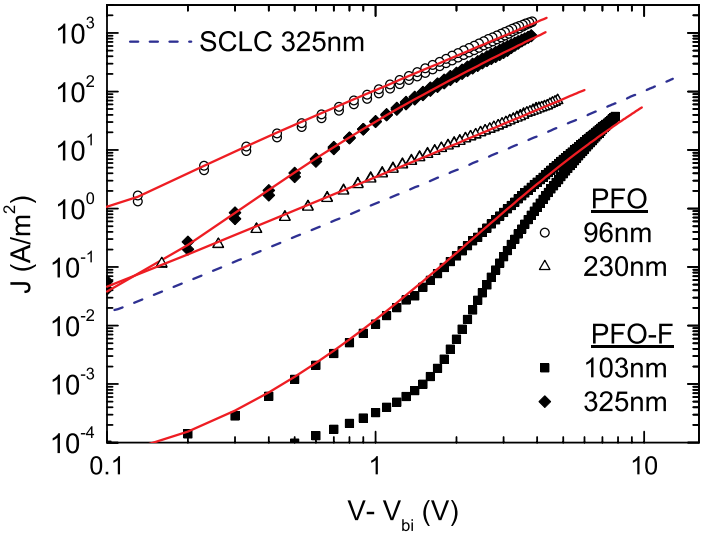

Figure 6. *Experimental and calculated J–V characteristics of hole-only devices for PFO (open symbols) and PFO-F (closed symbols) at 295K. The solid lines represent the calculations from a drift-diffusion model. The dashed line represents the calculated J–V characteristics of a 325 nm PFO device according to the Mott-Gurney square law,* ***Eq . (6)****.*

In agreement with the observation of Nicolai *et al.* [15], the deep blue emitting PFO exhibits a clearly discernible quadratic dependence of the current density on voltage for both the 96 and 230 nm device over almost the whole measured voltage regime. This indicates a weak dependence of the mobility on charge

carrier density, originating from the narrow width of the PFO density of states (DOS). As a first estimate, the mobility at low electric fields can therefore be considered constant and can be directly obtained from the *J–V* characteristics using the Mott-Gurney square law, **Eq. (6)**.[22] For a complete description, charge carrier diffusion from the electrodes[23] and the charge carrier density and electric field dependence of the mobility needs to be taken into account. [24], [25] Previous work on disordered organic semiconductors showed that the dependence of the mobility on carrier density governs the hole conduction at room temperature, whereas at low temperatures the field dependence dominates.[24], [25] These effects are responsible for the enhancement of the SCLC at higher voltages. Fitting the *J–V* characteristics with the Mott-Gurney relation for the defect free PFO results in a zero field mobility of 2.0×10^{-9} m^2/Vs, in excellent agreement with transient electroluminescence (TEL)[26] and steady-state *J–V* measurements.[15] The PFO-F current does not show a quadratic voltage dependence at low fields, but at higher voltages the thin PFO and PFO-F devices exhibit similar characteristics. Moreover, as can be clearly seen from **Figure 6**, the difference is more pronounced when comparing the thick devices. In fact, the *J–V* characteristics of the thick PFO-F devices show the fingerprints of trap-limited transport, exhibiting several important features. First, the thick PFO-F based device shows hysteresis in the back scan, resulting from the disturbance of the electrostatic equilibrium due to trapped charges. Second, the recalculated PFO hole current for a 325 nm device using **Eq. (6)**, is substantially higher than the experimental current from the PFO-F device with the same thickness, especially at lower voltages. Finally, where the pristine PFO device exhibits a clearly discernible quadratic dependence of the current of the voltage, indicative of being limited by space-charge, the thick PFO-F device current strongly deviates from that, showing a higher-power dependence on voltage. The increased slope for trap-limited electron currents in disordered organic semiconductors is generally explained by describing the transport with an exponential trap distribution according to the Mark and Helfrich [27] formalism, **Eq. (13**), as discussed in **Chapter 2**.

The total trap concentration N_{tr} is constant, but since E_a is temperature activated with $\sigma^2/2k_BT$ and E_{tc} is generally not known beforehand, the actual trap depth can only be calculated when the trap concentration N_{tr} is known, and vice versa. As a consequence the denominator in the first term of **Eq. (13)** is taken as the effective trap density, $N_{tr(eff)}$, **Eq. (14)**.[28] It should be noted that in a disordered system of localized states, there are no real free carriers since all carriers are localized. The distinction made is between mobile carriers that hop between localized states and are referred to as "free", and immobile ones which are trapped. It follows from **Eq. (13)** that the trapping behavior is more pronounced for thicker devices, in agreement with the measurements as

depicted in **Figure 6**. The convergence of the characteristics at higher voltages stems from the current approaching the trap-filled limit. As in previous chapters, the numerical drift-diffusion model derived by Koster *et al.* [29] was used to fit the experimental data. Performing a temperature sweep from 295K to 210K for the pristine PFO device enables us to determine the temperature dependence of the mobility. Applying the extended Gaussian disorder model (EGDM, **Eq. (10) & (11)**)[25] leads to a σ of 0.13 eV for PFO. [15] Since PFO-F exhibits hysteresis, all temperature scans for this material have been performed on fresh devices. Using the mobilities obtained from pristine PFO, the PFO-F curves can be fitted by introducing the trap parameters $N_{tr(eff)} = 2\times10^{23}$ m^{-3} and $T_t = 1350$ K. For the thick device the temperature dependence of $N_{tr(eff)}$ leads to a calculated σ of 0.12 eV. This value for the Gaussian variance is close to the value of 0.13 eV obtained for regular PFO by using the EGDM. It should be noted that for the thin device the variation of $N_{tr(eff)}$ with temperature is weaker: the average charge carrier densities in the thin device are higher due to diffusion from the contacts, thereby screening the trapping effect for a large part.[23] The trapping parameters deduced from the hole transport do not directly provide the actual trap depth and concentration of traps since the concept of an effective trap density is applied. Since the trap depth is an important quantity in relating these traps to fluorenone species, additional measurements on the electron transport are required.

Electron transport in PFO and PFO-F

For the characterization of the electron transport we fabricated electron-only diodes based on a glass/Al/polymer/Ba/Al structure. The *J–V* characteristics of a thick and a thin electron-only device of PFO and PFO-F are depicted in **Figure 7**.

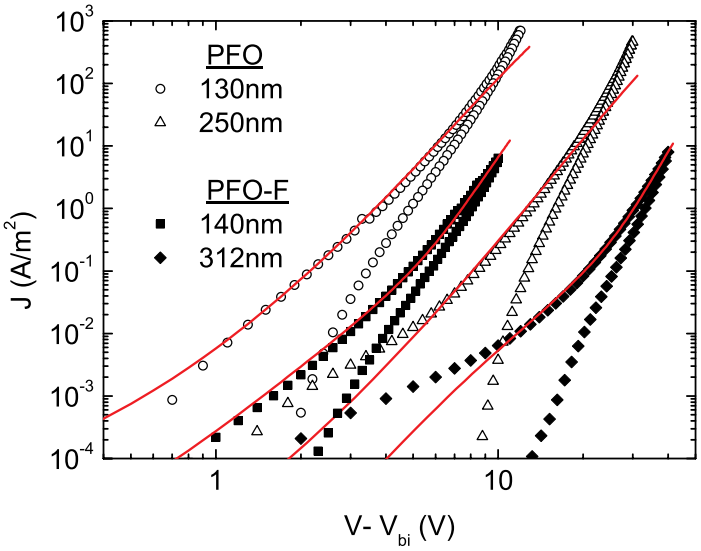

Figure 7. *Experimental and calculated J–V characteristics of electron only devices for PFO (open symbols) and PFO-F (closed symbols) at 295K. The solid lines represent the calculations from a drift-diffusion model incorporating the exponential trap distribution.*

The measured currents in **Figure 7** clearly reveal a trap-limited electron transport, also in the fluorenone defect-free PFO. Furthermore, it is also apparent that the transport in PFO-F is more severely trap-limited as compared to the regular PFO, for both the thin and thick devices. This suggests that, similar to the hole-only measurements, also in the electron transport the fluorenone defects have an influence on the charge transport. Again, the exponential trap model was used for modeling the electron current of pristine PFO for both thicknesses over a range of temperatures. The *J–V* characteristics from 295K down to 210K could be fitted by introducing the trap parameters $N_{tr(eff)} = 1.6\times10^{24}$ m^{-3} and $T_t = 1600$K in the numerical model. Similar to the PFO-F hole-only devices, all temperature scans have been performed on fresh devices. From the temperature dependence of the effective concentration of traps, the σ was calculated to be 0.13 eV (**Figure 8**), in excellent agreement with the value derived from the EDGM model on the PFO trap-free hole transport.

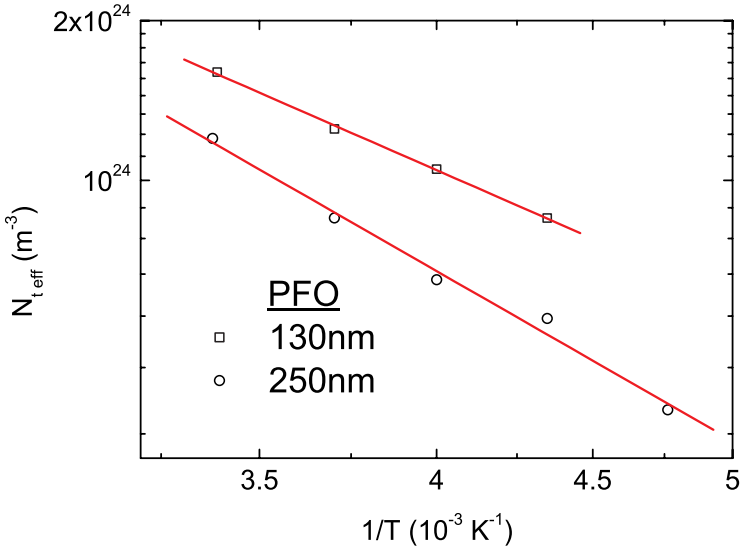

Figure 8. *Temperature dependence of the effective density of traps Nt eff of the electron current for PFO devices following* ***Eq. (14)****.*

In order to fit the simulations to the PFO-F electron-only characteristics, it is required to impose an additional trap level that can be attributed to be originating from a ketone defect. The similarity in slopes of the J–V characteristics for PFO-F with respect to pristine PFO require the addition of a single energy trap level to the already present exponential distribution of trap levels in PFO. The expression for the concentration of trapped electrons n_t in a single energy level trap follows from the Boltzmann distribution and the Fermi-Dirac expression and is described as[30]

$$n_t = \frac{N_{tr}}{1+\frac{N_{tr}}{n}e^{\frac{E_{tc}}{k_B T}}} \tag{43}$$

where E_{tc} in this case represents the single energy trap depth and n the free electron concentration. Analogous to the case of the exponential trap distribution, this relation has to be corrected for the Gaussian distribution of the density of states, which implies that the depth E_{tc} has to be corrected for $E_a = \sigma^2/2k_BT$, to obtain the effective trap level

$$E_{tc(eff)} = E_{tc} - E_a \tag{44}$$

where again E_a mimics the role of the conduction band edge.[31] For a concentration N_{tr} of single-level traps of 4.5×10^{22} m^{-3} with a trap depth E_{tc} of 0.46 eV, the 140 nm as well as the 312 nm thick device curves could be fitted (**Figure 9**).

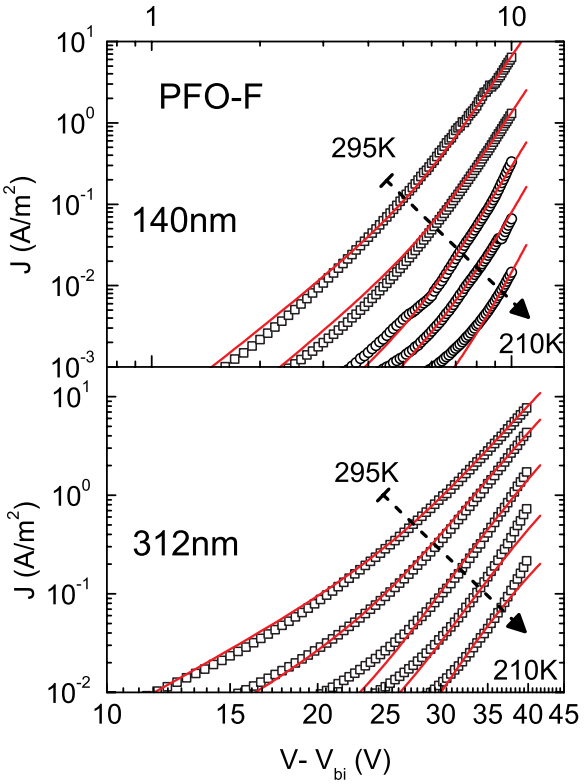

Figure 9. *Experimental (open symbols) and calculated (solid lines) J–V characteristics of the 140 nm and 312 nm PFO-F electron-only device for 295 K down to 210 K.*

The temperature dependence of $E_{tc(eff)}$ (**Figure 10**) leads to a σ of 0.13 eV, which is again in agreement to the σ determined from the EGDM model.

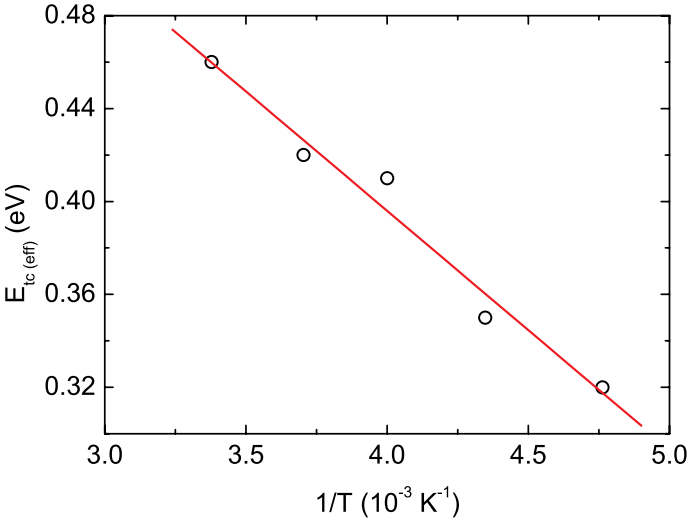

Figure 10. *Temperature dependence of the effective single-level trap depth Etc (eff) of the electron current for PFO-F devices following* ***Eq. (35)*** *and* ***Eq. (36)****, applied in* ***Figure 9*** *for both thicknesses.*

The advantage of the single-level trap model is that it directly provides the total amount of fluorenone related traps N_{tr}. Since the fluorenone defect is simultaneously responsible for the electron- and hole trapping, we now also know the total amount of hole traps. With the effective trap concentration already known from the modeling of the PFO-F hole-only devices, we can now also directly calculate the depth of the hole traps. Using **Eq. (14)**, the depth E_{tc} of the hole trap was calculated to be 0.18 eV. Taking the HOMO and LUMO of PFO into account, the energetic positions of the trapping specie with respect to the vacuum level were obtained. With the LUMO at 2.6 eV and an electron trap depth of 0.46 eV the LUMO of the fluorenone is located at 3.06 eV. Furthermore, with the HOMO at 5.8 eV and a hole trap of 0.18 eV the HOMO of the fluorenone is located at 5.62 eV. These energy levels, obtained from temperature dependent charge transport measurements, coincide very well with the respective HOMO and LUMO levels of 5.67 eV and 3.14 eV for the fluorenone moiety as obtained from CV measurements.[16] The resulting energy-band diagram for PFO and PFO-F is schematically depicted in **Figure 11**.

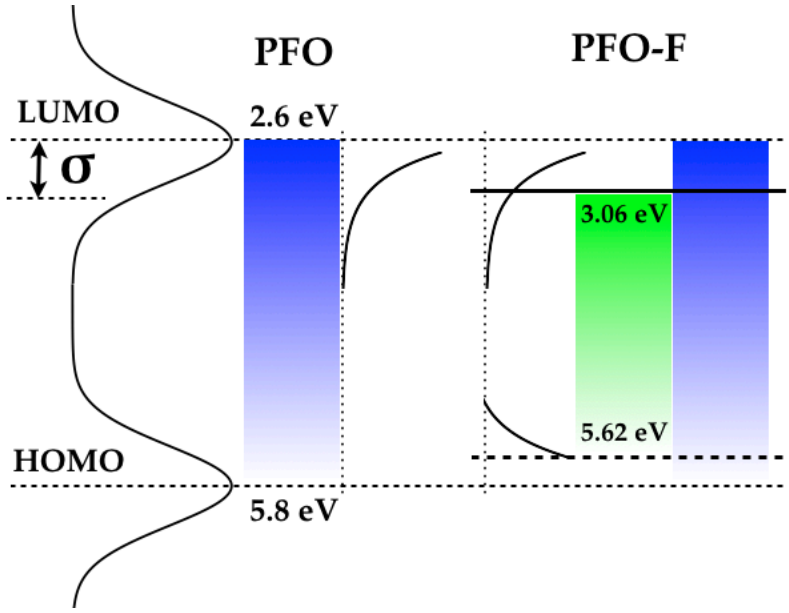

Figure 11. *Schematic representation of the energy levels for the PFO and PFO-F system. For PFO the exponential electron trap distribution is depicted, as used for the electron transport calculations. For the PFO-F system the presence of the fluorenone moiety requires the addition of a single level electron trap along with an exponential hole trap distribution. These calculated additional trap levels are in excellent agreement with the energy levels obtained from CV measurements.*

Since the fluorenone defects act as traps for both electrons and holes, albeit with different trap depths, the additional green electroluminescence originates from recombination of holes and electrons that are trapped on the fluorenone moieties. Therefore, the fluorenone defect acts as a recombination center. This is also reflected in the different voltage dependence of the blue (bimolecular recombination) and green (trap-assisted recombination) emission.

Conclusion

In conclusion, the effect of on-chain ketone defects on the electronic transport of a polyfluorene derivative has been studied using, amongst others, the techniques discussed in previous chapters. The presence of ketone defects in PFO can be unambiguously established through investigation of the electroluminescence, which shows that fluorenone moieties act as recombination centers for a trap-assisted SRH mechanism. Moreover, the energy levels of the fluorenone as determined by CV measurements suggest that both the hole and electron transport of PFO will be trap limited when this type of impurities are present.

Using MoO_3 as ohmic hole contact, the hole transport of fluorenone contaminated PFO-F was shown to be trap limited, in contrast to pristine PFO, where the hole transport is limited by space-charge. It was demonstrated that this current–voltage behavior can be accurately described by introducing an exponential trap distribution in a drift-diffusion model. With regards to the electron transport, pristine PFO was observed to also exhibit trap-limited electron transport, similar to other conjugated polymers, also arising from an exponential trap distribution. In order to describe the current–voltage behavior of the electron-only diodes of PFO-F, an additional trap level had to be introduced in the simulation. The calculated energy levels of the fluorenone trapping sites are in close agreement with CV measurements reported in literature.

References

[1] X. Gong, P. K. Iyer, D. Moses, G. C. Bazan, A. J. Heeger, and S. S. Xiao, "Stabilized Blue Emission from Polyfluorene-Based Light-Emitting Diodes: Elimination of Fluorenone Defects," *Adv. Funct. Mater.*, vol. 13, no. 4, pp. 325–330 (2003).

[2] E. Zojer, A. Pogantsch, E. Hennebicq, D. Beljonne, J. L. Bredas, P. S. de Freitas, U. Scherf, and E. J. W. List, "Green emission from poly(fluorene)s: The role of oxidation," *J. Chem. Phys*, vol. 117, no. 14, pp. 6794–6802 (2002).

[3] J. M. Lupton, M. R. Craig, and E. W. Meijer, "On-chain defect emission in electroluminescent polyfluorenes," *Appl. Phys. Lett.*, vol. 80, no. 24, pp. 4489–4491 (2002).

[4] K. L. Chan, M. Sims, S. I. Pascu, M. Ariu, A. B. Holmes, and D. D. C. Bradley, "Understanding the Nature of the States Responsible for the Green Emission in Oxidized Poly(9,9-dialkylfluorene)s: Photophysics and Structural Studies of Linear Dialkylfluorene/Fluorenone Model Compounds," *Adv. Funct. Mater.*, vol. 19, no. 13, pp. 2147–2154 (2009).

[5] V. N. Bliznyuk , S. A. Carter, J. C. Scott, G. Klärner, R. D. C. Miller, and D. C. Miller, "Electrical and photoinduced degradation of polyfluorene based films and light-emitting devices," *Macromolecules*, vol. 32, no. 2, pp. 361–369 (1999).

[6] M. Sims, D. D. C. Bradley, M. Ariu, M. Koeberg, A. Asimakis, M. Grell, and D. G. Lidzey, "Understanding the Origin of the 535 nm Emission Band in Oxidized Poly(9,9-dioctylfluorene): The Essential Role of Inter-Chain/Inter-Segment Interactions," *Adv. Funct. Mater.*, vol. 14, no. 8, pp. 765–781 (2004).

[7] X. Gong, P. K. Iyer, D. Moses, G. C. Bazan, A. J. Heeger, and S. S. Xiao, "Stabilized Blue Emission from Polyfluorene-Based Light-Emitting

Diodes: Elimination of Fluorenone Defects," *Adv. Funct. Mater.*, vol. 13, no. 4, pp. 325–330 (2003).

[8] E. J. W. List, M. Gaal, R. Guentner, P. S. de Freitas, and U. Scherf, "The role of keto defect sites for the emission properties of polyfluorene-type materials," *Synthetic Met*, vol. 139, no. 3, pp. 759–763 (2003).

[9] L. Romaner, A. Pogantsch, P. S. de Freitas, U. Scherf, M. Gaal, E. Zojer, and E. J. W. List, "The origin of green emission in polyfluorene-based conjugated polymers: On-chain defect fluorescence," *Adv. Funct. Mater.*, vol. 13, no. 8, pp. 597–601 (2003).

[10] U. Scherf and E. J. W. List, "Semiconducting polyfluorenes - Towards reliable structure-property relationships," *Adv. Mater.*, vol. 14, no. 7, pp. 477 (2002).

[11] A. Grice, D. D. C. Bradley, M. Bernius, M. Inbasekaran, W. Wu, and E. P. Woo, "High brightness and efficiency blue light-emitting polymer diodes," *Appl. Phys. Lett.*, vol. 73, no. 5, pp. 629–631 (1998).

[12] M. Redecker, D. D. C. Bradley, M. Inbasekaran, and E. P. Woo, "Nondispersive hole transport in an electroluminescent polyfluorene," *Appl. Phys. Lett.*, vol. 73, no. 11, pp. 1565–1567 (1998).

[13] A. J. Campbell, D. D. C. Bradley, and H. Antoniadis, "Quantifying the efficiency of electrodes for positive carrier injection into poly(9,9-dioctylfluorene) and representative copolymers," *J. Appl. Phys.*, vol. 89, no. 6, pp. 3343–3351 (2001).

[14] N. Koch, A. Vollmer, and A. Elschner, "Influence of water on the work function of conducting poly(3,4-ethylenedioxythiophene)/ poly(styrenesulfonate)," *Appl. Phys. Lett.*, vol. 90, no. 4, p. 043512 (2007).

[15] H. T. Nicolai, G. Wetzelaer, M. Kuik, A. J. Kronemeijer, B. de Boer, and P. W. M. Blom, "Space-charge-limited hole current in poly (9, 9-dioctylfluorene) diodes," *Appl. Phys. Lett.* vol. 96, no. 172107 (2010).

[16] X. Gong, D. Moses, A. J. Heeger, and S. S. Xiao, "Excitation energy transfer from polyfluorene to fluorenone defects," *Synthetic Met*, vol. 141, no. 1, pp. 17–20 (2004).

[17] A. Kadashchuk, R. Schmechel, H. von Seggern, U. Scherf, and A. Vakhnin, "Charge-carrier trapping in polyfluorene-type conjugated polymers," *J. Appl. Phys.*, vol. 98, no. 2, p. 024101 (2005).

[18] D. E. Markov, E. Amsterdam, P. W. M. Blom, A. B. Sieval, and J. C. Hummelen, "Accurate Measurement of the Exciton Diffusion Length in a Conjugated Polymer Using a Heterostructure with a Side-Chain Cross-Linked Fullerene Layer," *J. Phys. Chem. A*, vol. 109, no. 24, pp. 5266–5274 (2005).

[19] W. Shockley and W. T. Read jr., "Statistics of the recombinations of holes and electrons," *Phys Rev*, vol. 87, no. 5, pp. 835–842, Jan. 1952.

[20] R. N. Hall, "Electron-hole recombination in Germanium," *Phys Rev*, vol. 87, no. 2, pp. 387–387 (1952).
[21] C. Sah, R. N. Noyce, and W. Shockley, "Carrier generation and recombination in p-n junctions and p-n junction characteristics," *P Ire*, vol. 45, no. 9, pp. 1228–1243 (1957).
[22] N. F. Mott and R. W. Gurney, "Electronic Processes in Ionic crystals" Oxford University Press (1948).
[23] N. I. Craciun, J. J. Brondijk, and P. W. M. Blom, "Diffusion-enhanced hole transport in thin polymer light-emitting diodes," *Phys. Rev. B*, vol. 77, no. 3, p. 035206 (2008).
[24] C. Tanase, E. W. Meijer, P. W. M. Blom, and D. M. de Leeuw, "Unification of the hole transport in polymeric field-effect transistors and light-emitting diodes," *Phys. Rev. Lett.*, vol. 91, no. 21, p. 216601, Jan. 2003.
[25] W. F. Pasveer, J. Cottaar, C. Tanase, R. Coehoorn, P. A. Bobbert, P. W. M. Blom, D. M. de Leeuw, and M. Michels, "Unified description of charge-carrier mobilities in disordered semiconducting polymers," *Phys. Rev. Lett.*, vol. 94, no. 20, p. 206601 (2005).
[26] T. van Woudenbergh, J. Wildeman, P. W. M. Blom, J. Bastiaansen, and B. Langeveld-Voss, "Electron-enhanced hole injection in blue polyfluorene-based polymer light-emitting diodes," *Adv. Funct. Mater.*, vol. 14, no. 7, pp. 677–683 (2004).
[27] P. Mark and W. Helfrich, "Space-Charge-Limited Currents in Organic Crystals," *J. Appl. Phys.*, vol. 33, no. 1, p. 205 (1962).
[28] M. M. Mandoc, B. de Boer, G. Paasch, and P. W. M. Blom, "Trap-limited electron transport in disordered semiconducting polymers," *Phys. Rev. B*, vol. 75, no. 19, p. 193202 (2007).
[29] L. J. A. Koster, E. C. P. Smits, V. D. Mihailetchi, and P. W. M. Blom, "Device model for the operation of polymer/fullerene bulk heterojunction solar cells," *Phys. Rev. B*, vol. 72, no. 8, p. 085205 (2005).
[30] M. Lampert, "Simplified theory of space-charge-limited currents in an insulator with traps," *Phys Rev*, vol. 103, no. 6, pp. 1648–1656 (1956).
[31] T. van Woudenbergh, P. W. M. Blom, and J. Huiberts, "Electro-optical properties of a polymer light-emitting diode with an injection-limited hole contact," *Appl. Phys. Lett.*, vol. 82, no. 6, pp. 985–987 (2003).

Summary

The market or and the development of displays and lighting applications is increasing fast. These days a typical western household owns more than just one tv set. There will be at least one personal computer present and every person in that household owns a mobile phone. In the US alone iPod households now own on average 1.3 iPod units per households. And on top of that, the latest development is that likely more and more household also own a tablet computer. Even in the car of this typical western household a color display for the route navigation system has become common good. But this covers just displays, the number of lighting applications is even bigger. Clearly every room in a typical house has at least one electrical light source, likely more. But what about all the other lighting displays? The ones on your oven, micro-wave, alarm clock, VCR, DVD-player, sound-system, heating system, climate control, landline phone, car dials and much much more. And we haven't even discussed the public domain yet; the displays and lighting panels on busses, airplanes, airports, billboards, trains, signs, computers at work and we can go on and on. When you take into account that the refresh rate of a typical electrical appliance has become higher over the years, it becomes dauntingly clear that unless science manages to introduce nuclear fusion soon it is of vital importance that the development of displays and lighting applications focusses on durable, energy saving innovations. Additionally, considering that this small example has only covered the typical western household and that the living standard in the developing countries is also increasing fast the general picture might become even more gigantic and impressive.

Organic light-emitting diode (OLED) technology is one of the most promising candidates to facilitate the need for durable and energy saving displays and lighting systems. The typical operating voltage is low, typically around 3V, and the processing techniques are relatively easy, especially spin-coating or inkjet printing are very promising methods for deposition. Particularly the flexible property of OLED technology can provide a new road to possibilities and durability. Dropping you phone, for example, will almost certainly destroy it's display, but a flexible OLED display will likely increase the chances that the display is still working much more. That is in fact why also military organizations and companies are very much interested in the development of OLED technology. Another well known feature of OLED technology is that it allows for a much higher contrast ratio than for example an LCD display.

Hence, less light intensity is needed to be able to see or read what is depicted screen. Morover, in OLED displays every pixel is a light-emitting diode therefor, contrary to LCD technology, OLED devices don't require a backlight, which saves battery life drastically. This is in fact one of the main reasons why in the last few year the product line Galaxy featuring an Active Matrix OLED (AMOLED) display by Samsung has gained that much popularity.

The OLED displays of today consist mostly of evaporated multilayered diodes. Meaning that the one organic semiconducting compound comprising all the excellent properties for usage in OLED devices has not been discovered yet and in order to compensate for this, the application of additional organic layers is a necessity. However, these additional layers also result in disadvantageous side effects as higher operating voltages or longer production times, for example. Additionally, although the light emission efficiency for OLED displays is fine, this efficiency is still to low for bulk usage in common lighting applications. Hence a better understanding of the workings of the materials in OLED devices is desired.

What is understood thus far is that in the vast majority of materials used in organic electronic devices the hole transport is typically higher then the electron transport. In some cases even orders of magnitude higher. Holes are observed to travel *freely* governed by a space charge behavior whereas the electron transport is found to be limited by the presence of traps, partially charging up the device. In a device where both electrons and holes are injected the recombination zone, the area in the device where electrons will recombine with holes, will be formed closely to the cathode simply because the holes travel faster. For the case that these electron-hole recombinations are emitting light, the presence of a metallic cathode will reduce the total amount of light output since the metallic cathode will reduce the emissive property of this recombination by means of quenching. Clearly this electron trapping behavior is a major problem for the general device performance. Unfortunately not a lot is known about this trapping behavior and it's origin yet. In this thesis we demonstrate that the trapping behavior is likely not a result of the design structure of a particular material but rather universal for the entire class of organic polymeric semiconducting materials and that the origin of trapping behavior is likely extrinsic and not a property of the material itself. Additionally, we determine that the presence of these electron traps not only result in a displacement of the recombination zone towards the cathode but also introduces an additional recombination channel of trapped electrons with free holes. However, this recombination is in most cases non-radiative, i. e. not resulting in light emission. Hence, a major loss mechanism in OLED devices is unveiled, not recognized until now. Resulting from a deeper investigation, we

show that the trap-assisted recombination rate is actually dominating the total recombination mechanism at low operating voltages, whereas at higher voltages the trap-free recombination prevails. This insight is particularly useful since it was already established by Sah that the so-called ideality factor in the famous Schottky diode equation is to 2 for when trap-assisted recombination is dominant and converges to 1 in the case of trap-free recombination. This awareness allows us to introduce a measurement technique of determining the individual recombination mechanisms in the device current of OLED devices. Moreover, for the cases that the trap-assisted recombination *does* result in light emission we demonstrate that the ideality factor of the so-called photocurrent, the response of the light detecting photodiode to the light emission of an OLED, can be used in a similar fashion to differentiate between both recombination mechanisms. This proves to be particularly useful in our investigation of the transport and recombination mechanisms in one of the most popular principal compounds for blue and white emitting diodes, polyfluorenes. Here we convey that during synthesis of this compound the often unintentional introduction of ketone defects, leads to additional trapping behavior in both hole and electron transport. Furthermore, the otherwise bleu emissive characteristic of this polyfluorene is, for the case of ketone contamination, dominated by a lower energetic green emission due to trap-assisted recombination on the ketone moiety. Additional green emission in the light spectrum of polyfluorenes had been the subject of a long-lasting debate in the field of organic light-emitting diodes. A further investigation of the temperature dependence of the mechanism of trap-assisted recombination leads to the understanding that the physics of this recombination can be approximated by the common, trap-free, recombination description where the electron mobility is set to zero, the electron resides immobile in the trap, which drastically simplifies the current physical picture of this mechanism and eliminates additional fitting parameters in the device model. Lastly, we calculate that non-radiative trap-assisted recombination is responsible for as much as up to 45% of the total current efficiency loss, the ratio of light emission over the device current, designating non-radiative trap-assisted recombination as one of the prime loss mechanisms in OLED devices. As a result, we come to the conclusion that the main focus of future research should be in identifying and eliminating the origin of the electron trapping specie, which will likely immediately improve the performance of most OLED devices.

Samenvatting

De markt en de ontwikkeling van beeldschermen en verlichtingstoepassingen groeit tegenwoordig zeer snel. Een typisch huishouden is tegenwoordig bezitter van op zijn minst meer dan één televisie set. Er zal op zijn minst één personal computer aanwezig zijn en elk individu heeft zijn eigen mobiele telefoon. In de Verenigde Staten alleen hebben huishoudens die een iPod hebben gemiddeld zo'n 1.3 stuks per huishouden. Daarbovenop is de laatste ontwikkeling dat steeds meer huishoudens ook in het bezit zullen zijn van een tablet computers als een iPad of iets soortgelijks. Zelfs in de auto van die typische westerse huishouden is een kleuren beeldscherm voor de route navigatie niet meer weg te denken. Maar dan hebben we het tot nu toe alleen nog maar gehad over beeldschermen, het gebruik van het aantal verlichtingstoepassingen is zelfs nog veel groter. Het moge duidelijk zijn dat in elke kamer van een typisch huis op zijn minst één elektrische verlichtingsbron aanwezig zal zijn, waarschijnlijk meer. Maar hoe zit het dan met alle andere verlichte displays? De displays in je oven, magnetron, wekker-radio, videorecorder, DVD-speler, geluidssysteem, CV-ketel, thermostaat, vaste telefoon, dashboard van je auto en nog veel meer. En dan hebben we het nog niet eens gehad over de displays in het publieke domein voor het dagelijkse leven. De beeldschermen en verlichtingstoepassingen in en op de bussen, vliegtuigen, vliegvelden, reclame-borden, treinen, verkeersborden, computer voor op het werk en zo kunnen we nog wel even door gaan. Als we ook nog eens bedenken dat vervangingssnelheid van elektronische apparatuur ook nog frequenter is geworden door de jaren heen, wordt het wel heel erg duidelijk dat, tenzij de wetenschap snel kernfusie introduceert, het van vitaal belang is dat de ontwikkeling van beeldschermen en verlichtingstoepassingen zal moeten focussen op duurzaam en energie besparende innovaties. Als het dan ook nog eens zo is dat we in dit kleine voorbeeld alleen nog maar gekeken hebben naar een typisch westers huishouden en bedenken dat de levensstandaard in de ontwikkelingslanden ook zeer snel aan het stijgen is, wordt het helemaal duidelijk hoe immens, groots het belang van de totale markt wordt voor deze toepassingen.

Organische licht emitterende diode (OLED) technologie is één van de meest prominente kandidaten om te voorzien in de behoefte naar duurzaam en energie besparende beeldschermen en verlichtingstoepassingen. De typische spanning waarbij een OLED functioneert is maar ongeveer 3V en de productie technieken zijn relatief simpel. Zeker technieken als spin-coaten en inkjet

printen zijn zeer veelbelovende productie methodes. In het bijzonder de flexibele eigenschap van OLEDs kan leiden tot een weg naar nieuwe mogelijkheden en duurzame producten. Je telefoon laten vallen bijvoorbeeld, zal ongetwijfeld leiden tot het beschadigen of kapot gaan van het beeldscherm. Met flexibele beeldschermen zal de kans dat het beeldscherm helemaal kapot is in ieder geval een stuk kleiner worden. Dit is dan ook meteen de reden waarom onder andere militaire organisaties en bedrijven ook zeer geïnteresseerd zijn in deze technologie. Een ander zeer bekende eigenschap van OLED technologie is dat het leidt tot beeldschermen met een veel hogere contrast ratio dan bijvoorbeeld LCD displays. Dus de licht intensiteit die nodig is om een beeldscherm te kunnen lezen is op deze mannier veel lager, wat energie bespaart. Sterker nog, in een OLED display is elke pixel een individuele diode waardoor, en dit in tegenstelling tot LCD technologie, er geen achtergrond verlichting nodig is, wat ook weer energie bespaart. Dit is zelfs één van de belangrijkste reden waarom in de laatste jaren het Galaxy telefoon model met een actieve matrix OLED (AMOLED) beeldscherm van Samsung zo populair geworden is.

De OLED beeldschermen van vandaag bestaan hoofdzakelijk uit opgedampte mulitlaag diodes, bestaande uit organische halfgeleiders. Dit is eigenlijk een consequentie van het feit dat *de* ideale organische halfgeleider met alle gunstige eigenschappen in één, voor OLED toepassingen, nog niet bestaat. En om hiervoor te compenseren zijn helaas meerdere laagjes van verschillende organisch materialen nodig. Echter, helaas hebben deze extra laagjes ook negatieve bijwerkingen. Zo zorgen meerdere laagjes ervoor dat de diode dikker wordt waardoor er meer spanning nodig is om de diode te laten werken. Tevens zorgt het aanbrengen van additieve laagjes voor een langere productie tijd. Daarbovenop moet ook in ogenschouw genomen dat hoewel de licht efficiëntie van OLEDs genoeg is voor beeldscherm toepassingen, voor verlichtingstoepassingen is het nog te laag en het zal daardoor nog niet toegepast kunnen worden op grote schaal. Kortom, er is nog het nodige aan kennis en onderzoek nodig naar de natuurkundige, scheikundige en elektronische eigenschappen in materialen die gebruikt worden voor OLED toepassingen.

Wat we onder andere tot nu begrijpen van de organische halfgeleiders in OLED toepassingen is dat in het overgrote deel van de materialen het gaten transport veel sneller is dan het elektronen transport. Gaten kunnen zich *vrij* voortbewegen door het materiaal volgens een ruimtelading begrensde stroom, terwijl elektronen stroom wordt waargenomen als een transport dat wordt gelimiteerd door de aanwezigheid van zogenaamde potentiaal putten, ook wel traps genoemd, waarbij de laag gedeeltelijk een lading krijgt door de

elektronen die blijven steken in deze traps. In een diode waarbij beide ladingsdragers wordt geïnjecteerd zal het recombinatie gebied, de plek in de laag waar beide ladingsdragers elkaar ontmoeten en waarbij het elektron met het gat zal recombineren, vlakbij de kathode komen te liggen, simpelweg omdat de gaten sneller gaan dan de elektronen. Voor het geval dat de recombinatie van de gaten en elektronen leidt tot licht uitstraling zal de aanwezigheid van de metallische kathode ervoor zorgen dat de intensiteit van die licht drastisch verlaagd wordt. Dit komt doordat het metallische contact het niet toe staat dat alle recombinatie licht uit zal kunnen zenden omdat veel ladingen vlakbij de kathode ervoor zullen kiezen om energie aan het metaal af te staan in plaats van licht uit te zenden. Het moge duidelijk zijn dat de aanwezigheid van deze zogenaamde elektronen traps zeer nadelig zijn voor het optimaal functioneren van een OLED. Helaas is het zo dat we nog niet erg veel weten over de exacte beschrijving van dit trap gedrag en de oorzaak ervan. In het werk van dit proefschrift laten we zien dat dit trap gedrag zeer waarschijnlijk niet het gevolg is van de moleculaire structuur van organische halfgeleiders in zijn geheel, maar dat waarschijnlijk eerder de oorsprong gezocht moet worden in een externe oorzaak. Tevens stellen we vast dat de aanwezigheid van traps niet alleen maar de oorzaak zijn van de verplaatsing van de recombinatie zone, maar ook leidt tot een extra recombinatie mechanisme waarbij getrapte elektronen recombineren met vrij gaten. Daarbij moet worden opgemerkt dat voor het geval van deze zogenaamde trap-geassisteerde recombinatie er in de meeste gevallen geen licht uitgestraald wordt dat bijdraagt tot de totale licht opbrengst in een OLED. Hierdoor zijn we via dit nieuwe inzicht gestuit op een nieuw verlies mechanisme in OLED materialen, voorheen nog niet erkend. Bij een verder onderzoek laten we zien dat bij lage spanning de total recombinatie wordt gedomineerd door trap-geassisteerde recombinatie waarbij uiteindelijk bij hogere spanningen de recombinatie van vrij elektronen met vrije gaten de overhand krijgt. Dit specifieke gegeven is uiteindelijk bijzonder handig omdat we via theoretisch werk van Sah weten dat de zogenaamde ideality factor in de wel bekende Schottky diode vergelijking voor trap-geassisteerde recombinatie 2 is en convergeert naar 1 voor het geval van vrije recombinatie. Dit wetende zijn we in staat gebleken om een nieuwe meet methodiek te introduceren waarbij we de individuele recombinatie mechanismen kunnen identificeren in de stroom van een OLED device. En voor de situaties waarbij de trap-geassisteerde recombinatie toch licht uit zendt laten we zien dat we een zelfde methodiek kunnen toepassen op de stroom van de licht sensor die de intensiteit van de licht uitstraling meet van de diode. Op deze manier kunnen we ook in het uitgestraalde licht de recombinatie mechanismen onderscheiden. Dit geven is in het bijzonder nuttig gebleken in ons onderzoek naar het ladingstransport en ladingsrecombinatie in één van de belangrijkste basis bestanddelen voor blauw

en wit licht emitterende materialen, polyfluoreen. Hier laten we zien dat de aanwezigheid van het, tijdens de synthese ontstane, keton defect leidt tot trapping in het gaten transport and extra trapping in het elektronen transport. Het normaal gesproken blauw light emitterende polyfloureen verandert in groen emitterend door de aanwezigheid van een grote groene piek in het licht spectrum veroorzaakt door emitterend trap-geassisteerde recombinatie op het keton defect. Dit verschijnsel van groen emissie veroorzaakt door keton vervuiling in polyfluoreen is lange tijd een punt van discussie geweest in het vakgebied en hebben we onder andere via onze nieuwe identificatie techniek middels ideality factor metingen inzichtelijk kunnen maken. Onderzoek naar de temperatuursafhankelijkheid van het trap-geassisteerde recombinatie mechanisme laat zien dat de natuurkundige beschrijving hiervoor benadert kan worden door de beschrijving voor de vrije ladingsdragers recombinatie waarbij de elektronen mobiliteit nul is, de elektronen zitten vast in de trap. Dit versimpelt de huidige beschrijving voor trap-geassisteerd recombinatie drastisch en staat ons toe het aantal parameters in het model voor de beschrijving van ladingstransport en recombinatie te verminderen. Tevens versimpelt dit het fysische plaatje voor de beschrijving van dit proces drastisch. Tot slot rekenen we voor dat de bijdrage voor het efficiëntie verlies door niet stralende trap-geassisteerde recombinatie op kan lopen tot wel 45% van de total stroom efficiëntie. Waarbij we concluderen dat uiteindelijk niet stralende trap-geassisteerde recombinatie één van de voornaamste verlies mechanismen is in de OLED materialen van vandaag. Het gevolg hiervan is dat we tot de conclusie komen dat de focus van toekomstig onderzoek zal moeten liggen bij het identificeren van de oorzaak van het trap gedrag en waar mogelijk dit trap gedrag verminderen vanwege het feit dat dit direct tot prestatie verbetering zal leiden in de meeste OLEDs.

List of publications

1. *Space-charge-limited hole current in poly(9,9-dioctylfluorene) diodes,*
H. T. Nicolai, G. A. H. Wetzelaer, **M. Kuik**, A. J. Kronemeijer, B. de Boer, and P. W. M. Blom, *Appl. Phys. Lett.* 96, 172107 (2010).

2. *Hysteresis-free electron currents in poly(p-phenylene vinylene) derivatives,*
N. I. Craciun, Y. Zhang, A. Palmaerts, H. T. Nicolai, **M. Kuik**, R. J. P. Kist, G. A. H. Wetzelaer, J. Wildeman, J. Vandenbergh, J. Lutsen, D. Vanderzande, and P. W. M. Blom, *J. Appl. Phys.* 107, 124505 (2010).

3. *Determination of the trap-assisted recombination strength in polymer light-emitting diodes,*
M. Kuik, H. T. Nicolai, M. Lenes, G. A. H. Wetzelaer, M. Lu, and P. W. M. Blom, *Appl. Phys. Lett.* 98(9), 093301 (2011)

4. *Trap-assisted and Langevin-type recombination in organic light-emitting diodes,*
G. A. H. Wetzelaer, **M. Kuik**, H. T. Nicolai, and P. W. M. Blom, *Phys. Rev. B* 83, 165204 (2011)

5. *Polymer light-emitting diodes with doped hole-transport layers,*
M. Lu, H. T. Nicolai, **M. Kuik**, G. A. H. Wetzelaer, J. Wildeman, A. Palmaerts, and P. W. M. Blom, *Phys. Status Solidi A* 208, 10, 2482 (2011)

6. *The effect of ketone defects on the charge transport and charge recombination in polyfluorenes,*
M. Kuik, G. A. H. Wetzelaer, J. G. Laddé, H. T. Nicolai, J. Wildeman, J. Sweelsen, and P. W. M. Blom, *Adv. Funct. Mater.* 21, 4502 (2011) (back cover, v21, 23b)

7. *Origin of the dark-current ideality factor in polymer:fullerene bulk heterojunction solar cells,*
G. A. H. Wetzelaer, **M. Kuik**, M. Lenes, and P. W. M. Blom, *Appl. Phys. Lett.* 99, 153507 (2011)

8. *Optical detection of deep electron traps in poly(p-phenylene vinylene) light-emitting diodes,*
M. Kuik, J. Vandenberg, L. Goris, E. J. Begemann, L. Lutsen, D. Vanderzande, J. V. Manca, and P. W. M. Blom, *Appl. Phys. Lett.* 99, 183305 (2011)

9. *Trap-assisted recombination in disordered organic semiconductors,*
M. Kuik, L. J. A. Koster, G. A. H. Wetzelaer, and P. W. M. Blom, *Phys. Rev. Lett.* 107, 256805 (2011)

10. *Non-radiative recombination losses in polymer light-emitting diodes,*
M. Kuik, L. J. A. Koster, A. G. Dijkstra, G. A. H. Wetzelaer, and P. W. M. Blom, *Org. Electron.* 13, 6, 969 (2012)

11. *Identifying the nature of charge recombination in organic solar cells from charge-transfer state electroluminescence,*
G. A. H. Wetzelaer, **M. Kuik**, and P. W. M. Blom, *Adv. Energy. Mater.*, Accepted for publication.

12. *Asymmetric electron and hole transport in a high-mobility n-type conjugated polymer,*
G. A. H. Wetzelaer, **M. Kuik**, Y. Olivier, V. Lemaur, J. Cornil, S. Fabiano, M. A. Loi, and P. W. M. Blom, Submitted for publication.

13. *Unification of trap-limited electron transport in semiconducting polymers*
H. T. Nicolai, **M. Kuik**, G. A. H. Wetzelaer, B. de Boer, P. W. M. Blom, C. Campbell, C. Risko, and J. L. Brédas, Submitted for publication.

14. *Trap-limited electron and exciton transport in conjugated polymers*
O. V. Mikhnenko, **M. Kuik**, N. J. van der Kaap, M. A. Loi, and P. W. M. Blom, Submitted for publication.

Acknowledgements

After having done my Bachelor research as well as my Master research in the group Molecular Electronics Physics of Organic Semiconductors (MEPOS) of Paul Blom, and after having done my international internship at Siemens AG in Erlangen, Germany, I was convinced that the scientific field of organic electronics is a very interesting field to work in. Especially because of it's multidisciplinary, international and even commercial elements. With the *the Groningen school* reputation, the outstanding research group of Paul Blom is the place I wanted to be. In hindsight, although it wasn't always easy, I do not regret one minute of that decision. The fact that I am doing my postdoc now in a beautiful as well as challenging place as UCSB, Santa Barbara, I owe all this to the work I was allowed to do in Groningen. As a result, I would like to take the opportunity here to first thank you, Paul, for inspiring and stimulating me in this part of my career. Your ideas, pragmatic approach, insights, as well as your ability to trust have been an example for me. I am still amazed how calm you always appear, even when the workload seems so high.

Originally my PhD work was part of the Technologiestichting STW and for that reason I would like to thank them for making my project possible. PhD work in this research field you never do alone, and in fact, as you may have guessed form the above, a lot of the collaborations are international. Therefore I would like to express my gratitude to Ludwig Goris, Laurence Lutsen, Jean Manca, Dirk Vanderzande and especially Joke Vandenbergh from the University of Hasselt, Belgium for collaborating with me on the work of electron trapping and hysteresis in PPVs. Additionally I would like to thank Jurjen Wildeman for accidentally synthesizing ketone contaminated PFO from which we managed to publish a really piece of work. Accordingly, I should also thank Jörgen Sweelsen, from TNO, for providing us with the pristine material. During the course of my PhD period I have attended many project meetings for the Seventh Framework Programmes (FP7); OLLA, Aeviom and ONE-P. For the vast majority of these meetings I was traveling all over Europe together with Herman. Herman, thanks for taking me along and thanks for all the fun we had during our traveling and stays!

I would also like to thank my reading committee, Dago de Leeuw, Neil Greenham and Gernot Paasch for taking the time to read my thesis and granting their approval.

Having said that, with delight I naturally have to thank the rest of the MEPOS crew with whom I have had the pleasure of sharing many memorable moments both work related as well as of duty. Herman, Johan, Auke, Hylke, Lenes, René, Arne, thank you for all the coffee brakes, De Negende Circel, Vlieland, San Francisco, Boston, Beijing, Belgium, most of Europe and much much more! Jan Anton, I already told you many times, I think the group has been very lucky to have had somebody like you return to Groningen. I owe a lot to you and I am very glad that we were able to be fruitful in our collaboration. I should not forget to put forward my appreciation for Renate without whom the MEPOS group would not run as smooth as it does today. I would like to especially thank Jan for all his skills, wisdom and playfulness, for being more then just the technician of our group, and for just being a friend. And lastly, Gert-Jan, I find it really remarkable how our collaboration turned into something so rewarding. I still have our little breakthrough moments vividly in my mind! Working here now in Santa Barbara I really miss having a buddy like you to bounce ideas off of, discuss research and drink the occasional good glass of wine. I would also like to thank the students I have had the pleasure of supervising. René, Jurre, Eline, Niels, I can honestly say that it has been a joy to work and hang out with you guys and I am pretty certain that we will stay in touch in the future! I feel proud that your work ended up in a paper, one way or the other. I wouldn't be writing this acknowledgement in English if I didn't intent to also thank my foreign friends and colleagues, Marianne, Kriszty, Ilias, Claudia, Kamal, Simone, Milo. And lastly, my colleague then and my colleague now, Alex, thanks for collaborating on some nice work and let's hope for a continuation of our interesting collaborations!

My buddy's and soccer-team, De Drinkende Dieren, from the early days of studying applied physics, I should also not forget to thank them for the many Risk games, soccer and just hanging out enjoying a good beer. Raatjes, Tinge, Triez, Koen, Blaauw, Peter, thanks for the healthy change in environment and perspective! Tinge, I would say things turned out pretty convenient having the same biorhythms and becoming neighbors at the Grote Beerstraat! Pleun and Laurens, thanks for giving me a place to sleep when I had to take an early flight again from Schiphol. In terms of change in environment and perspective, Johan, thanks for all the guitar sessions and all the concerts we have been to, and Bernadette, thanks for actually allowing all these jam sessions in the first place! Joost, thanks for all the SC Heerenveen games, drinking coffee, discussing everything sport related and picking me up at the airport in LA! It was a pleasure having you and Else for a brief period as neighbors at the Grote Beerstraat and sharing our experiences! Arend (Dijkstra), interesting how we managed to eventually collaborated on some work, all the best in Kyoto! Evert-

Jan, although lately the times we meet are rare, since you resided mostly in either Russia or New Zealand, thanks for your good advice when I needed it! And Mo, thanks for designing my beautiful thesis cover!

To my paranymphs Arend Hiddema and Martijn Lenes, I am honored that you both are willing to stand by my side at my defense ceremony. That's what true friends are for I suppose.

I would also like to take this opportunity to remember Bert de Boer who, as a professor at the MEPOS group, sadly passed away much to early during my PhD period. We did not differ in age that much. Your kind, clear, firm but open personality and unprecedented drive to achieve has been an inspiration for all of us. I will never forget the personal talks we had and the Ribhouse Texas visits we made during the summer months. Sandra, I still wish you all the strength you need!

En als allerlaatste, Pap, mam, Eric en Heidi, dank voor alle vertrouwen, geduld en steun door al die jaren heen.